

**Clinical, functional, and genetic analysis of
NER defective patients
and characterization of five novel *XPG* mutations**

Doctoral Thesis

In partial fulfillment of the requirements for the degree
“Doctor rerum naturalium (Dr. rer. nat.)”
in the Molecular Medicine Study Program
at the Georg-August University Göttingen



submitted by
Annika Schäfer
born in Göttingen

Göttingen, 2012

Thesis Committee

Prof. Dr. Michael P. Schön

E-Mail

sekretariathautklinik@med.uni-goettingen.de

Phone

0049-551-396401

Postal Address

Universitätsmedizin Göttingen
Zentrum Arbeits-, Sozial-, Umweltmedizin und
Dermatologie
Abteilung Dermatologie, Venerologie und
Allergologie
Robert-Koch-Straße 40
37075 Göttingen

PD Dr. Wilfried Kramer

E-Mail

wkramer@gwdg.de

Phone

0049-551-39-9653

Postal Address

Institut für Mikrobiologie und Genetik
Abtl. Molekulare Genetik
Grisebachstr. 8
37077 Göttingen

Prof Dr. Jürgen Brockmöller

E-Mail

s.mueller@med.uni-Göttingen.de

Phone

0049-551-395822

Postal Address

Universitätsmedizin Göttingen
Zentrum Pharmakologie und Toxikologie
Abteilung Klinische Pharmakologie
Robert-Koch-Straße 40
37075 Göttingen

Date of Disputation:

Affidavit

By this I declare that my doctoral thesis entitled:

**“Clinical, functional, and genetic analysis of NER defective patients
and characterization of five novel XPG mutations”**

has been written independently with no other sources and aids than quoted.

Annika Schäfer

Göttingen, June 2012

Table of contents

Abstract	I
List of figures	III
List of tables	IV
Abbreviations	VI
1. Introduction	1
1.1. The need for DNA repair	1
1.2. Mutagens attacking DNA	1
1.3. DNA repair mechanisms and associated syndromes	2
1.4. The Nucleotide excision repair pathway	4
1.4.1. Initiation of the NER	4
1.4.2. Unwinding of the DNA.....	5
1.4.3. DNA incision step	5
1.4.4. Refilling of the gap and ligation.....	6
1.5. Multiple functions of TFIIH and its “assistant” XPG	8
1.6. Defects in the NER pathway result in multiple clinical entities	9
1.6.1. Xeroderma pigmentosum (XP)	10
1.6.2. XP plus neurological symptoms (De Sanctis-Cacchione syndrome).....	10
1.6.3. Trichothiodystrophy (TTD)	11
1.6.4. Cockayne Syndrome (CS).....	11
1.6.5. Xeroderma pigmentosum/Trichothiodystrophy complex (XP/TTD)	12
1.6.6. Xeroderma pigmentosum/Cockayne Syndrome complex (XP/CS)	12
1.6.7. Cerebro-Oculo-Facio-Skeletal Syndrome (COFSS).....	12
Aim of the study	13
2. Materials and Methods	15
2.1. Biological material	15
2.1.1. Primary cell cultures.....	15

2.1.2. Cell line	15
2.1.3. Bacteria.....	15
2.2. Equipment.....	15
2.3. Consumable supplies	16
2.4. Chemicals	17
2.5. Buffers, solutions, and media.....	19
2.6. Ready to use reaction systems	21
2.7. Antibodies and immunoreagents	22
2.8. Enzymes	24
2.9. Marker	24
2.10. Oligonucleotides.....	25
2.11. Plasmids	29
2.12. Cell culture techniques.....	31
2.12.1. Culture of primary human fibroblasts and HEK293A cells	31
2.12.2. Transient transfection of primary human fibroblasts	32
2.12.3. Transient transfection of HEK293A cells	33
2.12.4. Functional Assays	33
2.12.4.1. Determination of post-UV cell survival	33
2.12.4.2. Determination of NER capability with Host Cell Reactivation Assay (HCR)	34
2.13. Microbiology	35
2.13.1. Preparation of chemical competent <i>E.coli XL1blue</i>	35
2.13.2. Transformation of <i>E.coli</i>	35
2.14. Molecular biology	36
2.14.1. Preparation of nucleic acids	36
2.14.1.1. Isolation of genomic DNA.....	36
2.14.1.2. Ultra fast alkaline lysis plasmid extraction and analysis	36
2.14.1.3. Isolation of plasmid DNA.....	36
2.14.1.4. Agarose gel electrophoresis (AGE)	37

2.14.1.5. Isolation of DNA from an agarose gel	37
2.14.1.6. Isolation of total RNA	38
2.14.1.7. Quantification of DNA and RNA	38
2.14.2. Enzymatic manipulation of DNA	38
2.14.2.1. Polymerase chain reaction (PCR)	38
2.14.2.2. Site directed mutagenesis	40
2.14.2.3. Reverse transcription PCR: Generation of cDNA.....	40
2.14.2.4. Quantitative real time PCR (qRT-PCR).....	41
2.14.2.5. Restriction of DNA.....	42
2.14.2.6. Ligation	42
2.14.2.7. DNA sequencing and sequence analysis	42
2.15. Protein biochemistry.....	43
2.15.1. Preparation of whole cell protein lysates	43
2.15.2. Immunoprecipitation (IP)	43
2.15.3. Horizontal SDS-PAGE and Western Blotting	44
2.15.4. Immunofluorescence (XP protein recruitment kinetics).....	45
3. Results.....	47
3.1. Results of the molecular-genetic and functional-genetic analysis	47
3.1.1. Clinical symptoms.....	47
3.1.1.1. Clinical symptoms of the 12 XPC patients.....	47
3.1.1.2. Clinical symptoms of the eight XP-D patients	47
3.1.1.3. Clinical symptoms of the three XPG patients.....	48
3.1.2. Characterization of XP fibroblast cells.....	48
3.1.2.1. Determination of post-UV survival.....	48
3.1.2.2. Determination of NER capability and XP complementation groups	52
3.1.2.3. Determination of mRNA expression levels of the mutated XP genes.....	54
3.1.2.4. Mutational analysis	57

3.1.2.5. Conservation status of amino acids in XPG changed by missense mutations in XPC	60
3.2. Characterization of the five novel XPG mutations	61
3.2.1. Functional relevance of the five novel XPG mutations	61
3.2.2. Interaction of XPG _{mut} with TFIIH.....	61
3.2.3. Influence of the XPG mutations on XP protein recruitment to sites of local DNA damage and on subsequent XP protein redistribution	65
4. Discussion.....	73
4.1. Clinical symptoms of the patients.....	74
4.1.1. Clinical symptoms of XP-C patients.....	74
4.1.2. Clinical symptoms of the XP-D patients	75
4.1.3. Clinical symptoms of the XP-G patients	76
4.2. Functional deficits in the NER deficient cells	76
4.2.1. Increased UV sensitivity in the NER deficient cells	76
4.2.2. Decreased relative NER capability in the NER deficient cells.....	78
4.3. mRNA levels of the mutated gene are only effected in XP-C patients	78
4.4. Mutational analysis pinpointed the genetic defect und revealed new disease-causing mutations	80
4.4.1. Mutational analysis of XP-C fibroblasts.....	80
4.4.2. Mutational analysis of XP-D fibroblasts	82
4.4.3. Mutational analysis of XP-G fibroblasts	84
4.5. Influence of the novel XPG mutations	85
4.5.1. All five XPG mutations influence the functionality of XPG in NER	85
4.5.2. Mutations impair interaction with TFIIH.....	86
4.5.3. Mutation-specific effects on repair factor assembly	87
5. Summary and conclusion.....	89
Bibliography	91
Appendix.....	109

Curriculum vitae	124
Publications.....	125
Acknowledgement.....	126

Abstract

Xeroderma pigmentosum (XP), Trichothiodystrophy (TTD), and Cockayne Syndrome (CS) are rare (incidence ~1 to 1 million) recessively inherited genetic diseases arising from genetic defects in the nucleotide excision repair (NER) which is responsible for the removal of UV-induced DNA lesions. Increased UV sensitivity is a common symptom, whereas only XP patients exhibit freckling within sun-exposed skin and a more than 1000-fold increased skin cancer susceptibility. Beyond that, a high phenotypic heterogeneity results in at least seven overlapping phenotypes: XP, XP plus neurological abnormalities, TTD, CS, XP/TTD complex, XP/CS complex, and COFSS (Cerebro-Oculo-Facio-Skeletal Syndrome). Additionally, different mutations affecting the same gene may result in different phenotypes depending on their localization.

In this by far largest analysis of 23 NER defective patients in Germany 12 XP-C, eight XP-D, and three XP-G patients were assessed by molecular-genetic characterization of their corresponding fibroblast cells and correlation with their clinical course of disease. Neurological symptoms were absent in all but one of the XP-C patients. Of the XP-D patients, generally phenotypically more variable, five patients exhibited the XP phenotype, two patients the TTD, and one patient the XP/CS complex phenotype. Two of the three XP-G patients exhibited a XP/CS complex phenotype. All patients' fibroblasts showed an increased UV sensitivity and a decreased NER capacity compared to wild type fibroblasts. Co-transfection of plasmids expressing *XPC*, *XPD*, or *XPG* cDNA increased relative NER capacity in XP-C, -D, and -G cells, respectively, thereby confirming patients' complementation groups. The mRNA expression of the mutated genes was determined compared to the mean expression level of nine wild type fibroblast cell cultures set to 100 %. *XPC* mRNA expression levels were significantly decreased (range 9.5 % – 25.7 %; $p < 0.001$, Student's T-test) in all but one XP-C patients' fibroblasts (274.1 %), whereas *XPD* and *XPG* mRNA expression in the corresponding patients' cells ranged nearly within the SEM of wild type cells. Mutational analysis revealed all XP-C patients being homozygous and identified four novel *XPC* mutations: p.A116YfsX4 (1/12), p.R475EfsX18 (1/12), p.G723SfsX44 (1/12), and p.I812del (1/12) which is a unique novel mutation resulting in an unusually elevated *XPC* mRNA expression. The novel *XPD* mutation, p.D681H (2/8), was identified in patients carrying the TTD-causing mutation p.R112H on the other allele. One patient exhibited TTD- and the other one CS-like symptoms indicating that dominance of the alleles is probably differently influenced by other factors such as epigenetic effects or SNPs. Five novel *XPG* mutations were identified. Four mutations, p.Q150X with p.L778P and p.E727X with p.W814S, were found in a compound heterozygous and one,

p.G805R, in a homozygous state. Correlation of missense mutations with a XP/CS phenotype was rather unexpected. Usually missense mutations impairing NER result in XP, whereas truncating mutations impairing NER and transcription result in XP/CS. Allele-specific complementation analysis of these five novel mutations identified only p.L778P and p.W814S retaining some residual repair activity. In line with the XP/CS phenotypes, even the missense mutations failed to interact with the transcription factor IIH subunits XPD and cdk7 in co-immunoprecipitation assays probably resulting in destabilized TFIIH. Immunofluorescence techniques revealed a mutation-specific effect on early XP protein recruitment to localized photodamage and a delayed redistribution *in vivo*.

In summary, in very rare diseases, novel *XPC*, *XPD*, and *XPG* mutations were identified. Comprehensive analysis of five novel *XPG* mutations identified the first single amino acids crucial for interaction with TFIIH.

List of figures

Figure 1: Simplified scheme of the NER pathway.	7
Figure 2: Simplified model for the transcription factor TFIIH and the role of XPG in maintenance of its architecture.....	9
Figure 3: Post-UV survival of XP-C fibroblast cells after 30 J/m ² UVC irradiation determined via MTT Assay.	49
Figure 4: Post-UV survival of XP-D fibroblasts determined via MTT Assay. Cells.....	51
Figure 5: Post-UV cell survival of XP-G fibroblast determined via MTT Assay.	52
Figure 6: Determination of relative NER capability and assignment of patients' fibroblast cells to their complementation groups with HCR.....	54
Figure 7: Determination of mRNA expression levels of the mutated genes via qRT-PCR.	56
Figure 8: Alignment of a stretch of amino acid sequences of the BHD3 domain from the XPC protein (A) and the I-region from the XPG protein (B).	60
Figure 9: Determination of the allele specific complementation ability of the novel XPG mutations by HCR.....	61
Figure 10: Schematic representation of pXPG(mut)mycHis constructs.	62
Figure 11: Determination of the complementation ability of XPGmycHis with HCR.	63
Figure 12: Co-immunoprecipitation of XPD and cdk7 with XPGmycHis.....	64
Figure 13: Quantification of XP protein and photodamage spot positive cell nuclei after local UVC irradiation.....	68
Figure 14: Immunofluorescence double staining of XP proteins and CPD photoproducts.	69
Figure 15A: Immunofluorescence staining of XP proteins in wild type and XP40GO fibroblasts.	70
Figure 15B: Immunofluorescence staining of XP proteins in wild type and XP40GO fibroblasts.	71
Figure 15C: Immunofluorescence staining of XP proteins in wild type and XP40GO fibroblasts.	72
Figure 16: Scheme of the primary structure of XPC with transglutaminase-homology domain (TGD) domain and the three β -hairpin domains.....	82
Figure 17: Scheme of the XPD protein with the helicase domains HD1 and HD2, the Fe-S domain and the CTE.....	84

List of tables

Table 2-1 Equipment.....	15
Table 2-2 Consumables.....	16
Table 2-3 Chemicals.....	17
Table 2-4 Buffers, solutions, and media.....	19
Table 2-5 Reaction systems.....	21
Table 2-6 Antibodies and immunoreagents.....	22
Table 2-7 Enzymes.....	24
Table 2-8 DNA- and protein standards.....	24
Table 2-9 Oligonucleotides.....	25
Table 2-10 Amount of plasmid DNA used for transfection with Lipofectamine 2000.....	33
Table 2-11 PCR reaction mix for Taq and Pfu DNA polymerase.....	39
Table 3-1 Summary of mutations found in XP-C, XP-D and XP-G patients.....	59
Table A-1 Post-UV survival of wt fibroblasts at a density of 5000 cells in percent.....	109
Table A-2 Post-UV survival of wt fibroblasts at a density of 5000 cells in the presence of 1 mM caffeine in percent.....	109
Table A-3 Post-UV survival of wt fibroblasts at a density of 7500 cells in percent.....	110
Table A-4 Post-UV survival of wt fibroblasts at a density of 7500 cells in the presence of 1 mM caffeine in percent.....	110
Table A-5 Post-UV survival of XP-C fibroblasts at a density of 5000 cells in percent.....	110
Table A-6 Post-UV survival of XP-C fibroblasts at a density of 5000 cells in the presence of 1 mM caffeine in percent.....	111
Table A-7 Post-UV survival of XP-C fibroblasts at a density of 7500 in percent.....	112
Table A-8 Post-UV survival of XP-C fibroblasts at a density of 7500 cells in the presence of 1 mM caffeine in percent.....	113
Table A-9 Post-UV survival of XP-D fibroblasts at a density of 5000 cells as well as 10000 cells in the case of XP188MA in percent.....	114
Table A-10 Post-UV survival of XP-D fibroblasts at a density of 5000 cells in the presence of 1 mM caffeine in percent.....	115
Table A-11 Post-UV survival of XP-C fibroblasts at a density of 7500 cells in percent.....	115
Table A-12 Post-UV survival of XP-D fibroblasts at a density of 7500 cells in the presence of 1 mM caffeine in percent.....	116
Table A-13 Post-UV survival of XP-G fibroblasts in percent.....	116

Table A-14 Relative NER capability of wt fibroblasts.....	118
Table A-15 Relative NER capability of XP-C fibroblasts	118
Table A-16 Relative NER capability of XP-D fibroblasts	119
Table A-17 Relative NER capability of XP-G fibroblasts	120
Table A-18 mRNA expression of the XP genes of NER deficient cells in %	121
Table A-19 Relative NER capability of XP40GO (XP-G) fibroblasts complemented with pXPG and pXPGmut plasmids	123

Abbreviations

Abbreviation	Denotation
ATP	Adenosine-5'-triphosphate
ATPase	adenosine triphosphatase
CAF-1	chromatin assembly factor 1
CAK	cdk-activating kinase
cdk	cyclin dependent kinase
COFS Syndrome	Cerebro-Oculo-Facio-Skeletal Syndrome
CPD	cyclubutane pyrimidine dimer
CS	Cockayne Syndrome
Ct	cycle threshold
DDR	DNA damage respose
DEPC	diethylpyrocarbonate
DMSO	dimethyl sulfoxide
DNA	deoxyribonucleic acid
dNTP	desoxyribonucleotide
ddNTP	dideoxyribonucleotide
DSB	double strand breaks
DTT	dithiothreitol
<i>E.coli</i>	<i>Escherichia coli</i>
EDTA	ethylenediaminetetracetic acid
GGR	global genome repair
HCl	hydrochlorid acid
HEK	Human Embryonic Kidney
HhH	helix-hairpin-helix
HNPCC	hereditary non-polyposis colorectal cancer
HRR	homologous recombination repair
ICL	interstrand crosslink
IR	ionizing radiation
KCl	Potassium chloride
mcs	multiple cloning site
MMR	miss match repair
NaCl	natrium chloride

NaOH	sodium hydroxide
NBS	Nijmegen breakage syndrome
NER	nucleotide excision repair
NHEJ	non-homologous end-joining
PAGE	polyacrylamide gel electrophoresis
PCNA	proliferating cell nuclear antigen
PCR	Polymerase Chain Reaction
PFA	paraformaldehyde
PMSF	phenylmethanesulfonylfluoride
qRT-PCR	quantitative Real Time Polymerase Chain Reaction
RFC	proliferating cell nuclear antigen loading complex Ctf18-replication factor C
RNA	ribonucleic acid
RPA	replication protein A
SDS	sodium dodecyl sulfate
ss	single strand
TCR	transcription coupled repair
TF	transcription factor
TFA	trifluoroacetic acid
TTD	Trichothiodystrophy
UV	ultraviolet radiation
XP	Xeroderma pigmentosum
CTE	C-terminal extension
<i>Sch.pombe</i>	<i>Schizosaccharomyces pombe</i>
SaXPD	XPD homolog from <i>Sulfolobus</i> <i>acidocaldarius</i>
TGD	transglutaminase-homology domain
BHD	β -hairpin domain
MTT	3-(4,5- Dimethylthiazol-2-yl)-2,5-diphenyl- tetrazoliumbromid
TMB	3,3',5,5'-Tetramethylbenzidine
N-region	N-terminal region
I- region	internal region
wt	wild type

6,4PP

pyrimidine (6-4) pyrimidone photoproduct

1. Introduction

1.1. The need for DNA repair

The Deoxyribonucleic acid (DNA) is carrier of the genetic information of all organisms and DNA-viruses. The genetic information is organized in chromosomes and the whole chromosome set is contained in every single cell. The diploid human genome consists of nearly 3 billion base pairs per chromosome set and encodes between 20,000 and 25,000 protein-coding genes (Venter *et al.*, 2001). Maintenance of the genomic sequence is essential for proper function and survival of every single cell and for the organism as a whole. Unrepaired DNA modifications severely affect the fidelity of DNA polymerases and, thus, can turn into permanent mutations during DNA replication. These permanent mutations present the basis for malignant transformation of the cells: accumulation of mutations can result in the activation of proto-oncogenes and the inactivation of tumor-suppressor genes over time (Bartek *et al.*, 2007). To face this problem, eukaryotic cells have developed a network of DNA damage signaling pathways and associated DNA repair systems collectively called the DNA damage response (DDR) (Giglia-Mari *et al.*, 2011).

1.2. Mutagens attacking DNA

Faulty alterations in the DNA can result from endogenous and exogenous sources. Endogenous sources are mistakes in DNA replication and (by)-products of the cellular metabolism like reactive oxygen and nitrogen species, lipid peroxidation products, estrogen and cholesterol metabolites, reactive carbonyl species, and endogenous alkylating agents (De Bont and van Larebeke, 2004). In addition, the DNA molecule itself is unstable and hydrolysis of nucleotide residues creates abasic sites and deamination of adenine, cytosine, and guanine (Lindahl, 1993; Sander *et al.*, 2005). Exogenous sources for DNA damage are ultraviolet radiation (UV), ionizing radiation (IR), and numerous genotoxic chemicals that cause alterations within the DNA (Hoeijmakers, 2001).

Among the various exogenous sources of DNA damage induction the UV radiation on Earth's surface represents one of the most effective carcinogenic agents altering the genome integrity from prokaryotes to mammals (Rastogi *et al.*, 2010). In 1928 a lethal effect due to UV light absorption (100-400 nm wavelength) of nucleic acids with an absorption maximum about 260 nm was described for the first time (Gates, 1928). Later on, in 1962, formation of thymine dimers after UV treatment was described in living cells (Wacker *et al.*, 1962). Today the genotoxic effect of solar irradiation is well established. Cyclobutane pyrimidine dimer (CPD) and pyrimidine (6-4) pyrimidone photoproducts (6,4PP) represent the two major cytotoxic,

mutagenic and carcinogenic UV-induced DNA damages in living cells. CPDs arise from the formation of two bonds between carbons four and five of each adjacent pyrimidine. 6,4PPs result from the formation of one bond between carbons six and four of adjacent pyrimidines (Pfeifer, 1997).

1.3. DNA repair mechanisms and associated syndromes

The importance of a proper DNA damage response is mirrored by different human syndromes which arise from defects in genes functioning in certain DNA repair pathways.

The homologous recombination repair (HRR) and the non-homologous end-joining (NHEJ) are responsible for the repair of DNA double strand breaks (DSB). This DNA lesion results from ionizing radiation, X-rays, or from chemical modifications causing replication fork stalling and collapse in actively cycling cells. Additionally, DSB occur during the repair of DNA interstrand crosslinks (ICLs) as well as in recombination processes of homologous chromosomes during meiosis (Kee and D'Andrea, 2010). HRR is active in the late S- and G2-phase of the cell cycle as the cut strand interacts with the homologous strand of the sister chromatid. The intact sister chromatid strand serves as a template and subsequently allows for error-free re-ligation of the DNA ends (Chodaparambil *et al.*, 2006; Liang *et al.*, 1998; Thompson and Schild, 2001). NHEJ, the more mutation prone pathway, is restricted to the G0, G1 and early S-phase of the cell cycle. During NHEJ the two DNA ends are ligated without any verification which often results in the insertion or deletion of a few base pairs (Lieber, 2008; Roth *et al.*, 1985; Thacker *et al.*, 1992). Consequences of non-repaired double strand breaks are chromosomal aberrations leading to cell death or mutations that, in turn, may result in cancer phenotypes (Aguilera and Gomez-Gonzalez, 2008). Thus, mutations in genes mediating initiation and repair of double strand breaks result in several genetic diseases (Thompson and Schild, 2002). Defects in genes mediating the initiation and procedure of the double strand break repair lead to ataxia telangiectasia (Rotman and Shiloh, 1998), ataxia telangiectasia-like disorder and to the Nijmegen breakage syndrome (NBS) (Petrini, 2000). All three syndromes commonly result in an increased cancer susceptibility as well as immunodeficiency, hypersensitivity to X-rays, and chromosomal instability (Hoeijmakers, 2001). The cancer-prone disorders Werner, Bloom and Rothmund Thomson syndrome result from defects in RecQ-like helicases RecQL12, RECQL3, RECQL4, respectively, which are described to interact with the DSB repair enzymes (Chun *et al.*, 2011; Larizza *et al.*, 2010; Monnat, Jr., 2010; Tikoo and Sengupta, 2010). Additionally, the Fanconi anemia is induced by mutations in 15 gene products involved in the removal of ICLs.

This genetic disorder is also characterized by increased tumor predisposition in combination with pancytopenia (Kee and D'Andrea, 2010).

The miss match repair (MMR) pathway is responsible for the correction of mispaired base pairs occurring spontaneously during replication. Moreover, MMR removes insertion and deletion loops in the DNA which lead to microsatellite instability if left unrepaired (Hoeijmakers, 2001; Thoms *et al.*, 2007). These loops result from DNA polymerase slippage at nucleotide repeats during replication (Canceill *et al.*, 1999; Canceill and Ehrlich, 1996). The MMR pathway recognizes the DNA aberration, identifies the modified DNA strand, which is subsequently degraded, and re-synthesizes the excised DNA tract. Microsatellite instability due to defective MMR results in the hereditary non-polyposis colorectal cancer (HNPCC) as well as the Muir Torre syndrome and the Turcot syndrome. However, the Muir Torre and the Turcot syndrome result in an increased skin and brain tumor susceptibility and are therefore considered as subtypes of the HNPCC (Hoeijmakers, 2001; Manceau *et al.*, 2011; Ponti and Ponz de, 2005; Thoms *et al.*, 2007).

The nucleotide excision repair pathway is generally responsible for the removal of a variety of DNA lesions inducing a distortion of the DNA double helix (Buschta-Hedayat *et al.*, 1999; Wood, 1999). This includes bulky chemical DNA adducts like interstrand crosslinks induced by chemotherapeutic agents such as cisplatin, or polycyclic aromatic hydrocarbons induced by components of tobacco smoke (Friedberg, 2006; Wogan *et al.*, 2004). Importantly, this pathway is responsible for the removal of UV-induced CPDs and 6,4PPs. NER consists of several steps: recognition of the DNA damage, opening of the DNA around the lesion, incision of the damaged strand 3' and 5' to the lesion and removal of the damage-containing single strand (ss) oligonucleotide, filling of the resulting gap and strand ligation (De Boer and Hoeijmakers, 2000). Genetic defects in genes contributing to the NER result in the three diseases Xeroderma pigmentosum, Cockayne Syndrome and Trichothiodystrophy (Bootsma, 2002). However, there is a very high clinical heterogeneity between these three main clinical entities. Patients from all three disorders exhibit increased sun sensitivity, whereas increased skin cancer susceptibility, a common feature of all DNA-repair-defect associated syndromes, is only found in XP-patients (Kraemer *et al.*, 2007).

1.4. The Nucleotide excision repair pathway

The NER pathway is subdivided into the transcription coupled repair (TCR) and the global genome repair (GGR). TCR removes lesions from actively transcribed genes (Mellon *et al.*, 1987), whereas GGR removes DNA lesions throughout the whole genome (Bohr *et al.*, 1985). A simplified scheme of the NER pathway is depicted in figure 1.

1.4.1. Initiation of the NER

The stalled RNA polymerase II together with the Cockayne Syndrome proteins CSA, and CSB initiate the repair process in TCR (Mu and Sancar, 1997). In contrast, the initial damage recognition in GGR is performed by XPC functioning in complex with HR23B and Centrin2. Rad23B (yeast homolog of HR23B) and Centrin2 are supposed to stimulate the DNA binding activity of XPC (Ng *et al.*, 2003; Nishi *et al.*, 2005; Xie *et al.*, 2004). XPC itself is a DNA binding protein that binds in particular to damaged DNA structures with considerable distortion (Araki *et al.*, 2001; Sugasawa *et al.*, 1998). Mailliard *et al.* reported that XPC has no direct contact with the bulky DNA lesion itself but rather interacts with ss DNA configurations on the complementary DNA strand (Mailliard *et al.*, 2007). Binding affinity of the protein to 6,4PPs (Hey *et al.*, 2002; Sugasawa *et al.*, 1998), *N*-(2'-deoxyguanosin-8-yl)-*N*-acetyl-2-aminofluorene adducts (Sugasawa *et al.*, 2001), intrastrand cisplatin crosslinks (Hey *et al.*, 2002; Trego and Turchi, 2006), and artificial cholesterol-like structures (Roche *et al.*, 2008) has been described previously. However, the UV-induced CPDs are poorly recognized by XPC (Hey *et al.*, 2002; Kusumoto *et al.*, 2001; Sugasawa *et al.*, 2001) although the removal of the CPD photolesions still depends on functional XPC protein (Hwang *et al.*, 1999; Venema *et al.*, 1991). Here the UV damaged DNA binding protein (UV-DDB or XPE) complex comes into play. UV-DDB is a heterodimer consisting of the proteins DDB1 and DDB2 (Keeney *et al.*, 1993; Takao *et al.*, 1993). The protein complex is involved in GGR, whereas it is dispensable for TCR. Fibroblasts with a defective *XPE* gene show an impaired removal of CPDs in GGR while 6,4PP removal is carried out in normal levels (Hwang *et al.*, 1999). This indicates a specific function of XPE in the initiation of CPD removal. In addition, binding of UV-DDB to UV damaged DNA results in a distortion of the DNA (Fujiwara *et al.*, 1999). Thus, recognition of CPDs by XPC is probably facilitated by prior binding of UV-DDB to the lesion (Tang and Chu, 2002). Beside its function in damage recognition, the UV-DDB complex is part of the multi-subunit E3 ubiquitin ligase complex (Groisman *et al.*, 2003) which ubiquitinylates DDB2 and the XPC protein with different consequences. While the ubiquitination of XPC is reversible and results in an increase of its DNA binding affinity, DDB2 ubiquitination leads to a rapid degradation of the protein within a

few hours. This probably results from a handover mechanism changing the initial damage recognition from UV-DDB complex to XPC/HR23B/Centrin2 complex (Sugasawa *et al.*, 2005; Sugasawa, 2006).

1.4.2. Unwinding of the DNA

The second step of the NER pathway comprises the XPC dependent recruitment of the transcription factor IIH (TFIIH) (Araujo *et al.*, 2001; Riedl *et al.*, 2003) and, subsequently, the unwinding of the DNA around the lesion. TFIIH consists of ten proteins and can be divided into two complexes. The core complex is composed of the six proteins XPB, p62, p52, p44, p32, and p8 (TTDA). The CAK (cdk-activating kinase) complex contains cdk7, cyclin H, and MAT1. Both complexes are bridged by XPD which interacts with MAT1 (CAK) and p44 (core) (Drapkin *et al.*, 1996; Reardon *et al.*, 1996). XPB and XPD represent the two helicase subunits of TFIIH which open the DNA around the lesion. However, it is the 5'→3' helicase function of XPD which is needed for DNA unwinding, whereas XPB mainly functions as a DNA-dependent ATPase (Coin *et al.*, 2007; Tirode *et al.*, 1999; Winkler *et al.*, 2000). Beside its function in DNA unwinding, the ATPase activity of XPB was also described to be necessary for the accumulation of TFIIH to sites of local DNA and the anchoring of the complex to the damaged DNA (Fan *et al.*, 2006; Oksenysh *et al.*, 2009).

The XPA protein is also recruited at this early time point and Riedl *et al.* reported that the absence of XPA abolished the recruitment of any following NER factor (Riedl *et al.*, 2003). XPA represents another DNA binding protein with slight preference for damaged DNA (Lao *et al.*, 2000; Matsuda *et al.*, 1995; Robins *et al.*, 1991). Therefore, the protein was originally thought to be involved in initial damage recognition together with XPC (Asahina *et al.*, 1994; Wakasugi and Sancar, 1999). The protein interacts with different NER proteins (Li *et al.*, 1995a; Li *et al.*, 1995b; Nocentini *et al.*, 1997; Park *et al.*, 1995; Park and Sancar, 1994; Saijo *et al.*, 1996) and was described to stimulate the DNA helicase function of TFIIH (Sugasawa *et al.*, 2009). In addition, there is indication that XPA is needed to dislodge the XPC protein (Hey *et al.*, 2002). Although the XPA protein is required for proper function of GGR and TCR (Kobayashi *et al.*, 1998), the specific role of the XPA protein still remains to be elucidated.

1.4.3. DNA incision step

The two structure specific endonucleases XPF-ERCC1 and XPG cut the DNA strand 5' and 3' to the lesion, respectively (Mu *et al.*, 1996; O'Donovan *et al.*, 1994). The heterodimer formation of XPF-ERCC1 is performed with helix-hairpin-helix (HhH) domains located at the C-termini of

both subunits (de Laat *et al.*, 1998; Tsodikov *et al.*, 2005). The endonuclease activity of the heterodimer is located adjacent to the HhH domain of the XPF subunit (Enzlin and Scharer, 2002), whereas the ERCC1 subunit only exhibits a stabilizing effect on XPF (Houtsmuller *et al.*, 1999). XPG belongs to the FEN-1 family of structure specific nucleases whose members are characterized by two highly conserved nuclease domains called N-region (N-terminal region) and I- region (internal region). These regions contain a number of highly conserved acidic residues which are required for nuclease function of the proteins (Constantinou *et al.*, 1999; Hosfield *et al.*, 1998; Lieber, 1997; Shen *et al.*, 1996). In addition, regions involved in DNA binding are also conserved within their amino acid sequence (Park *et al.*, 1997; Stucki *et al.*, 2001). The domain between N- and I-region spans about 70 amino acids in FEN-1 and most of the other family members (Ceska *et al.*, 1996; Hosfield *et al.*, 1998; Hwang *et al.*, 1998). In the XPG protein this so called “spacer region” or “R-Region” spans about 600 amino acids (Scherly *et al.*, 1993). Differences in the amino acid sequence between N- and I-region define substrate specificity of the FEN-1 endonucleases. Bubble substrates are cleaved by XPG but not by FEN-1, which removes 5' flaps on single stranded DNA (Evans *et al.*, 1997; Tomlinson *et al.*, 2010). Accordingly, bubble substrate cleavage of XPG is decreased when the spacer region is replaced by a sequence ($\alpha 4$ and $\alpha 5$) from an archaeal FEN endonuclease, whereas 5' flaps can still be processed properly (Sarker *et al.*, 2005; Tsutakawa *et al.*, 2011).

In NER the mere presence of XPG, independent from its catalytic activity, is required for the 5' incision by XPF implicating a structural role of XPG beside its endonuclease function. In contrast, for efficient 3' incision by XPG catalytically active XPF is necessary (Constantinou *et al.*, 1999; Staresincic *et al.*, 2009; Tapias *et al.*, 2004; Wakasugi *et al.*, 1997). Moreover, initiation of partial DNA repair synthesis after 5' incision of XPF as well as recruitment of the following repair synthesis factors PCNA (proliferating cell nuclear antigen) and CAF-1 (chromatin assembly factor 1) in the presence of catalytically inactive XPG has been shown *in vitro*. These findings suggest that 5' incision occurs first and is sufficient for the initiation of the DNA repair synthesis, while the 3' incision is needed for completion of DNA synthesis (Staresincic *et al.*, 2009).

1.4.4. Refilling of the gap and ligation

The excised fragment comprises a length of 25-30 nucleotides depending on the lesion (Matsunaga *et al.*, 1995; Moggs *et al.*, 1996; Svoboda *et al.*, 1993). The resulting gap is subsequently filled by the DNA polymerase δ and ϵ in the presence of PCNA, RFC (proliferating cell nuclear antigen loader complex Ctf18-replication factor C), and RPA (replication protein A)

(Shivji *et al.*, 1995). The last NER step comprises the ligation of the newly synthesized DNA fragment with the adjacent 3' and 5' ends. This step was originally thought to be carried out mainly by DNA ligase I (Aboussekhra *et al.*, 1995; Shivji *et al.*, 1995) as mutations in the corresponding gene result in a UV sensitive phenotype (Barnes *et al.*, 1992). However, meanwhile ligase III together with XRCC1 was described to be the dominant ligase complex in NER (Moser *et al.*, 2007).

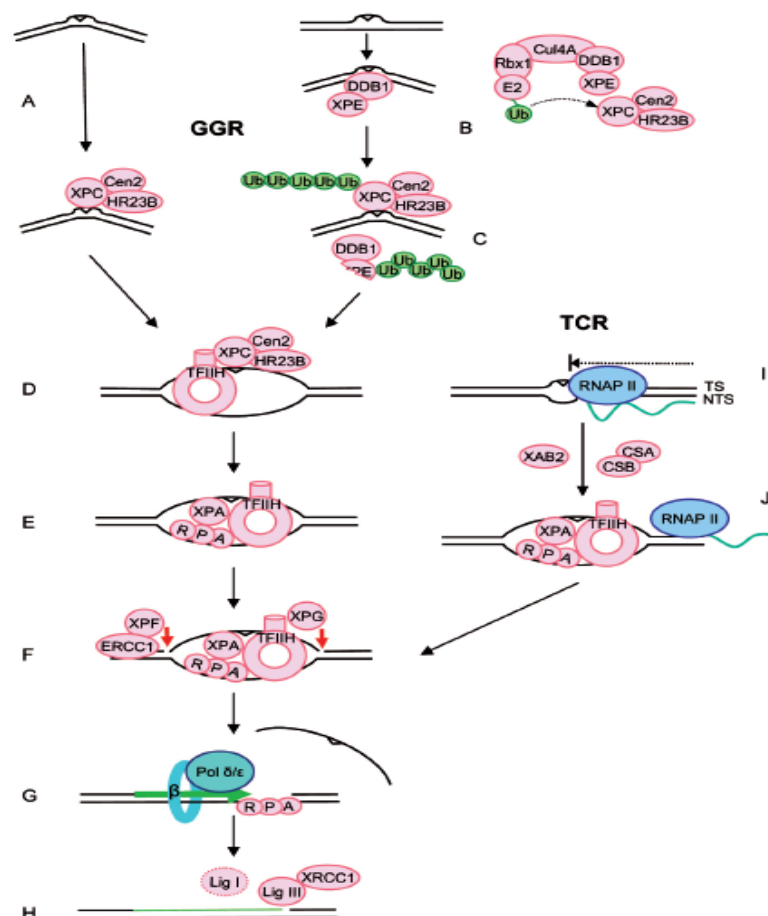


Figure 1: Simplified scheme of the NER pathway. **A:** Many lesions are recognized by XPC in complex with HR23B and Centrin2. **B:** Lesions resulting in little distortion are first recognized by UV-DDB (XPE/DDB1). **C:** The UV-DDB containing E3 ubiquitin ligase complex ubiquitinylates XPC and UV-DDB, resulting in an increased DNA binding affinity of XPC and the degradation of XPE. **D:** The TFIH complex unwinds the DNA around the lesion. **E:** XPA and RPA join in, while the XPC complex leaves. **F:** Endonucleases XPG and XPF incise the damaged DNA strand 3' and 5' to the lesion, respectively. **G:** DNA polymerases δ and ϵ refill the resulting gap. **H:** Mainly ligase III in complex with XRCC1 and to a little extent ligase I seal the newly synthesized strand with the old one. **I and J:** TCR is initiated by the stalling of RNA polymerase III in front of a lesion on the transcribed strand. Proteins CSA, CSB, and XAB2 are required for initiation of the NER, although their exact functions are unclear. Figure taken from Nospikel *et al.* 2009.

1.5. Multiple functions of TFIIH and its “assistant” XPG

TFIIH has a dual role: transcription (core complex and CAK) and repair (core complex only). In transcription, TFIIH is part of the pre-initiation complex composed of the general transcription factors TFIIA, TFIIIB, TFIIIE, and TFIIIF as well as RNA Polymerase II. In this context TFIIH is engaged in transcription initiation and promoter escape (Dvir *et al.*, 2001) as well as in transcription re-initiation (Yudkovsky *et al.*, 2000). In transcription initiation the helicase subunit XPB is required for promotor opening around the start side, whereas the XPD subunit stimulates transcription and anchors the CAK complex to core TFIIH (Tirode *et al.*, 1999). The CAK protein cdk7 phosphorylates the C-terminal domain of the RNA polymerase II required for promotor escape (Lu *et al.*, 1992; Svejstrup *et al.*, 1996; Tirode *et al.*, 1999). Furthermore, cdk7 phosphorylates different nuclear receptors including retinoic acid receptors, the thyroid hormone receptor, and the peroxysome proliferator-activated receptors (Le *et al.*, 2010; Rochette-Egly *et al.*, 1997) which, once activated, transactivate the transcription of certain genes in turn (Bastien *et al.*, 2000; Chen *et al.*, 2000; Compe *et al.*, 2005; Drane *et al.*, 2004; Ito *et al.*, 2007; Rochette-Egly *et al.*, 1997). In NER the helicase function of XPD and the ATPase activity of XPB are required for DNA opening (Coin *et al.*, 2007; Tirode *et al.*, 1999; Winkler *et al.*, 2000), whereas the activity of CAK is dispensable (Arab *et al.*, 2010).

Interactions of the TFIIH proteins XPD, XPB, p62, p44, and cdk7 with XPG have been shown *in vivo* and *in vitro* (Dunand-Sauthier *et al.*, 2005; Ito *et al.*, 2007; Iyer *et al.*, 1996; Thorel *et al.*, 2004). The architecture of TFIIH was found to depend strongly on interaction with XPG. Impaired interaction due to truncating mutations, found in XP/CS patients, result in the dissociation of CAK and core TFIIH (figure 2) (Arab *et al.*, 2010; Ito *et al.*, 2007). Again, this implicates a structural role of the endonuclease beside its catalytical function in DNA incision during NER. A general participation of XPG in transcription remains to be elucidated. However, importance of the XPG-TFIIH interaction in transcriptional context is reflected by the observation of impaired TFIIH mediated nuclear receptor transactivation due to mutations in XPG impairing interaction (Ito *et al.*, 2007).

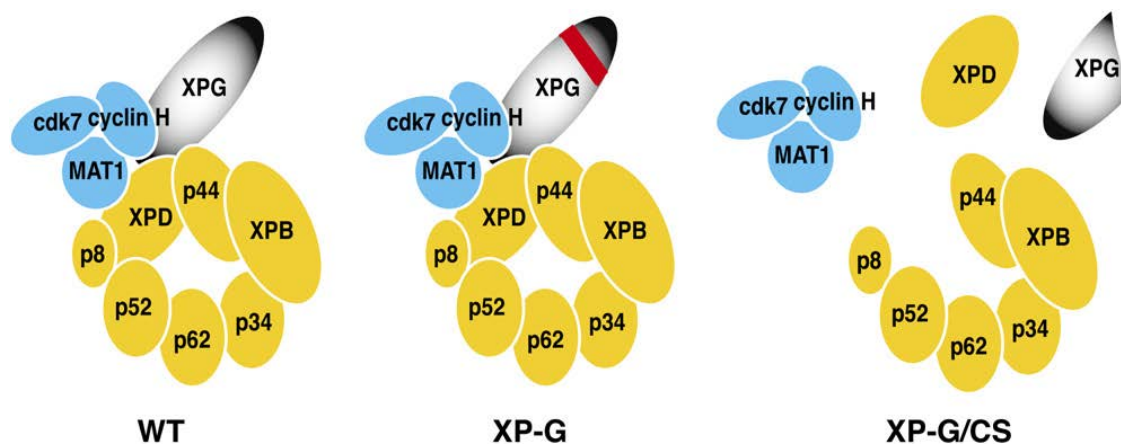


Figure 2: Simplified model of the transcription factor TFIIH and the role of XPG in maintenance of its architecture. The architecture of TFIIH is maintained in wild type and XP-G cells while truncating *XPG* mutations in XP-G/CS patients result in the dissociation of TFIIH. Figure taken from Ito *et al.* 2007.

1.6. Defects in the NER pathway result in multiple clinical entities

Mutations in genes functioning in the NER pathway result in the autosomal recessive disorders Xeroderma pigmentosum (XP, OMIM 278700-278780), Cockayne Syndrome (CS, OMIM 216400 (CSA), 133540 (CSB)) and Trichothiodystrophy (TTD, OMIM 601675). All three syndromes cause increased sun sensitivity. However, only XP patients additionally suffer from an increased risk to develop sun induced skin cancer. Moreover, freckling within sun-exposed skin is a typical marker for XP (Bootsma, 2002; Kraemer *et al.*, 2007). NER defect syndromes are very rare disorders: incidences in Western Europe were established at 2.3 per million for XP, 2.7 per million for CS and 1.2 per million for TDD (Kleijer *et al.*, 2008).

To date seven XP genes, *XPA* to *XPG*, involved in the nucleotide excision repair pathway have been identified by cell fusion experiments (De Weerd-Kastelein *et al.*, 1972). Accordingly, patients can be assigned to seven complementation groups, XP-A to XP-G, depending on the mutated gene. In addition, a XP variant form (XPV, OMIM 278750) is caused by mutations in the gene coding for translesion DNA polymerase eta (*XPV*) (Masutani *et al.*, 1999). Defects in genes *CSA* and *CSB* result in the Cockayne Syndrome (Henning *et al.*, 1995; Tanaka *et al.*, 1981; Troelstra *et al.*, 1990) and a defective *TTDA* gene was found to induce TTD (Giglia-Mari *et al.*, 2004). Beyond that, there is a pronounced variability between the different phenotypes. Mutations in one gene can result in different phenotypes, depending on their localization, and thus, their impact on the protein function. Therefore genetic defects in NER associated genes may result in seven different clinical phenotypes: XP, XP plus neurological abnormalities, TTD,

CS, XP/TTD complex, XP/CS complex, and COFSS (Cerebro-Oculo-Facio-Skeletal Syndrome) (Kraemer *et al.*, 2007).

1.6.1. Xeroderma pigmentosum (XP)

XP arises from defects in genes *XPA* to *XPG* and *XPV*. It was the first NER associated disorder to be described in 1874 by M. Kaposi (Hebra and Kaposi, 1874). Later on, in 1968, J. Cleaver identified the underlying DNA repair defect (Cleaver, 1968). Typical symptoms of XP include increased sun sensitivity since birth as well as freckling, hyper- and hypopigmentations, skin atrophy, and premature skin aging (i.e. poikiloderma) within sun-exposed skin starting as early as two to three years of age. Interestingly, about one third of the XP patients may not exhibit any sun sensitivity at all. Eventually, development of non-melanoma (~10,000-fold increased risk) as well as melanoma skin cancer (~2,000-fold increased risk) occurs in XP patients starting at a median age of about nine and 22 years, respectively. Tumors are preferentially located to sun-exposed areas of the body (Bootsma, 2002; Bradford *et al.*, 2011; Kraemer *et al.*, 1987).

1.6.2. XP plus neurological symptoms (De Sanctis-Cacchione syndrome)

XP plus neurological symptoms is mainly found in complementation groups XP-A, -B, -D, and -G, whereas XP-C, XP-E and XP-V patients rarely exhibit neurological symptoms (Cleaver *et al.*, 2009). A study from Bradford *et al.* evaluated the long term outcome of 106 XP patients: 24 % (25 patients) exhibited neurologic abnormalities. In addition, patients suffering from neurologic symptoms mainly exhibited mutations in the *XPD* (16 patients) or the *XPA* gene (six patients) (Bradford *et al.*, 2011). The course of neurological degeneration is generally variable among the patients. Intellectual capacity may initially develop during childhood, but later on deterioration follows. It begins in the fifth to tenth year of life. Earliest clinical signs are diminished or absent deep tendon reflexes, followed by progressive high-frequency hearing loss. This may necessitate the use of a hearing aid. Mental deterioration with disabilities in speaking, walking, and balance may follow (spasticity, ataxia). An abnormal gait and difficulty to walk eventually can be included and may result in the need of using a wheelchair. At late stages of the disease swallowing difficulties may become problematic, leading to the aspiration of food, and necessitate the implantation of a gastric feeding tube. Neuro-imaging abnormalities show atrophy of the cerebrum and cerebellum with sparing of white matter due to neuronal degradation (Kraemer *et al.*, 2007).

1.6.3. Trichothiodystrophy (TTD)

TTD results from mutations in genes *TTDA*, *XPB* and prevailing from mutations in *XPD*. All affected genes are components of TFIIH (Botta *et al.*, 2009; Friedberg, 2006; Kleijer *et al.*, 2008; Kraemer and Ruenger, 2008). Additionally, a non-photosensitive form of TTD results from mutations in *TTDN1*, a gene of unknown function (Nakabayashi *et al.*, 2005). Photosensitivity of the skin, reflecting the NER defect, occurs in half of the TTD patients although patients do not exhibit the XP typical freckling (Itin *et al.*, 2001; Kraemer *et al.*, 2007). Characteristic for all TTD patients is the sulphur deficient, short, and brittle hair. An early diagnostic tool is the observation of alternating dark and light banding appearance (tiger tail) of the hair utilizing a polarizing microscope (Liang *et al.*, 2005; Price *et al.*, 1980). Clinical features among the patients may range from exhibiting only tiger tail hair to severe neurological and somatic developmental abnormalities such as mental retardation, microcephaly, unusual facies, ichthyotic skin, and reduced stature (Itin and Pittelkow, 1990). Thus, several acronyms are used to describe the clinical features of TTD patients. PIBIDS (Crovato *et al.*, 1983), IBIDS (Jorizzo *et al.*, 1980; Jorizzo *et al.*, 1982) and BIDS (Baden *et al.*, 1976) describe six clinical symptoms of TTD: photosensitivity, ichthyosis, brittle hair, intellectual impairment, decreased fertility, and short stature. A review from Faghri *et al.*, summarizing 112 TTD cases, described developmental delay or intellectual impairment to be found in 86 % of the patients (Faghri *et al.*, 2008). However, while TTD patients may suffer from intellectual impairment, they are usually characterized by an outgoing and friendly personality (Kraemer *et al.*, 2007). Neuro-imaging analysis of TTD patients exhibiting neurological abnormalities shows dysmyelination, cerebellar atrophy, and dilated ventricles (Faghri *et al.*, 2008).

1.6.4. Cockayne Syndrome (CS)

Cockayne Syndrome may result from mutations in the CS genes *CSA* and *CSB* as well as from mutations in the XP genes *XPB*, *XPD*, and *XPG* (Cleaver *et al.*, 2009). Similar to TTD, patients suffering from CS exhibit photosensitivity, whereas freckling within sun-exposed skin is not observed. An unusual bird-like facies with deep set eyes, prominent ears, flat cheek bones, and prominent pointy nose is characteristic for CS patients. Additional typical features are growth retardation, disturbed neurological and psychomotor development including mental retardation, loss of ability to walk, microcephaly, deafness, and progressive visual loss due to pigmentary retinal degeneration (Dollfus *et al.*, 2003; Nance and Berry, 1992). Patients often suffer from profound cachexia necessitating food intake with a gastric tube. Like TTD patients,

CS patients exhibit a social and outgoing personality. Neuro-imaging analysis shows dysmyelination comparable to TTD patients. Cerebral atrophy may also be present. Additionally, calcification of the cerebral ganglia and other areas of the brain are seen in CS patients (Kraemer *et al.*, 2007; Wang *et al.*, 2011).

1.6.5. Xeroderma pigmentosum/Trichothiodystrophy complex (XP/TTD)

XP/TTD complex is a very rare clinical entity. Taylor *et al.* investigated mutations of XP and TTD patients and described mutations shared by both phenotypes to result in null mutations. Thus, the other mutation would be predisposing for development of either XP or TTD phenotype (Taylor *et al.*, 1997). Therefore, individuals with XP/TTD are expected to be compound heterozygous for mutations predisposing to TTD and XP. Two patients with compound heterozygous *XPD* mutations exhibiting XP/TTD complex symptoms have been described. One patient, XP189MA, carried two novel mutations and the other patient, XP38BR, carried one mutation known to result in TTD (p.R112H) and a second missense mutation generally leading to a non-functional protein (p.L485P). TTD typical tiger tail hair was not observed in both patients, although chemical analysis of the hair revealed reduced sulfur content compared to healthy individuals. Both were photosensitive and exhibited dry skin as well as the XP typical freckling of the sun-exposed skin. XP38BR additionally developed a squamous cell and a basal cell carcinoma in the face at the age of 23 years. Both suffered from TTD like symptoms like short statures, microcephaly, and unusual facies. XP189MA was described to suffer from mental retardation, whereas XP38BR showed mild to moderate learning difficulties. Diagnosis of XP/CS was excluded by the lack of retinal abnormalities, deafness, ataxia, and brain calcification (Broughton *et al.*, 2001).

1.6.6. Xeroderma pigmentosum/Cockayne Syndrome complex (XP/CS)

XP/CS complex patients belong to XP complementation groups XP-G and XP-D. These patients show combined symptoms of XP and CS. They exhibit photosensitivity as well increased risk of cutaneous malignancies combined with CS symptoms such as delayed mental and physical development, short stature, bird-like facies, retinal degeneration, and progressive neurological degeneration, deafness and brain calcification (Emmert *et al.*, 2006a; Kraemer *et al.*, 2007).

1.6.7. Cerebro-Oculo-Facio-Skeletal Syndrome (COFSS)

The COFS Syndrome may arise from mutations in genes coding for *CSB* (Meira *et al.*, 2000), *XPD* (Graham, Jr. *et al.*, 2001), and *ERCC1* (Jaspers *et al.*, 2007). Patients may exhibit

photosensitivity within sun-exposed skin. Symptoms of COFSS are very similar to those of CS, although eye defects are more severe in patients having COFSS (Graham, Jr. *et al.*, 2001).

Aim of the study

Seven different clinical entities may arise from mutations in the genes with functions in the NER pathway. The different clinical entities are not restricted to mutations in different genes. Mutations affecting the same gene may result in different clinical outcome depending on the localization of the mutation and its impact on gene function.

The aim of this study was to assess the correlation of underlying molecular defects and the resulting phenotypic characteristics in the NER defective patients. Phenotype-genotype correlations build the fundament to understand the phenotypic heterogeneity among NER defective patients and might help to develop therapeutic strategies in the future as different gene functions become visible which can be further explored by molecular means. Furthermore, the expanded knowledge about the mutation-predisposed course of disease is a benefit for newly diagnosed patients.

For this purpose, a collection of 75 NER deficient primary fibroblast cell cultures, isolated from skin punch biopsies of the patients, was provided from the University Clinics of Mannheim and Göttingen. In particular the fibroblast cells from Mannheim represent Germany's largest collection of NER defective fibroblasts, which has been assembled over the last 30 years. Fibroblasts were analyzed for their specific pheno- and genotypic characteristics and the molecular results of 23 completely analyzed fibroblasts were correlated with clinical findings of the corresponding patients.

As XP-G is very rare, XPG has multiple functions, and only 20 XPG mutations have been reported world-wide. Thus, the five novel *XPG* gene mutations were comprehensively analyzed for their impact on the protein function in NER and TFIIH interaction.

2. Materials and Methods

2.1. Biological material

2.1.1. Primary cell cultures

Primary human fibroblasts cell cultures have originally been isolated from skin punch biopsies from NER deficient patients as well as healthy controls either at the Department of Dermatology in Mannheim (MA) or in Göttingen (GO). Fibroblasts are summarized in appendix table A-18.

2.1.2. Cell line

HEK293A is a cell line originated from human embryonic kidney cells. HEK293A cells were purchased from Invitrogen, Karlsruhe GER.

2.1.3. Bacteria

Escherichia coli (*E. coli*) BIOblue 10⁹, Genotype *recA1 endA1 gyrA96 thi-1 hsdR17 (r_k⁻m_k⁺) supE44 relA1 lac [F' proAB lacI^qZ Δ M15 Tn10(Tet^r)]*, from BIO LINE, Luckenwalde GER were used for the transformation and amplification of plasmid DNA.

2.2. Equipment

Table 2-1 Equipment

Equipment	Manufacturer
CO ₂ -Incubator	Sanyo, München GER
Du 640® Spectrophotometer	Beckmann, München GER
Elektrophorese chamber	Biometra, Göttingen GER
Gel documentation system	Biometra, Göttingen GER
Controller/UV-table Fluo-Link	
Hera freeze -80°C freezer	Heraus Instruments, Hanau GER
Incubator model 200	Memmert, Büchenbach GER
LAS 4000	Fujifilm, Düsseldorf GER
Lightcycler	Roche, Mannheim GER
Luminometer	Promega, Mannheim GER
Mega fuge 1,0, model G25	Thermo Fisher Scientific, Schwerte GER
Mikroskop Axiovert 100	Carl Zeiss, Oberkochen GER
Microscope Axio Imager.M1	Carl Zeiss, Oberkochen GER

Microwave	Panasonic, Hamburg GER
Mini Rocking Platform	Biometra, Göttingen GER
NANO-DROP ND-1000	Biometra, Göttingen GER
pH meter	Schütt, Göttingen GER
Pipetboy acu	Integra Biosciences, Fernwald GER
Spectral photometer Dynatech MR 5000	Dynatech, Denkendorf GER
Spectrophotometer Du® 640	Beckmann Coulter, Brea USA
3100-Avant Genetic Analyzer	Applied Biosystems, Foster City USA
Sorvall RC6+	Thermo Fisher Scientific, Schwerte GER
Power Supply Ease 500	Invitrogen, Karlsruhe GER
Laminat flow Hera Safe	Thermo Fisher Scientific, Schwerte GER
Thermo mixer 5436	Eppendorf, Hamburg GER
Thermotron incubation shaker	Infors, Bottmingen CH
T-Gradient Thermo block	Biometra, Göttingen GER
Benchtop centrifuge 5415 C	Eppendorf, Hamburg GER
UNO Thermo block	Biometra, Göttingen GER
UVC 500 Ultraviolet Crosslinker	Amersham Bioscience, Piscataway USA
Vortexer Vibrofix VF1 Electronic	IKA Labortechnik, Staufen GER
Video Monitor WV-BM 900	Panasonic, Hamburg GER
Video Graphic Printer UP-890CE	Sony, Berlin GER
Analytic balance BP2100; MC1	Sartorius, Göttingen GER
XCell II Blot Module	Invitrogen, Karlsruhe, GER

2.3. Consumable supplies

Table 2-2 Consumables

Consumables	Manufacturer
96 well Glomax™ 96 Microplate	Promega, Mannheim GER
ABI PRISM® 384-Well Clear Optical	Applied Biosystems, Foster City USA
ABI PRISM® Optical Adhesive Covers	Applied Biosystems, Foster City USA
Cell culture flasks (25 cm ³ , 75 cm ³ , 175 cm ³)	Greiner bio-one, Frickenhausen
Cell scraper 25 cm	BD Biosciences, Pharmingen, Oxford UK
Cryo box	Nunc, Wiesbaden GER

Cryo tubes (2 ml)	Greiner bio-one, Frickenhausen
Erlenmeyer flask	Schott, Mainz GER
Glass cover slips, round, 20 mm	Roth, Karlsruhe GER
Glass bottles	Schott, Mainz GER
Microscope slight, 26 x 27 mm	Roth, Karlsruhe GER
Multiply μ Strip Pro 8 tubes per chain	Sarstedt, Numbrecht-Rommelsdorf GER
Neubauer cell counting chamber	Brand, Wertheim GER
Nitrocellulose, 0.45 μ M Protran BA85	Whatman, Madstone UK
Parafilm	Brand, Wertheim GER
Pasteur-pipettes 230 mm	Brand, Wertheim GER
Pipettes 10 ml	Brand, Wertheim GER
Pipettes sterile (2.5 ml, 10 ml)	Eppendorf, Hamburg GER
Pipette tips (10 μ l, 100 μ l, 1000 μ l)	Sarstedt, Numbrecht-Rommelsdorf GER
Polystyrene tubes	BD Biosciences, Pharmingen, Oxford UK
Reaction tubes 1.5 ml and 2 ml	Eppendorf, Hamburg GER
Tissue culture 6-well-plate	Greiner bio-one, Frickenhausen GER
Tissue culture 96-well-plate	Greiner bio-one, Frickenhausen GER
Tissue culture dish 10 cm	Greiner bio-one, Frickenhausen GER
Whatman filter paper	Whatman, Maidstone UK

2.4. Chemicals

Table 2-3 Chemicals

Chemicals	Manufacturer
5x Loading Dye	Qiagen, Hilden GER
Agar Fluka	Chemie, Neu-Ulm GER
Agarose-Seakem [®]	Fluka Chemie, Neu-Ulm GER
Ammonium persulfate	Sigma-Aldrich, Taufkirchen GER
Ampicillin	Sigma-Aldrich, Taufkirchen GER
Boric acid	Merck, Darmstadt GER
Bradford Mix Roti [®]	Quant Roth, Karlsruhe GER
Bromphenolblue	Sigma-Aldrich, Taufkirchen GER
Calcium chloride	Merck, Darmstadt GER
Complete ULTRA Tablets Mini EDTA	Roche, Mannheim GER

free EASYpack	
Diethylpyrocarbonate (DEPC)	Invitrogen, Karlsruhe GER
Dimethyl sulfoxide (DMSO)	Merck, Darmstadt GER
dNTP mix (dATP, dTTP, dGTP, dCTP)	Fermentas, St. Leon-Rot GER
Double distilled water	Sartorius, Göttingen GER
Dithiothreitol (DTT)	Sigma-Aldrich, Taufkirchen GER
Ethylenediaminetetraacetic acid (EDTA)	Sigma-Aldrich, Taufkirchen GER
Ethanol 98 % (p.a.)	Merck, Darmstadt GER
Ethidium bromide (1 %)	Roth, Karlsruhe GER
GelRed	Biotium Inc., Hayward CA
Glycine	Sigma-Aldrich, Taufkirchen GER
Hydrochlorid acid (HCl) (37 %)	Merck, Darmstadt GER
Hi-Di Formamide	Applied Biosystems, Foster City USA
Isopropanol	Merck, Darmstadt GER
Isopropanol	Merck, Darmstadt GER
KH_2PO_4	Merck, Darmstadt GER
Potassium chloride (KCl)	Merck, Darmstadt GER
Lipofectamin 2000	Invitrogen, Karlsruhe GER
Magnesium chloride	Merck, Darmstadt GER
Methanol	Mallinckrodt Baker, Griesheim GER
$\text{Na}_2\text{HPO}_4 \times 2\text{H}_2\text{O}$	Merck, Darmstadt GER
Sodium chloride (NaCl)	Merck, Darmstadt GER
Sodium hydroxide (NaOH)	Merck, Darmstadt GER
Non-fat dry milk	Roth, Karlsruhe GER
Nonidet P40	Sigma-Aldrich, Taufkirchen GER
Paraformaldehyde	Merck, Darmstadt, GER
Phenylmethanesulfonylfluoride (PMSF)	Sigma-Aldrich, Taufkirchen GER
Ponceau S	Sigma-Aldrich, Taufkirchen GER
Sodium dodecyl sulfate (SDS)	Roth, Karlsruhe GER
Trifluoroacetic acid (TFA)	Sigma-Aldrich, Taufkirchen GER
3,3',5,5'-Tetramethylbenzidine (TMB)	Invitrogen, Karlsruhe GER
Tris-Base	Merck, Darmstadt GER
Trypton	Difco, Augsburg GER
Tween 20	Merck, Darmstadt GER

Vectashield Mounting Medium for Fluorescence with DAPI	Vector Laboratories, Inc., Burlingame CA
β -mercaptoethanol	Merck, Darmstad GER
Zeocin	Invitrogen, Karlsruhe GER

2.5. Buffers, solutions, and media

Commonly used Buffers, solutions, and media are listed below

Table 2-4 Buffers, solutions, and media

Cell culture	Manufacturer
DMEM	PAA, Cölbe GER
Freezing medium	40 % DMEM 40 % (v/v) FBS 20 % (v/v) DMSO
Fetal Bovine Serum (FBS)	Biochrom AG, Berlin GER
Opti-MEM	Gibco, Invitrogen, Karlsruhe GER
Penicillin-Streptomycin (100x)	PAA, Cölbe GER
Trypanblue	Sigma-Aldrich, Taufkirchen GER
Trypsin/EDTA	Biochrom AG, Berlin G
Bacterial culture	Manufacturer
LB Broth Base	Invitrogen, Karlsruhe GER
LB Agar	Invitrogen, Karlsruhe GER
Ampicillin stock solution	100 mg/ml Ampicillin in <i>aqua bidest</i> Working concentration 100 μ g/ml
Zeocin stock solution	25 mg/ml Zeocin in <i>aqua bidest</i> Working concentration 25 μ g/ml

Protein biochemistry	
Buffer /Solution	Recipe
Blotto-PBS	1x PBS 0.05 % (v/v) Tween-20 5 % (w/v) Non-Fat Dry Milk
9 % Laemmli buffer, pH 7.4	30 mM Tris 9 % SDS (w/v) 15 % Glycine (w/v) 0.04 % Bromphenol blue 10 % β -Mercaptoethanol
Immunoblot transfer buffer, pH 8.3	0.192 M Glycin 0.025 M Tris-Base 20 % MeOH (v/v)
IP lysis buffer	20 mM Tris-HCl, pH 7.3 at 4°C 150 mM NaCl 1 mM EDTA 1 mM PMSF 1 Complete ULTRA Tablets Mini EDTA free (protease inhibitor) per 10ml
Ponceau S-solution	0.2 % (v/v) Ponceau S 3 % (v/v) TFA
3.7 % Paraformaldehyde (PFA)	1.85 g PFA 2.5 ml <i>aqua bidest</i> 5 drops 1 M NaOH →incubate stirring at 80°C until PFA is dissolved →add 50 ml with 1x PBS
SDS PAGE running buffer, pH 8.3	0.192 M Glycin 0.025 M Tris-Base 0.1 % SDS

Additional commonly used buffers and solutions

Buffer/ Solution	Recipe
10x PBS, pH 7.2	1.5 M NaCl 30 mM KCl 80 mM Na ₂ HPO ₄ x 2H ₂ O 10 mM KH ₂ PO ₄
DNA loading buffer	0.5 M EDTA 50 % (v/v) Glycerol 0.01 % (w/v) Bromphenol blue
10x TBE, pH 8.3	0.9 M Tris 0.89 M boric acid 25 mM EDTA
10x TBS, pH 7.4	0.25 M Tris 1.37 M NaCl 50 mM KaCl 6 mM Na ₂ HPO ₄
TE buffer	10 mM Tris-HCl, pH 7.5 1 mM EDTA

2.6. Ready to use reaction systems

The following ready to use reaction systems were utilized in this thesis.

Table 2-5 Reaction systems

Reaction systems	Manufacturer
Attractene Transfection Reagent	Qiagen, Hilden GER
BigDye Terminator v3.1 Cycle Sequencing Kit	Applied Biosystems, Foster City USA
Lipofectamine® 2000 Transfection Reagent	Invitrogen, Karlsruhe GER
NucleoBond® Xtra MiDi/Maxi	Machery-Nagel, Düren GER
NucleoSpin® Extract II	Machery-Nagel, Düren GER
NucleoSpin® Plasmid	Machery-Nagel, Düren GER
QIAamp® DNA Blood Kit	Qiagen, Hilden GER
QuantiTect® SYBR green PCR Kit	Applied Biosystems, Foster City USA
RevertAid H Minus First strand cDNA	MBI Fermentas, St. Leon-Rot GER

synthesis Kit

RNase free DNase Set	Qiagen, Hilden, GER
RNeasy Mini Kit	Quiagen, Hilden GER
Roti®-Quant Protein quantification assay	Roth, Karlsruhe GER
According to Bradford	
USB® Exo-SAP IT® PCR Prdukt Cleanup	USB Products, Cleveland USA
WesternBreeze Chemoluminescent Immunodetection Systems (anti mouse and anti rabbit)	Applied Biosystems, Foster City USA

2.7. Antibodies and immunoreagents

Antibodies and immunoreagents utilized in this thesis are listed below. Name, application and dilution as well as manufacturer are depicted in the table.

Table 2-6 Antibodies and immunoreagents

Name	Application/ dilution	Manufacturer
α XPA (FL-273)	Immunofluorescence/1:50 in 1x PBS containing 20 % FBS (v/v)	Santa Cruz Biotechnology, Santa Cruz USA
α XPB (S-19)	Immunofluorescence/1:50 in 1x PBS containing 20 % FBS (v/v)	Santa Cruz Biotechnology, Santa Cruz USA
α XPC (H-300)	Immunofluorescence/1:50 in 1x PBS containing 20 % FBS (v/v)	Santa Cruz Biotechnology, Santa Cruz USA
α XPD (XXX)	Immunofluorescence/1:50 in 1x PBS containing 20 % FBS (v/v)	Santa Cruz Biotechnology, Santa Cruz USA
α ERCC1 (FL-297)	Immunofluorescence/1:50 in 1x PBS containing 20 % FBS (v/v)	Santa Cruz Biotechnology, Santa Cruz USA
α XPG (8H7)	Immunofluorescence/1:50 in 1x PBS containing 20 % FBS (v/v)	Santa Cruz Biotechnology, Santa Cruz USA

α cdk7 (MO1)	Western Blot/ 1:1000 in Blotto PBS	Cell Signaling, Danvers USA
α myc (9B11)	Western Blot/ 1:1000 in Blotto PBS Immunoprecipitation/ 1:1000 in IP lysis buffer	Cell Signaling, Danvers USA
α CPD	Immunofluorescence 1:1000 in 1x PBS containing 20% FBS (v/v)	a gift from Toshio Mori JP
α 6,4PP	Immunofluorescence 1:500 in 1x PBS containing 20 % FBS (v/v)	a gift from Toshio Mori JP
α mouseDylight594	Immunofluorescence 1:500 in 1x PBS containing 20 % FBS (v/v)	Dianova, Hamburg GER
α rabbitDylight488	Immunofluorescence 1:500 in 1x PBS containing 20 % FBS (v/v)	Dianova, Hamburg GER
α mouse IgG	Immunoprecipitation control 1:500 in IP lysis buffer	DAKO, Glostrup, DEN
Protein A Agarose	Immunoprecipitation	Santa Cruz Biotechnology, Santa Cruz USA
Protein G+ Agarose	Immunoprecipitation	Santa Cruz Biotechnology, Santa Cruz USA

2.8. Enzymes

The following enzymes were utilized in this thesis.

Table 2-7 Enzymes

Enzyme	Manufacturer
NotI 10 u/μl	New England Biolabs, Frankfurt, GER
KpnI 10 u/μl	New England Biolabs, Frankfurt, GER
DpnI 10 u/μl	Fermentas, St. Leon-Roth, GER
T4 DNA Ligase 1u/μl	Fermentas, St. Leon-Roth, GER
Rnase T1 1000 u/μl	Fermentas, St. Leon-Roth, GER
Taq DNA Polymerase 5 u/μl	Fermentas, St. Leon-Roth, GER
Pfu DNA Polymerase 2.5 u/μl	Fermentas, St. Leon-Roth, GER

2.9. Marker

The following DNA- and protein standards were used for the fragment length control of DNA- and protein molecules, respectively.

Table 2-8 DNA- and protein standards

Standard	Manufacturer
Gene Ruler™ 100 bp DNA Ladder Plus	Fermentas, St. Leon-Roth, GER
Gene Ruler™ 1 kb DNA Ladder	Fermentas, St. Leon-Roth, GER
Spectra™ Multicolor High Range Protein Ladder SM#1851	Fermentas, St. Leon-Roth, GER
Page Ruler™ Prestained Protein Ladder #26616	Thermo Fisher Scientific, Scherte GER

2.10. Oligonucleotides

Oligonucleotides separated for their application are listed in table 2-9.

Table 2-9 Oligonucleotides

Oligonucleotides for cloning		
Name	Sequence 5' → 3'	Restriction site
XPGmycHis_for	AAT <u>GCGGCCG</u> CTTAGAGTAGAAGTTGTCTG	NotI
XPGmycHis_rev	ATT <u>GGTACCG</u> TTTTCTTTTTCTTCC	KpnI
XPGQ150mycHis_rev	ATT <u>GGTACCT</u> TGTAAAGGAGGCAAAC	KpnI
XPGE727mycHis_rev	ATT <u>GGTACCT</u> TTCATGGAGCGAATCTTCCGC	KpnI
Oligonucleotides for site directed mutagenesis		
Name	Sequence 5' → 3'	
Q150Xfor	GCCTCCTTTA <u>TAA</u> GAGGAAGAAAAACAC	
Q150Xrev	CTTCCTCTTA <u>TAA</u> AGGAGGCAAACATAG	
E727Xfor	CGCTCCATTA <u>TAA</u> TGGCAAGATATTAATTTG	
E727Xrev	TATCTTGCCATTA <u>TAA</u> TGGAGCGAATCTTCC	
G805Rfor	CAGACTTCCAGA <u>ACC</u> ATCACTGATGACAG	
G805Rrev	GTGATGGTTCT <u>GGA</u> AGTCTGATCAGTCAG	
L778Pfor	ACTCCTGCGCC <u>CG</u> TTCGGCATTCCCTAC	
L778Pprev	GAATGCCGAAC <u>G</u> GGCGCAGGAGTTCCTGG	
W814Sfor	ACAGTGATATCT <u>CG</u> CTGTTTGGAGCGCG	
W114Srev	CCAAACAGC <u>G</u> AGATATCACTGTCATCAG	
Oligonucleotides for amplification/sequencing of genomic DNA		
Name	Sequence 5' → 3'	
XPC ex1f	GGAGGATACAATACACCGGAAATAGAGAGAAAC	
XPC ex1r	ACAACGGGAGCGGGAAAAAAG	
XPC ex2f	GGAGACAGGTCGTAGAGCCG	
XPC ex2r	GGACCCAGTGACAAGTAAG	
IXPCex3f	TGGAGGAAGTGAGGCTCAGA	

IXPCex3r	TGCAATTAGTGATCTGACTCCAA
XPC ex4f	TTCCTCCTTCCCAGCAGAAC
XPC ex4r	CGACCACTTTGATACTCAGTCC
XPCex5.1f	TGTAGGGAAACAGGGAGAG
XPC ex5.1r	CAGCAAAGCCAGAAATAAAG
XPC ex5.2f	CTTTGGCAGCAAAAATTCC
XPC ex5.2r	CCAGCCTCTGAGAGAAACAC
XPC ex6f	TCTCACGATTCACTCCCTC
XPC ex6r	GGCTTCAGCAGCTATCAAC
I XPC ex7f	CTGGAGTTTCCGTCGCCTAC
I XPC ex7r	CAATTCCTGTCAATTGCTCCTC
IXPC ex8af	ACTGTCTGAGCTGGGGACAT
IXPC ex8ar	TTCCTCCTGCTCACAGAACA
Seq.8a rev	GTTGCCTTCTCCTGCTTCTC
XPC ex8bf	CTCCAAAGCAGAGGAAAG
XPC ex8br	CCCATTA AAAACACCCAAC
XPC ex19f	CAGATGCGATGTTACAAAACCA
XPC ex19r	GAATGCTGTCCAGTCAGATGAG
XPC ex10f	TTGCCTAGCACAGCTTCTC
XPC ex10r	TCCAACCTGTAGAACCTTTG
XPC ex11f	TGGATGCCTTTGTTGTAAAC
XPC ex11r	GAGCAAGTCAGCATTGG
XPC ex12f	TAAGGGCAGCATCAGAAGGG
XPC ex12r	CAGCTTCCATCCCCATCTC
XPC ex13f	GCCCACTGTTTTCCACAACTG
XPC ex13r	AGTGTTGCTTCCCGCTTCTG
XPC ex14f	TGGAAGTGAGACTTGGTG
XPC ex14r	ATCCCTGACTTGAGGATG
XPC ex15f	TGGGAACTTGCTGCCTCTTC
XPC ex15r	ACTGGTGGGTGCCCTCTA
XPD ex1for	GAGCCCTCGAGGATGTCCA
XPD ex2rev	CGTCCTGCAATCTGTCTTAGGC
XPD ex3for	GTTTGTGTGCCCAAGGTTCT
XPD ex5rev	ATCCAGGACTTGTGGTTGGA

XPD Seq 3-5for	GTTCCCTAGGCCCTATTGGT
XPD Seq 3-5rev	GGAGCTTGTGCTCATTGGAG
XPD ex6for	GAAGAGTGGTTGGGTTTTCCA
XPD ex7rev	ACCAACAGGGAGATGCAGAC
XPD ex8for	GTGCCCGTATCTGTTGGTCT
XPD ex9rev	CTGGGGACAAGTCAGACAGG
XPD ex10for	CTGGAGACCCTGCAGAAGAC
XPD ex11rev	GAGGACACGGCTCTGCATAA
XPD I ex12for	GACTCTGGAGTGTCTGATTATTGCTC
XPD I ex12rev	ATCTGAGCACAAAGGCTTACTCAAG
XPD ex13for	GGGTAATCTCACCCCTCCTT
XPD ex15rev	TAAAGCTCTCCTGCCTGAGC
XPD ex16for	GCTTAGAACAGCACCAGCAG
XPD ex16rev	TGATACACCTCCCCTCTTGG
XPD ex17for	AGAGAAGGGAGGAGGACCTG
XPD ex17rev	ATGCTGCACACACTCTCCTG
XPD ex18for	CCCAGAGACATGGTGATGTG
XPD ex19rev	GAGCTCTGGGAAGACACCTG
XPD ex20for	CCAACTCAGACACAGCATCC
XPD ex21rev	CAGGGACAGAAGGTCATTCCG
XPD ex22for	AGGCTGTTTCCCGTTCATTT
XPD ex22rev	AGGGGACTTTCTGGAGGAGA
XPD ex23for	CTTCATAAGACCTTCTAGCACCA
XPD ex23rev	CGCTCTGGATTATACGGACA
XPG 5'UTR fwd	GCCATTCTCTGGACCTGTCTT
XPG Intron 1 rev	CCGAGGGACGACTGTACTIONTAGA
XPG Intron 1 fwd	GGAAATTGAAGTTGTGAGGATG
XPG Intron 2 rev	TCATTGTACCCATGATGAACTCTC
XPG Intron 2 fwd	TGGCAATTAGGAGGAAATGC
XPG Intron 3 rev	AGGGAAAGAGAATCGCAGGA
I,XPG Intron 3 fwd	CGTGTTGCGTCATGTACACTTT
I,XPG Intron 4 rev	AGCCCTGGCAGAAGTTCTTTAG
XPG Intron 4 fwd	AACGAGCAGAGCCTTGCATA
XPG Intron 5 rev	CAACCAAAAAGCCATCTGTC

XPG Intron 5 fwd	GCCTACTCACTTTGTTGCCTGT
XPG Intron 6 rev	CCTAGTCTCGGGTCAAAAGTCA
XPG Intron 6 fwd	GGGAAAGGGTGGAAATATGG
XPG Intron 7 rev	TCATTTAATCGGCAACTAGGAG
XPG Intron 7 fwd	GAACCAGTGTTCTCTTATCCATCTT
XPG Intron 8 rev	AGCTGTGACTCCCTGGGAAA
XPG Intron 8 fwd	GCATTTTTCAGGTTCCCTCCAG
XPG Intron 9 rev	GCCATCAGCAACCACAAGAT
XPG Intron 9 fwd	CAGAGTCTTGGTTAGACATCCAGTG
XPG Intron 11 rev	CCTGCAATTTCCATCAATGC
I,XPG Intron 11 fwd	GTGGTTCAGAGAGACTCAGGCTA
I,XPG Intron 12 rev	CCAGCACCACTAAGAAGTACTGACTC
XPG Intron 12 fwd	AGTGCCAAGCACAGAGGAAG
XPG Intron 13 rev	GTGAAAAGGAGAGCGGGATA
I,XPG Intron 13 fwd	GAACATAGTGCCAGATGATTATGC
I,XPG Intron 14 rev	ACTCAAAGTTCAGCCCTAAGAG
XPG Intron 14 fwd	GGGAGAGAACTGGGTTTTGG
XPG 3' UTR rev	TGACCGTGCCACCAGTTAAT

Oligonucleotides for amplification/sequencing of cDNA

Name	Sequence 3'→5'
XPG g285rev	CCCCATCAAACACAAAAATAGG
XPG g870rev	AATAATGTTCTTGTCCTTGG
XPG t10 for	ACCTCTATGTTTTGCCTCCTT
XPG 594r4 for	TGCTGCTGTAGACGAAGGC
XPG 593R86 rev	GCTCACCATCCACGTCGTCCC
XPG 2472-2492for	CGGATCGCTGCTACTGTCACC
XPG xp5 100 for	TAAGACCTAATCCTCATGACA
XPD d11	CTCAGGTCTGCAATCTTGG
XPD d12	ACCAGGTCTGCAATCTTGG
seq.XPD ex1for	GAGCCCTCGAGGATGTCCA
seq. XPD d12r	CTTGGGGTCCAGGAGGTAGT
XPD d21	GCCAATGTGGTGGTTTATAGCT
XPD d22	TGATGACAGACTGGAAACGC

XPD d31	ATCGAGCCCTTTGACG
XPD d32	TCTCACGAATCTGGAAGTGG
seq. XPD d32r	GAACTGGTCCCGCAGGTAT
XPD d41	AAAGTGTCCGAGGGAATCG
XPD d42	AAGACCTTCTAGCACCACCG
seq. XPD d41f	GCGTCCCCTACGTCTACACA
seq. XPD d42r	GGCAAGACTCAGGAGTCACC

Oligonucleotides for quantitative Real Time PCR purchased from Qiagen, Hilden GER

Gene	Order number
<i>XPA</i>	QT00029519
<i>XPB</i>	QT00080276
<i>XPC</i>	QT00080381
<i>XPD</i>	QT00086758
<i>DDB2 (XPE)</i>	QT00062986
<i>XPF</i>	QT00063091
<i>XPG</i>	QT00029246
<i>GAPDH</i>	QT00079247
<i>β-actin</i>	QT00095431

2.11. Plasmids

Commercially available plasmids, plasmids containing a certain cDNA generated during this thesis, and plasmids provided from other researcher are listed and described concerning their source and purposes below. Plasmids containing cDNA sequences generated during the thesis were always controlled by DNA sequencing for proper nucleotide sequences (see 2.14.2.7.).

pcDNA3.1/myc-His(-)A was purchased from Invitrogen, Karlsruhe GER. The 5.5 kB vector has a human cytomegalovirus immediate-early (CMV) promoter and is used for high level expression of recombinant proteins in eukaryotic cells (Boshart *et al.*, 1985; Nelson *et al.*, 1990). The vector has a Neomycin resistance gene allowing for selection of stable transfections in mammalian cells (Heffron *et al.*, 1975; Southern and Berg, 1982) and an ampicillin resistance gene (β -lactamase) for selection of transformation-positive bacterial cells when the vector is cloned *E.coli*. The coding sequence of a myc- and a His-tag (eleven amino acids myc epitope, six amino acids His epitope (6 x His) bridged by five amino acids) is located downstream of the

multiple cloning site (mcs). Thus, cDNA cloning in the mcs, within the reading frame, results in the expression of recombinant proteins with a C-terminal mycHis-tag after transfection into eukaryotic cells. The myc-tag enables immunoprecipitation and/or detection of the recombinant protein via Western Blot using α myc antibody. The His-tag enables purification of the recombinant protein on metal-chelating resin, but also immunoprecipitation and/or detection of the recombinant protein via Western Blot using α His antibody.

pXPGmycHis: XPG wild type protein was cloned into the pcDNA3.1/myc-His(-)A expression vector utilizing oligonucleotides XPGmycHis_for and XPGmycHis_rev for amplification of XPG cDNA from pXPG. Enzymes NotI (5') and KpnI (3') were used for restriction of insert and vector.

pXPG_{Q150}mycHis: XPG amino acids 1-150 were cloned from pXPG into the pcDNA3.1/myc-His(-)A expression vector utilizing oligonucleotides XPGmycHis_for and XPGQ150mycHis_rev for amplification. Enzymes NotI (5') and KpnI (3') were used for restriction of insert and vector.

pXPG_{E727}mycHis: XPG amino acids 1-727 were cloned from pXPG into the pcDNA3.1/myc-His(-)A expression vector utilizing oligonucleotides XPGmycHis_for and XPG_{E727}mycHis_rev for amplification. Enzymes NotI (5') and KpnI (3') were used for restriction of insert and vector.

pXPG_{L778P}mycHis: XPG with amino acid change p.L778P was generated subjecting pXPGmycHis to site directed mutagenesis using primer L228Pfor and L778Pprev.

pmycHis_XPG_{G805R}: XPG with amino acid change p.G805R was generated subjecting pXPGmycHis to site directed mutagenesis using primer G805Rfor and G805Rrev.

pXPG_{W814S}mycHis: XPG with amino acid change p.W814S was generated subjecting pXPGmycHis to site directed mutagenesis using primer W814Sfor and W814Srev.

pXPG_{Q150X}: XPG protein, containing amino acids 1-150, was generated subjecting pXPG to site directed mutagenesis using primer Q150Xfor and Q150Xrev.

pXPG_{E727X}: XPG protein, containing amino acids 1-727, was generated subjecting pXPG to site directed mutagenesis using primer E727Xfor and E727Xrev.

pXPG_{G805R}: XPG protein containing amino acid exchange p.G805R was generated subjecting pXPG to site directed mutagenesis using primer G805Rfor and G805Rrev.

pXPG_{L778P}: XPG protein containing amino acid exchange L778P pXPG was generated subjecting pXPG to site directed mutagenesis using primer L778Pfor and L778Pprev.

pXPG_{W814S}: XPG protein containing amino acid exchange W814S was generated subjecting pXPG to site directed mutagenesis using primer W814Sfor and W814Srev.

pXPA, pXPB, pXPC, pXPD, pXPE, pXPF, pXPG were all provided from Dr. K.H. Kreamer MD, NCI, NIH Bethesda, USA. The vectors were used for the expression *XPA, XPB, XPC, XPD, XPF*, and *XPG* cDNA in eukaryotic cells, respectively. All vectors, except pXPE, have an ampicillin resistance gene. XPE contains a zeocin resistance gene. Resistance genes are used for selectivity purposes when the vectors are cloned in *E.coli*.

pcmvLUC was provided from M. Hedayati und L. Grossman, Johns Hopkins University, Baltimore, MD, USA. The vector was used for the expression of firefly luciferase in eukaryotic cells. The non-replicative vector has an ampicillin resistance gene used for selectivity purposes when it is cloned in *E.coli*.

pRL-CMV (catalog no. E2261) was purchased from Promega, Mannheim, GER. The 4079bp vector encodes the renilla luciferase and exhibits a cytomegalovirus immediate-early (CMV) promoter. It was used for constitutive expression of renilla luciferase in eukaryotic cells. The non-replicative vector has an ampicillin resistance gene for selectivity purposes when the vector is cloned in *E.coli*.

2.12. Cell culture techniques

2.12.1. Culture of primary human fibroblasts and HEK293A cells

All cells were cultivated in 175 cm² culture flasks with 30 ml DMEM culture media supplemented with 10 % FCS (v/v) and 1 % P/S (v/v) in a humidified atmosphere at 37 °C and 5 % CO₂. The adherent cells were passaged when they were grown to confluency. HEK293A were passaged 1:10 and primary fibroblasts 1:2.

For passaging, cells were rinsed with 10 ml PBS and dissociated from the culture flask by incubation with 5 ml trypsin. HEK293A cells were trypsinized at room temperature, whereas

fibroblasts were incubated for 5 min at 37 °C. Trypsinization was stopped by adding 8 ml culture medium to the cells. The cell suspension was centrifuged at 188 x g for 10 min. Cells were resuspended in an appropriate volume of culture media. One-tenth of the HEK293A cell suspension and one-third to one-half of the fibroblast cell suspension was transferred back into the culture flask.

If cells had to be seeded in a specific density for further experimental procedures, 10 µl cell suspension was mixed with 90 µl trypan blue and cells were counted in a Neubauer chamber. To cultivate cells from a frozen aliquot, cells were thawed and washed with 10 ml culture medium (centrifugation 188 x g, 5 min at room temperature). The resulting cell pellet was resuspended in 10 ml medium, transferred into a culture flask and incubated at 37 °C, 5 % CO₂. To freeze cells, approximately 5x10⁶ HEK293A cells or 1x10⁶ primary human fibroblasts were sedimented as described above resuspended in 500 µl culture media and transferred into pre-cooled cryo tubes containing 500 µl freezing medium. Cells were frozen at -80 °C in cryo boxes containing isopropanol to obtain a constant cooling of approximately 1 °C/min before they were stored in liquid nitrogen at -196 °C.

2.12.2. Transient transfection of primary human fibroblasts

Primary human fibroblast cells were transfected with Lipofectamine 2000 transfection reagent. The reagent contains cationic lipids that accumulate with the negatively charged DNA and the resulting precipitates are absorbed by the cells via endocytosis.

Cells were seeded in 6-well-plates with a density of 1.3x10⁵ cells per well. Next day, the culture medium was changed to 2 ml Opti-MEM and cells were further incubated, while the transfection mix was prepared. Preparation of the DNA-Lipofectamine-mix was performed in polystyrene tubes. For the exact amounts of plasmid DNA, please refer to values in table 2-10. For transfection of one well, the appropriate amount of plasmid was diluted in 97.5 µl Opti-MEM (plasmid-mix). In a second tube, 2.5 µl Lipofectamine 2000 and 97.5 µl Opti-MEM (Lipofectamine-mix) were pre-incubated for 5 min at room temperature before the Lipofectamine-mix was added to the plasmid-mix. The plasmid-Lipofectamine-mix was incubated for 45 min at room temperature. Afterwards, 800 µl Opti-MEM were added and the tube was inverted for five times. The 2 ml Opti-MEM were changed by the transfection mixture and the cells were further incubated for 4 h until the transfection mixture was changed to normal culture medium.

Table 2-10 Amount of plasmid DNA used for transfection with Lipofectamine 2000

Firefly luciferase plasmid	Renilla Luciferase plasmid	pXPA to pXPG
150 ng (50 ng/ μ l)	250 ng (50 ng/ μ l)	250 ng (50 ng/ μ l)

2.12.3. Transient transfection of HEK293A cells

HEK293A cells were transfected with Attractene Transfection Reagent, a non-liposomal transfection reagent, which forms a complex with the DNA resulting in micelles that are absorbed by the cells via endocytosis.

Cells were seeded in 10 cm dishes in a density of 1.2×10^6 cells per dish. Next day, cells were transfected according to manufacturer's instructions: 300 μ l medium without supplements were mixed with 5 μ g plasmid DNA (1 μ g/ μ l) and 15 μ l Attractene Transfection Reagent. The plasmid-Attractene-mix was incubated at room temperature for 15 min. During this time the medium of the cells was changed to 10 ml fresh culture medium. The plasmid-Attractene-mix was added to the cells and the cells were further incubated for 6 h until the transfection mixture was changed to normal culture medium.

2.12.4. Functional Assays

2.12.4.1. Determination of post-UV cell survival

To test the cells for their sensitivity against UV irradiation, the cell proliferation after UV treatment was determined using the CellTiter96[®] Non-Radioactive Cell Proliferation Assay. The test is based on the determination of the activity of a mitochondrial dehydrogenase which can metabolize 3-(4,5-Dimethylthiazol-2-yl)-2,5-diphenyl-tetrazoliumbromid (MTT) to its blue coloured formazan salt. Primary fibroblasts were seeded in two different densities (7500 and 5000 cells per well in 100 μ l culture media) in 96-well-plates. Next day cells were washed twice with 1x PBS, the 1x PBS was removed and the cells were irradiated with an ultraviolet crosslinker with 254 nm UV light bulbs in increasing doses from 6 J/m² to 30 J/m². Afterwards, fresh culture medium was added to the cells and they were further incubated at 37 °C and 5% CO₂. After at least two days or until the cells in the unirradiated control well were 90 % confluent, 15 μ l Dye-Solution was given to each well and the plate was further incubated for 4 h at 37 °C. The reduction of MTT to its blue coloured salt was stopped by adding 100 μ l Stop-Solution to each well. Afterwards, the plate was incubated over night at room temperature and protected from light to achieve complete cell lysis. The amount of formazan correlating with cells' viability was measured with a Dynatech MR 500 photometer at 550 nm. The software BioLynx 2.0. was used for quantitative analysis. The mean absorption value (n=4) of

the unirradiated cells was set to 100 % survival to calculate the relative post-UV survival of the irradiated cells.

2.12.4.2. Determination of NER capability with Host Cell Reactivation Assay (HCR)

The relative NER capability and the complementation group (XP-A to XP-G) of primary fibroblast cells was determined by host cell reactivation assay (HCR). The HCR assay has the following principle: a non-replicating reporter gene plasmid is irradiated with 250 J/m² UVC irradiation generating DNA photoproducts pyrimidine-6,4-pyrimidones (6,4PPs) and cyclobutane-pyrimidine-dimer (CPDs). Transfection of an irradiated plasmid into a host cell will only result in enzyme expression if the cell reactivates the plasmid by removing all photoproducts from the transcribed strand of the reporter gene. Therefore, activity of the enzyme expressed from the irradiated plasmid correlates with NER capability and is simplified termed as relative NER capability.

Fibroblast cells were transfected with either non-irradiated or irradiated pcmvLUC reporter gene plasmid coding for firefly luciferase together with unirradiated pRL-CMV reporter gene plasmid coding for renilla luciferase for normalization. The enzyme expression was determined after 72 h with a Promega's Dual-Luciferase Reporter Assay System. Therefore, cells were washed with 1x PBS and lysed with 200 µl lysis buffer for 45 min at room temperature. Cell lysates were transferred into eppendorf tubes and centrifuged for 10 min at 1300 x g. 20 µl of the supernatant containing the proteolytic fraction was transferred into a 96 well Glomax™ 96 Microplate. The enzyme activities were measured as relative light units (RLUs) with a Glomax™ 96 Microplate Luminometer by adding the specific substrate solutions beetle luciferine (for firefly luciferase) and coelenterazine (for renilla luciferase) to the supernatant. Firefly luciferase RLUs were divided through corresponding renilla luciferase RLUs. Relative luciferase activity (or relative NER capability) is expressed as percentage activity obtained from UVC treated plasmids divided through corresponding untreated control plasmids.

For determination of the complementation group, the fibroblasts were simultaneously co-transfected with pcmvLUC, pRL-CMV, and 250 ng of a wild type XP cDNA containing plasmid (pXPA, pXPB, pXPC, pXPD, pXPE, pXPF, pXPG). At least triplicate experiments were performed.

2.13. Microbiology

2.13.1. Preparation of chemical competent *E.coli XL1blue*

Competent cells have the ability to take up extracellular foreign DNA. This process occurs naturally in many bacteria (natural competence) and can also be induced artificial. Chemical competent cells are treated with calcium ions which facilitate the attachment of the DNA to the competent cell membrane.

10 ml LB medium without antibiotics was inoculated with *E.coli BIOblue* and incubated shaking at 37 °C for 16 h. 190 ml LB medium without antibiotics was inoculated with 10 ml from the overnight culture and were further incubated shaking at 37 °C until OD₆₀₀ was 0.5. Cells were centrifuged (188 x g, 10 min, 4 °C) and the pellet was resuspended in 25 ml ice-cold 100 mM MgCl₂ solution. Cells were incubated on ice for 5 min before they were centrifuged (188 x g, 10 min, 4 °C) again. Next, cells were resuspended in 5 ml ice-cold 100 mM CaCl₂ solution and incubated on ice for 20 min before they were centrifuged again (188 x g, 10 min, 4 °C). The pellet was resuspended in 1 ml 100 Mm CaCl₂ solution containing 15 % Glycerol (v/v), aliquoted in 50 µl portions, and frozen in liquid nitrogen. Afterwards, the competent bacteria were stored at -80 °C until further use.

2.13.2. Transformation of *E.coli*

Competent *E.coli BIOblue* were thawed on ice before 100 ng plasmid DNA was mixed with 50 µl competent cells. The suspension was incubated on ice for 30 min until cells underwent a heat shock for 1 min at 42 °C. Afterwards, the bacteria were incubated on ice for 2 min before 200 µl LB medium without antibiotics was added to the cells. Cells were incubated shaking for 1 h. To select for positively transformed cells, 100 µl bacteria suspension was plated on LB agar plates containing 100 µg/ml of specific antibiotic (corresponding to the selection marker of the plasmid) and plates were incubated at 37 °C for 16 h.

2.14. Molecular biology

2.14.1. Preparation of nucleic acids

2.14.1.1. Isolation of genomic DNA

Genomic DNA was isolated from fibroblast cell pellets with QIAamp DNA Blood Kit according to manufactures instructions. The DNA concentration was measured photometrically at 260 nm (see 2.14.1.7.).

2.14.1.2. Ultra fast alkaline lysis plasmid extraction and analysis

This DNA extraction method (Cormack and Somssich, 1997) was used for simultaneous analysis of several bacterial colonies. Single *E.coli* colonies were screened for containing a plasmid with previously inserted cDNA after transformation.

Two ml LB medium containing 100 µg/ml of specific antibiotic (corresponding to the selection marker of the plasmid) were inoculated with bacteria from a single colony and the bacterial culture was incubated shaking at 37 °C for 16 h. Next day, 300 µl of the bacterial suspension were mixed with 300 µl lysis buffer (0.2 N NaOH, 1 % SDS) and incubated for 5 min at room temperature. 300µl neutralization buffer (3 M potassium-acetate, pH 5.5) were added and the suspension was further incubated for 5 min at room temperature before the sample was centrifuged (16000 x g, 10 min, room temperature) to remove cell debris and chromosomal DNA. 800 µl of the resulting supernatant were mixed with 600 µl isopropanol to achieve precipitation of the DNA. Precipitated DNA was pelleted by centrifugation (16000 x g, 15 min, room temperature), the pellet was washed with 250 µl 70 % EtOH and centrifuged (16000 x g, 15 min, room temperature) again. DNA was dried at room temperature and re-dissolved in TE buffer with a final volume of 15 µl containing two appropriate restriction enzymes à 0.3 µl (10 u/µl), one tenth (v/v) of the corresponding 10x buffer, one tenth (v/v) 10x BSA (depending on the requirements of the enzyme) and 0.3 µl RNase T1 (1000 u/µl). The sample was incubated for 1 h at 37 °C. The selected enzymes allow for a restriction digest that gives information about the insertion of the cDNA into the plasmid when the resulting DNA fragments are separated by agarose gel electrophoresis (see 2.14.1.4.).

2.14.1.3. Isolation of plasmid DNA

For preparation of small amounts of plasmid DNA (~40 µg) 5 ml LB medium containing 100 µg/ml of specific antibiotic (corresponding to the selection marker of the plasmid) were inoculated with bacteria from a single colony. The bacterial culture was incubated shaking at 37 °C for 16 h. Isolation of plasmid DNA was performed with the NucleoSpin® Plasmid from

Machery and Nagel according to manufacturer's instructions. The DNA concentration was measured photometrically at 260 nm (see 2.14.1.7.).

The NucleoBond® Xtra MiDi/Maxi from Machery and Nagel was applied for isolation of greater amounts of plasmid DNA (~250 µg). Therefore, 100 ml LB medium containing 100 µg/ml of specific antibiotic (corresponding to the selection marker of the plasmid) were inoculated with bacteria from a single colony and the bacterial culture was incubated shaking at 37 °C for 16 h. Isolation of plasmid DNA was performed according to manufacturer's instructions. The DNA concentration was measured photometrically at 260 nm (see 2.14.1.7.).

2.14.1.4. Agarose gel electrophoresis (AGE)

DNA fragments, generated by PCR or by restriction digestion of plasmids, were subjected to agarose gel electrophoresis for analysis or preparative purpose. The negatively charged DNA fragments move towards the anode in an electric field. DNA fragments exhibit different mobility due to the DNA fragment size and the pore size of the agarose gel: smaller fragments move faster than bigger ones. Therefore, DNA fragments are separated by size and can be visualized using fluorescence dyes (GelRed, ethidium bromide) which intercalate into DNA and fluoresce under UV light.

Depending on the fragment size, agarose gels were generated by diluting a suitable amount of agarose powder, 0.8 % to 1.5 % (w/v), in 1x TBE buffer and dissolving it by boiling. 1x TBE buffer was also used as running buffer during electrophoresis with a current of 100 V. Samples were mixed with 5x LDS before they were loaded on the gel together with an appropriate molecular weight size standard (see table 2-8). Visualization of the DNA fragments was performed using the gel documentation system from Biometra and either GelRed (added directly when the gel is generated) or ethidium bromide (incubation of the gel in an ethidium bromide containing *aqua bidest* bath).

2.14.1.5. Isolation of DNA from an agarose gel

Isolation of specific DNA fragments from agarose gels was performed with the NucleoSpin® Extract II Kit from Machery and Nagel. Therefore, DNA fragments were separated by agarose gel electrophoresis (see 2.14.1.4.). The DNA fragment of interest was excised and purified with the NucleoSpin® Extract II from Machery-Nagel according to manufacturer's instructions.

2.14.1.6. Isolation of total RNA

Total RNA was isolated from fibroblast cell pellets using the Rneasy Mini Kit and the DNase-free-set from Qiagen, according to manufacturer's instructions. The RNA concentration was measured photometrically at 260 nm (see 2.14.1.7.).

2.14.1.7. Quantification of DNA and RNA

The DNA concentrations were determined photometrically at 260 nm. Either 1 µl of the undiluted sample or 100 µl of diluted sample (1:100 with *aqua bidest*) were used for determination using a NANO-DROP ND-1000 or the Beckmann Du® 640 spectrophotometer, respectively. RNA concentration was measured similarly in a 1:50 dilution with *aqua bidest* with the Beckmann Du® 640 spectrophotometer.

To calculate the concentration of the sample from the absorption value following formula was applied:

$$\text{Concentration } (\mu\text{g}/\mu\text{l}) = (A_{260} \times V \times U \mu\text{g}) / 1000 \mu\text{l}$$

A_{260} = absorption

V = sample volume

U = conversion factor (50 for double stranded DNA, 40 for single stranded/double stranded RNA)

Absorbance of a DNA sample is determined at wavelength of 260 nm and 280 nm. DNA absorbs mainly UV light of 260 nm and aromatic proteins absorb UV light at 280 nm. A relatively pure DNA or RNA sample has a 260/280 quotient of 1.8 or 2.0, respectively. A lower quotient indicates protein contamination.

2.14.2. Enzymatic manipulation of DNA

2.14.2.1. Polymerase chain reaction (PCR)

PCR is a technique to amplify a specific DNA region of a target DNA strand (template) similar to endogenous DNA replication (Mullis *et al.*, 1986). Two specific oligonucleotides (primer), complementary to the target region of the DNA template, are used to create free 3' hydroxyl ends for the DNA polymerase. The PCR consists of a series of three repeating steps:

1. Denaturation of the template DNA results in single stranded DNA molecules
2. Annealing of the oligonucleotide primer to the single stranded DNA templates
3. Elongation/extension of the oligonucleotide primer complementary to the DNA template strand

Repetitions of these steps for 30 to 40 times lead to a million fold amplification of a single DNA molecule. Fusing restriction site sequences to the 5' ends of each oligonucleotide primer results in PCR products which can be inserted into a vector after incubation with the corresponding restriction enzymes (DNA molecules and vector).

For mutational analysis genomic DNA was amplified using Taq DNA polymerase, whereas Pfu DNA polymerase with proofreading activity was used to amplify template DNA for cloning purpose. Each PCR reaction mix is listed in table 2-11.

Table 2-11: PCR reaction mix for Taq and Pfu DNA polymerase

	Taq polymerase	Pfu polymerase
dNTP-Mix (3.75 mM)	1µl	1µl
10x Buffer	5µl*	5µl**
MgCl ₂ , 25 mM	4µl	-
forward-primer (10 pmol/µl)	2µl	2µl
reverse-primer (10 pmol/µl)	2µl	2µl
DMSO	2µl	2µl
DNA polymerase	0,5µl (5u/µl)	0.5µl (2.5u/µl)
template DNA	100ng	100ng
<i>ad aqua bidest.</i>	ad 50µl	ad 50µl

*10x Taq DNA Polymerase Buffer – MgCl₂

**10x Pfu DNA Polymerase Buffer + MgSO₄

The PCR reaction was performed in a thermo cycler with following basic program:

Step 0: 95°C 2min
 Step : 95°C 30sec
 Step 2: n°C 30sec
 Step 3: 72°C n* min

Repetition of Step 1 to Step 3 for 30 to 40 cycles

Step 4: 72°C n* + 5 min
 Step 5: 10°C ∞

The annealing temperature of step 2 depends on the melting temperature of the oligonucleotide primer. The elongation time of step 3 depends on the length of the expected PCR product and on the applied DNA polymerase (Taq polymerase: 1 kb/min, Pfu Polymerase: 1 kb/2 min).

5 µl of the PCR product were analyzed by agarose gel electrophoresis (see 2.14.1.4.) for control purpose. For subsequent sequence analysis, unincorporated oligonucleotide primer and dNTPs were removed either with the USB[®] Exo-SAP IT[®] PCR Product Cleanup kit or with the NucleoSpin[®] Extract II from Machery-Nagel according to manufacturer's instructions.

2.14.2.2. Site directed mutagenesis

Site directed mutagenesis is a technique to introduce mutations, such as base changes, deletions or insertions, into DNA via PCR. Each oligonucleotide primer used for amplification has to contain the desired mutation. Recombinant proteins with desired mutations can be expressed in host cells using the corresponding expression plasmid as PCR template.

The oligonucleotide primers were complementary to the DNA template around the site where the mutation was to be introduced and contained the desired mutation (see table 2-9). Using Pfu DNA polymerase, with proof reading activity, the plasmid was amplified in a common PCR (see 2.14.2.1.) with about 18 cycles. The mutation was subsequently included in every PCR product. Template DNA was digested by incubation with 1 µl DpnI (10 u/µl), which was directly added to the 50 µl PCR sample, for 3 h at 37 °C. Dam⁺ *E.coli* methylates DNA with the sequence GATC at the N6 position of the adenine (G^{m6}ATC) and DpnI cleaves DNA at this sequence (Palmer and Marinus, 1994). The template plasmid was previously cloned in Dam⁺ *E.coli* BIOblue. Thus, the methylated template plasmid was digested by DpnI. The PCR product, containing the mutation, remained and was transformed into *E.coli* BIOblue (see 2.13.2.).

2.14.2.3. Reverse transcription PCR: Generation of cDNA

The reverse transcriptase is a polymerase which uses RNA templates to synthesize complementary DNA (cDNA) (Baltimore, 1970; Temin and Mizutani, 1970). An oligo dT primer which binds to the poly-A tail of each mRNA molecule is used for reverse transcription of the whole mRNA of a sample. Reverse transcription of a certain mRNA into cDNA can also be performed using a template specific primer.

The cDNA was generated with the RevertAid H Minus First strand cDNA synthesis Kit using 1 µg total RNA and 500 ng oligo dT. The reaction was performed as follows:

1. 1 µg total RNA
1 µl Oligo (dT)₁₈ (0.5 µg/µl)
Add 12 µl Rnase free water

The first sample was incubated for 5 min at 70 °C for in the thermo cycler and cooled down on ice for at least one minute.

2. 4 µl 5x reaction buffer
- 1 µl RiboLock™RNase Inhibitor
- 2 µl 10 mM dNTP mix

First and second sample were mixed and incubated at 37 °C for 5 min in the thermo cycler. Afterwards, 1µl RevertAid™ H Minus Reverse Transcriptase was added and the sample was further incubated for 60 min at 42 °C followed by incubation for 10 min at 70 °C.

2.14.2.4. Quantitative real time PCR (qRT-PCR)

The qRT-PCR technique is based on PCR but enables detection and quantification of the PCR product after every single PCR cycle. Thus, mRNA expression level of certain genes can be investigated by this technique using gene specific (exon priming) oligonucleotide primer pairs and cDNA as PCR template. qRT-PCR was performed with QuantiTect® SYBR green PCR Kit according to manufacturer's instructions. SYBR green is an asymmetrical cyanine dye which intercalates in double stranded DNA thereby enabling quantification of the PCR products by determination of the fluorescence intensity at 530 nm after each PCR cycle (Zipper *et al.*, 2004). The cycle threshold (Ct) value defines the PCR reaction level at which a significant exponential increase in fluorescence is detected. The Ct value directly correlates with the number of copies of cDNA template present in the reaction. Thus, different Ct values of individual samples result from different amounts of template cDNA indicating different expression levels of the corresponding gene.

Determination of the mRNA expression levels of two housekeeping genes, *GAPDH* (glyceraldehyde-3-phosphate dehydrogenase) and *β-actin*, was used for normalization purposes. Additionally, standard curves were generated using specific PCR products (spectrophotometrical quantificated) in a dilution series from 500 atm/µl to 5×10^{-4} atm/µl. All primers were purchased from Qiagen (see table 2-9) and uniform cycle conditions according to manufacturer's instructions were applied. The mRNA Expression level of a certain gene was determined in duplicates for each sample. For calculation of relative mRNA expression levels, the mean mRNA expression of nine wild type fibroblast cell cultures (wt1 to wt9) was set to 100 %. One qRT-PCR probe was prepared as follows:

qRT-PCR reaction mix:	5 µl SYBR green
	1 µl Primer
	1 µl cDNA
	<u>4 µl <i>aqua bidest</i></u>
	11µl

2.14.2.5. Restriction of DNA

Restriction of double stranded DNA is performed with restriction enzymes cleaving the phosphate-desoxyribose-backbone at specific recognition nucleotide sequences. Enzymes used in this thesis generated DNA with short single stranded overhangs, so called sticky ends. Enzyme restriction digestion of plasmid DNA or PCR products was performed according to restriction enzymes' manufacturer's instructions. Restriction digestion products were subjected to AGE for control (see 2.14.1.4.) and preparative purposes (see 2.14.1.5.).

2.14.2.6. Ligation

DNA ligases are enzymes which catalyze the formation of covalent phosphodiester bonds between free 3' hydroxyl and 5' phosphate ends of DNA molecules thereby fusing two DNA fragments together. Ligation utilizing the T4 DNA ligase can be used for the insertion of cDNA fragments (insert) into a plasmid.

Prior to ligation, plasmid and insert DNA were digested with the same enzymes generating two DNA molecules with complementary sticky ends which were fused together by subsequent ligation with T4 DNA ligase. A threefold molecular overspill of insert DNA was calculated with the following formula:

$$x \mu\text{g insert} = \text{insert size} / \text{vector size} * 3 * y \text{ ng vector}$$

Ligation was performed in a 15 µl reaction mix containing 1 µl T4 DNA ligase (1 u/µl) with its corresponding buffer (1x concentrated) for 16 h at 4°C.

2.14.2.7. DNA sequencing and sequence analysis

Sequencing was performed with the chain-termination method after Sanger (Sanger et al, 1977). This technique basically requires a DNA template, a DNA polymerase, and an oligonucleotide primer. The PCR reaction mix contains dideoxynucleotides (ddATP, ddGTP, ddCTP, ddTTP), labeled with four different fluorescent dyes (emitting light of different wavelengths), beside the deoxynucleotides (dATP, dGTP, dCTP, dTTP). The ddNTPs terminate the elongation by the DNA polymerase due to their lacking 3' hydroxyl group, which is required

for formation of the phosphodiester bond with the next dNTP. Thus, randomly incorporated ddNTPs lead to DNA molecules of different length, which are separated by size using capillary gel electrophoresis. Detection is performed when the molecules cross a laser and a fluorescence detector. The fluorescence of the terminal ddNTP of each molecule, induced by the laser, is getting detected. Therefore, a red, a yellow, and a blue fluorescence signal (one after another), for example, correspond to DNA sequence TCG when ddTTP, ddCTP, and ddGTP are labeled with fluorescent dyes emitting red, yellow, and blue light, respectively.

For sequencing of DNA samples, the BIGDYE TERMINATOR v3.1 CYCLE SEQUENCING KIT was applied with a specific primer complementary to the template DNA according to manufacturer's instructions. The resulting cycle sequencing product was cleared by ethanol/sodium acetate precipitation. The sample was transferred into a 1.5 ml reaction tube, mixed with 10 μ l Na-acetate pH 4.7, 120 μ l H₂O and 220 μ l 100 % EtOH and centrifuged (20 min, 16000 x g, room temperature). The supernatant was discarded and 400 μ l 70 % EtOH were added to the DNA pellet before the sample was centrifuged again (10 min, 16000 x g, room temperature). The DNA was dried at 40 °C for 5 min and resuspended in 10 μ l Hi-Di Formamide for analysis with a 3100-Avant Genetic Analyzer. The resulting DNA sequence was analysed with Chromas Lite version 2.01 (Technelysium Pty Ltd, Brisbane, Australia).

2.15. Protein biochemistry

2.15.1. Preparation of whole cell protein lysates

Cells were harvested by trypsinization (see 2.12.1.), resulting cell pellets were washed twice with 50 ml 1x PBS, and cells were diluted in an appropriate volume of 1x PBS. Cells were disrupted by rotational freezing in liquid nitrogen followed by thawing on ice for three times. The cell lysates were centrifuged to sediment the residual cell debris (10 min, 16000 x g, 4 °C). Resulting supernatant was transferred into a new reaction tube. Photometric quantification of protein concentrations was performed by the Bradford method (Bradford, 1976) using the Roti[®]-Quant Kit according to manufacturer's instructions.

2.15.2. Immunoprecipitation (IP)

HEK293A cells were transiently transfected with Attractene transfection reagent (see 2.12.3.) and harvested 24 h after transfection by trypsinization (see 2.12.1.). The resulting cell pellets were diluted in 1 ml IP lysis buffer, containing freshly added 1 mM PMSF and protease inhibitor (Complete ULTRA Tablets Mini EDTA free EASYpack), and were incubated on ice for 1 h. Cell suspension was centrifuged (10 min, 16000 x g, 4 °C) before the protein concentration

in the supernatant was determined by the Bradford method using the Roti[®]-Quant Kit. For later control purpose an aliquot containing 65 µg protein was taken from the supernatant (input), mixed with 9 % Laemmli buffer and stored at -20 °C. The remaining supernatant was divided into half (myc IP and control IP). To increase the amount of protein for the co-immunoprecipitation, total protein from one 175 cm² culture flask with confluent grown, untransfected HEK293A cells was added to a final volume of 4 ml IP lysis buffer. Precipitation of XPG_(mut)mycHis protein was performed over night on a rotating wheel at 4 °C by adding an αmyc antibody in a dilution of 1:1000 to the myc IP sample. Control IP was performed under similar conditions using an αmouse IgG control antibody. Next day, 50 µl of a 1:1 mixture of AgaroseA beads (50 % slurry) and AgaroseG+ beads (50 % slurry), equilibrated with IP lysis buffer, were added to each sample and samples were further incubated for 2 h. The antibodies bind to the agarose beads and, subsequently, the antibody-protein complexes are immobilized on the beads. Beads with bound protein complexes were washed five times with IP lysis buffer. Beads were resuspended in 30 µl 9 % Laemmli buffer and boiled for 5 min at 96 °C. The 9 % Laemmli buffer contains 10 % (v/v) β-mercaptoethanol reducing disulfide bridges of proteins needed for protein unfolding. Boiling the samples results in the dissolution of protein-antibody-agarose-complexes. Subsequently, the proteins can be separated by size with SDS-PAGE (see 2.15.3).

2.15.3. Horizontal SDS-PAGE and Western Blotting

Dilution and boiling (5 min at 96 °C) of protein samples in Laemmli buffer containing SDS (sodium dodecyl sulphate) results in denaturated and negatively charged proteins. Therefore, samples can be separated by size in an electric field using polyacrylamide gel electrophoresis (PAGE) (Laemmli, 1970).

Protein samples were analyzed by horizontal SDS-PAGE followed by immunoblotting. For SDS-PAGE the Amersham[™] ECL[™] electrophoresis system with a precast 4 % to 12 % polyacrylamide gradient gel was used according to manufacturer's instructions. Protein transfer from the polyacrylamide gel to a nitrocellulose membrane was performed applying the wet-blot method using an XCellIII Blot Module at a voltage of 25 V and a current of maximal 300 mA for 2.5 h at 4°C. Afterwards, free protein binding sites were saturated by incubation of the membrane for 30 min at room temperature in blocking buffer (blocking buffer was used for each antibody according to manufacturer's instructions). Incubation with the specific antibodies was performed rocking over night at 4 °C. All following steps were performed at room temperature using solutions from the WesternBreeze Chemiluminescent Immunodetection Systems (anti

mouse or anti rabbit). The membrane was washed four times for 5 min with washing buffer before incubation with the secondary antibody was performed for 30 min. Afterwards, the membrane was washed four times for 5 min with washing buffer again and rinsed with *aqua bidest* before chemiluminescent substrates were added. The resulting chemiluminescent signal was detected with a luminescent image analyzer LAS-4000.

2.15.4. Immunofluorescence (XP protein recruitment kinetics)

Fibroblast cells were seeded at a density of 2×10^4 cells per well on glass cover slips in 24-well-plates. Next day, medium was taken from the cells, kept for later use, and cells were washed twice with 1x PBS. 1x PBS was removed and cells were covered with 8 μ m isopore polycarbonate membrane before they were irradiated with 100 J/m² UVC using an ultraviolet crosslinker with 254 nm UV light bulbs. The medium was given back to the cells and cells were further incubated for time intervals of the kinetic (6 min, 15 min, 30 min, 3 h, 6 h, 24 h). Cells were washed three times with 1x PBS to remove the media before they were fixed with 300 μ l 3.7 % PFA for 15 min at room temperature. Cells were washed again three times with 1x PBS to remove remaining PFA before they were permeabilized with 0.1 % Triton-X-100 in 1x PBS for 15 min at room temperature. Additional threefold washing with 1x PBS was performed and cells were blocked with 20 % FCS in 1x PBS for 20 min at room temperature. Again, cells were washed threefold with 1x PBS before incubation with an antibody directed against one of the XP-proteins (XPA, XPB, XPC, ERCC1, or XPG) in a 1:50 dilution for 1 h at 37 °C was carried out. Afterwards, cells were washed three times with 1x PBS containing 0.05 % Tween-20 (1x PBS-Tween) and incubated with the secondary α rabbit antibody conjugated with DyLight488 in a 1:400 dilution for 1 h at 37 °C. For single staining against a XP protein, the glass cover slip was mounted with mounting medium for fluorescence containing DAPI and stored at 4 °C and protected from light until further use.

For a double staining of a XP protein and a photoproduct or single staining of a photoproduct the DNA had to be denaturated to become accessible for the antibody directed against the DNA photoproduct. Denaturation was performed by incubation with 2 M HCL for 20 min (double staining) or 30 min (single staining) at room temperature. After that, cells were washed three times with 1x PBS-Tween and then incubated with either CPD antibody in a 1:1000 or with 6,4PP antibody in a 1:500 dilution for 30 min at 37 °C. Cells were washed threefold with 1x PBS-Tween and incubated with secondary α mouse antibody conjugated with Dylight594 in a 1:500 dilution for 1 h at 37 °C. Cells were washed three times with 1x PBS and glass cover slips were subsequently mounted with mounting medium containing DAPI. Digital

images were taken with an Axio Imager.M1. For quantification at least 100 nuclei were counted for positive staining (percent positive stained nuclei).

3. Results

3.1. Results of the molecular-genetic and functional-genetic analysis

3.1.1. Clinical symptoms

3.1.1.1. Clinical symptoms of the 12 XPC patients

The age of the XP-C patients from whom fibroblasts for functional and molecular-genetic analysis were obtained ranged from four to 45 years at last observation with a mean age of 8.75 and a median age of nine years. There were seven male and four female XP-C patients. For one patient (XP23GO) no information about the sex was known. XP20MA and XP117MA were of German ancestry. XP47MA, XP98MA and XP99MA came from Iran and XP23GO came from Afghanistan. XP102MA was of Libyan, XP155MA and XP156MA of Balkan ancestry. XP150MA was of Turkish, XP114MA and XP115MA of Arab ancestry. XP98MA and XP99MA, XP114MA and XP115MA as well as XP155MA and XP156MA were siblings. Four of the 12 patients were described to exhibit increased sun sensitivity (XP20MA, XP47MA, XP98MA, and XP150MA), whereas all patients developed poikiloderma, i.e hyper- and hypopigmentations on atrophic dry premature-aged skin. Seven patients developed skin cancers already in childhood (XP20MA, XP47MA, XP98MA, XP102MA, XP114MA, XP155, and XP156MA). Sun sensitivity and poikiloderma in sun-exposed skin enabled clinical XP diagnosis at a median age of nine years (range from two to 16 years). First skin cancers evolved at a median age of eight years (range from three to 14 years). Eight of the XP-C patients developed more than one skin malignancy and different types of skin cancer including squamous and basal cell carcinomas as well as cutaneous melanomas (XP20MA, XP47MA, XP98MA; XP102MA, XP114MA, XP117MA, XP150MA, and XP155MA). Interestingly, XP47MA, the only patient who was later found to carry no protein-truncating mutation, did not exhibit milder symptoms compared with the other patients. Of note, none of the XP-C patients exhibited typical neurological symptoms classically found in the XP plus neurological symptoms entity like absence of deep tendon reflexes, progressive high-tone deafness. An overall reduced intellectual capacity was described for XP20MA.

3.1.1.2. Clinical symptoms of the eight XP-D patients

The age of the XP-D patients at last observation ranged from two to 64 years with a mean age of 29 years and a median age of 27 years. There were five male and three female patients. Four of the patients, XP19MA, XP71MA, XP89MA, and XP90MA were of German ancestry. XP40MA was of Swedish, XP46MA of Portuguese, XP87MA of French and XP188MA of Turkish ancestry. Five of the XP-D patients suffered from XP phenotype (XP19MA, XP40MA, XP46MA,

XP71MA, and XP90MA). All these patients, except XP71MA, exhibited freckling within sun-exposed skin. An increased sun sensitivity was described for three of them (XP40MA, XP71MA, XP90MA), whereas XP19MA was described to be not sun sensitive. Four of the five patients exhibiting the XP phenotype developed NMSC skin cancers: patients XP40MA and XP46MA developed first skin cancers at the age of 15 and 17 years, respectively, whereas XP71MA was 52 years old. No exact age at first skin cancer development was described for XP19MA. Additionally, XP19MA, XP40MA, and XP71MA developed more than one skin cancer. Patient XP89MA suffered from a mild XP/CS complex phenotype with sun sensitivity and freckling within sun-exposed skin as well as short stature, underweight, reduced muscle proprioceptive reflexes, impaired vision, and a slight mental retardation. The patient did not develop a tumor until the age of 15 years. Two patients, XP87MA and XP188MA, exhibited the TTD phenotype. Unfortunately, the further clinical outcome was not described for these two TTD patients.

3.1.1.3. Clinical symptoms of the three XPG patients

Patients XP72MA and XP165MA were from German ancestry. Both were sun sensitive since birth and developed freckling within the sun-exposed skin as toddlers. They suffered from the XP/CS complex; however, XP72MA exhibited a somewhat milder phenotype compared to XP165MA with respect to CS symptoms. XP72MA developed no skin cancer up to the age of seven years but exhibited microcephaly, ataxia, and neurological impairment. XP165MA exhibited a severe XP/CS phenotype with dwarfism, microcephaly, muscular hypotension, ataxia, reduced muscle proprioceptive reflexes and neurological impairment. This patient died at the age of two years from meningitis. Unfortunately, no clinical data were available for the third XP-G patient, XP40GO.

3.1.2. Characterization of XP fibroblast cells

3.1.2.1. Determination of post-UV survival

The post-UV cell survival of the patients' fibroblasts was assessed with MTT Assay (see 2.12.4.1.). This assay reveals the viability of cells by determination of the activity of a mitochondrial dehydrogenase which metabolizes 3-(4,5-Dimethylthiazol-2-yl)-2,5-diphenyl-tetrazoliumbromid (MTT) to its blue coloured formazan salt. The amount of formazan correlates with cells viability and can be measured at 550 nm. A reduced post-UV cell survival is typical for XP cells compared to wild type cells, while survival of XP variant cells only decreases in the presence of caffeine (Arlett *et al.*, 1975; Despras *et al.*, 2010). Thus, all cells were tested with media containing 1 mM caffeine and without caffeine at a density of 5000

(n=4) and 7500 (n=4) cells per well in 96-well-plates. Some cells, which were tested in the beginning of the thesis, were tested without caffeine (n=8). A repetition of the test in the presence of 1 mM caffeine (n=8) was only performed if cells revealed to be un-sensitive against UVC irradiation. Later on during the thesis, the test was performed simultaneously with and without caffeine (each n=4).

Post-UV survival of wild type cells was assessed by the mean survival of three wild type fibroblasts (wt1, wt5, wt6). The wild type cells exhibited a mean post-UV survival of 81 % (5000 cells per well) and 87 % (7500 cells per well) at the highest UVC dose of 30 J/m² compared with their unirradiated counterparts. All patients' cells showed a reduced post-UV cell survival compared to wild type fibroblasts but the UV sensitivity differed between the patients' cells. Complete mean values of the post-UV survival with and without caffeine at both cell densities in % are summarized in appendix tables A-1 to A-13.

All 12 XP-C cells were irradiated with UVC doses from 6 J/m² to 30 J/m². The post-UV cell survival of XP-C fibroblast cells at the highest dose of UVC irradiation is depicted in figure 3. UVC irradiation of XP-C fibroblasts at 30 J/m² resulted in a mean post-UV survival of 50 % and 49 % at 5000 (range from 26 % to 77 %) and 7500 cells (range from 27 % to 78 %), respectively. The ability to cope with UV-induced cell damage was disabled the most in XP23GO fibroblasts (26 % at 5000 and 31 % at 7500 cells, both at 30 J/m² UVC) whereas XP150MA cells exhibited the mildest sensitivity to UV irradiation (77 % at 5000 cells and 78 % at 7500 cells, both at 30J/m² UVC).

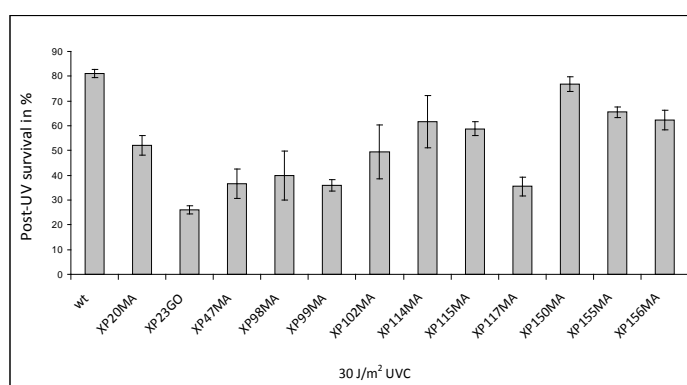


Figure 3: Post-UV survival of XP-C fibroblast cells after 30 J/m² UVC irradiation determined via MTT Assay. Cells were seeded in quadruplicates at a density of 5000 cells per well in 96-well-plates and irradiated with increasing doses of UVC from 6 J/m² to 30 J/m². Survival of the unirradiated cells was set to 100 %. Post-UV survival of wild type cells is the mean survival of three different wild type cells.

Four of the eight XP-D cells were irradiated with doses from 6 J/m² to 30 J/m² UVC. Within these fibroblasts (XP46MA, XP71MA, XP87MA, XP90MA) the mean level of relative post-UV survival at 30 J/m² UVC was 56 % at a density of 5000 (range from 42 % to 74 %) and 52 % at a density of 7500 cells (range from 46 % to 61 %). XP90MA and XP71MA exhibited a post-UV survival of 42 % and 44 % (5000 cells) as well as 48 % and 46 % (7500 cells) after irradiation with 30 J/m² UVC, respectively. In contrast, XP87MA and XP46MA fibroblasts revealed a slightly milder UV sensitivity with 74 % and 67 % (5000 cells) as well as 61 % and 52 % (7500 cells) cell survival after irradiation with 30 J/m² UVC, respectively. Post-UV cell survival of these four patients' fibroblast cell cultures at a density of 5000 cells per well after irradiation at the highest dose of 30 J/m² UVC is depicted in figure 4A.

UV sensitivity of XP-D cells XP19MA, XP40MA, XP89MA, and XP188MA has been determined at an early time point of the thesis. At this time, the later standard UVC irradiation from 6 J/m² to 30 J/m² was not obligatory used for irradiation. Thus, these cells were irradiated with UVC doses of a minimum of 3 J/m² and a maximum of 25 J/m².

XP19MA exhibited a post-UV survival of 22 % (5000 cells) and 19 % (7500 cells) at the highest dose of 16 J/m² UVC. XP40MA showed a survival of 22 % (5000 cells) and 23 % (7500 cells) after irradiation with a maximum of 20 J/m². XP89MA fibroblasts revealed a cell survival of 34 % (5000 cells) and 25 % (7500 cells) at 15 J/m² UVC. XP188MA cells were irradiated at a density of 10,000 cells per well and exhibited a post-UV survival of 48 % at the highest dose of 25 J/m². Due to the different maxima of UVC irradiation, complete survival curves of these cells at a density of 5000 cells (10,000 cells for XP188MA) per well are depicted in figure 4B.

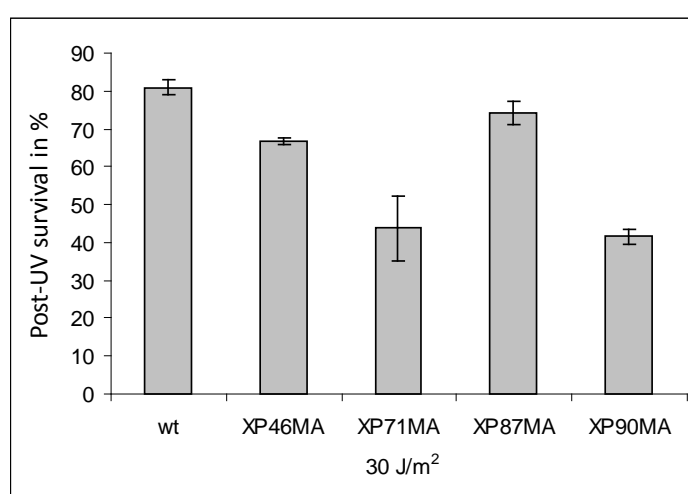


Figure 4A (legend see next page)

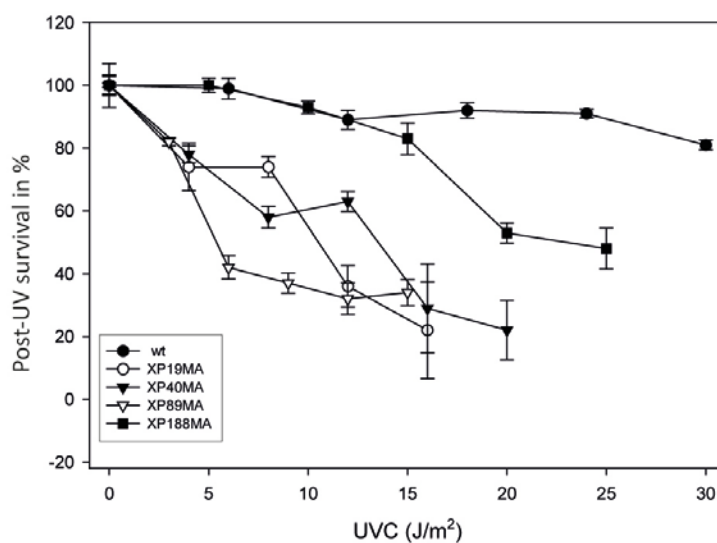


Figure 4: Post-UV survival of XP-D fibroblasts determined via MTT Assay. Cells were seeded in quadruplicates at a density of 5000 cells per well in 96-well-plates and irradiated with increasing doses of UVC irradiation (3 J/m² minimum to 30 J/m² maximum). Survival of the unirradiated cells was set to 100 %. Post UV-survival of the wild type cells is the mean survival of three different wild type cells. **A:** Cell survival of XP-D fibroblasts after irradiation with the highest dose of 30 J/m² UVC. **B:** Post-UV survival curves of XP-D fibroblasts after irradiation with increasing doses of UVC irradiation.

UV sensitivity of XP-G fibroblasts from patients XP165MA and XP72MA was more pronounced compared to all XP-C and XP-D fibroblasts (Emmert *et al.*, 2002). Therefore, these cells were irradiated with UVC doses from 0-20 J/m² (XP165MA) and 0-15 J/m² (XP72MA). Post-UV cell survival curves of the three XP-G fibroblasts at a density of 5000 cells per well are depicted in figure 5. Of the three XP-G patients' cells, fibroblasts from XP165MA were most sensitive with a post-UV survival of 54 % (5000 cells) and 62 % (7500 cells) at 4 J/m². All cells died at 12 J/m² (both cell densities). XP72MA fibroblasts were also very UV sensitive and nearly all cells were killed with 15 J/m² UVC irradiation (2 % and 4 % survival at densities of 5000 and 7500 cells per well, respectively). In contrast, fibroblast cells from XP40GO exhibited the mildest sensitivity to UV with a survival of 46 % (5000 cells) and 52 % (7500 cells) at 30 J/m² UVC. Thus, survival of XP40GO is comparable to the post-UV survival of the XP-C and XP-D cells although it is still lower than the average XP-C cell survival of 50 %.

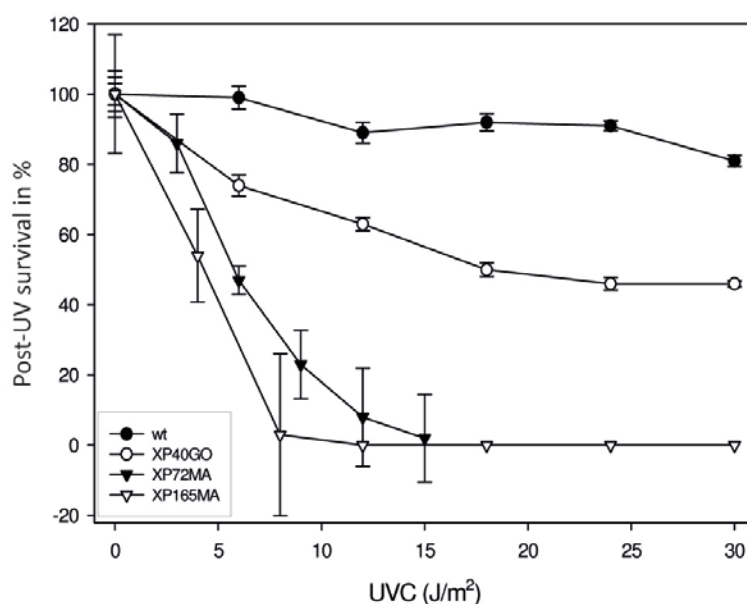


Figure 5: Post-UV cell survival of XP-G fibroblast determined via MTT Assay. 5000 cells were seeded in quadruplicates in 96-well-plates and irradiated with increasing doses of UVC (3 J/m² minimum to 30 J/m² maximum). Cell survival was determined via MTT assay and survival of unirradiated cells was set to 100 %. Post-UV survival curve of wild type cells is the mean survival of three wild type fibroblasts.

3.1.2.2. Determination of NER capability and XP complementation groups

NER capability and complementation group assignment was examined using Host Cell Reactivation Assay (see 2.12.4.2.). Cells were transfected in triplicates with either irradiated (250 J/m² UVC) or non-irradiated pcmvLUC plasmid together with non irradiated pRL-CMV plasmid (see 2.12.2.). Relative NER capability of the cells correlates with the activity of the firefly luciferase expressed from the UV irradiated plasmid vs. the activity of the firefly luciferase expressed from non-irradiated plasmid. This relative enzyme activity in % is simplified termed as “% of relative NER capability”.

The NER defect of the XP fibroblast cells is complemented by co-transfection of expression plasmids encoding cDNA of the XP gene which is mutated in the cell. Thus, an increased relative NER capability after co-transfection of a certain expression plasmid (pXPA, pXPB, pXPC, pXPD, pXPE, pXPF, pXPE) reveals the XP gene responsible for patients’ phenotype and accordingly patients’ complementation group (XP-A to XP-G).

All XP patient fibroblasts showed a reduced relative nucleotide excision repair capability compared to the mean value of five wild type fibroblasts cell cultures (Figure 6: A, B, C). The

complete values (n=3) and the resulting mean values in % are summarized in appendix tables A-14 to A-17.

The mean relative NER capability ranged from 0.7 % (XP114MA) to 11.3 % (XP20MA) and from 0.4 % (XP19MA, XP89MA) to 4.7 % (XP46MA) in the uncomplemented XP-C and XP-D fibroblasts, respectively. The three XP-G fibroblasts exhibited relative NER capabilities of 1.6 % (XP40GO), 0.6 % (XP72MA), and 2.6 % (XP165MA). In contrast, a mean relative NER capability of 30.7 % (range from 20.2 % to 47.3 %) was determined for the five wild type fibroblast cell cultures (wt1 to wt5). XP-C, XP-D and XP-G complementation groups were assessed by co-transfection with plasmids expressing wild-type *XPC*, *XPB*, and *XPG* cDNA (pXPC, pXPB, pXPG), respectively. Co-transfection resulted in increased relative NER capabilities depicted in figure 6A (XP-C cells), 6B (XP-D cells), and 6C (XP-G cells). The increase in relative NER capability ranged from twofold (XP20MA) to 13-fold (XP117MA) in the XP-C cells and from threefold (XP71MA, XP188MA) to 47-fold (XP87MA) in the XP-D fibroblasts. In the XP-G cells relative NER capability increased 13-fold, twofold, and 38-fold in the XP40GO, XP72MA and XP165MA fibroblasts, respectively. Accordingly, cells could be clearly assigned to the XP complementation groups C, D, and G.

Four of the XP-C fibroblasts (XP23GO, XP98MA, XP99MA, and XP115MA) could not be assigned to the XP-C complementation group by HCR and co-transfection of the pXPC plasmid: it was difficult to obtain enough cells due to their poor cell growth. Therefore, the defect *XPC* gene was determined by measurement of the *XPC* mRNA expression level.

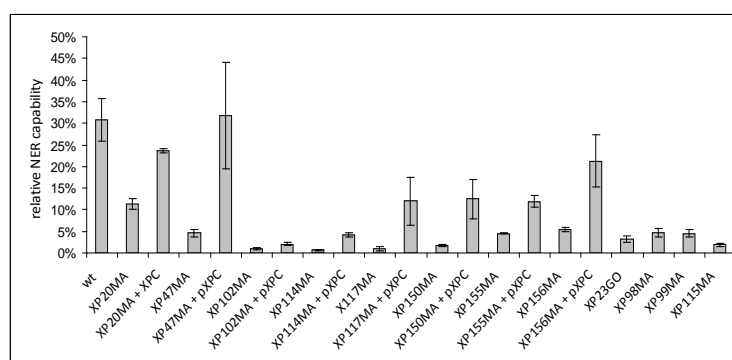
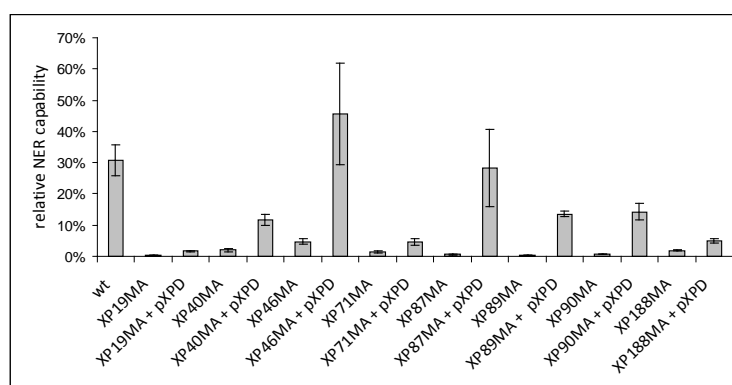
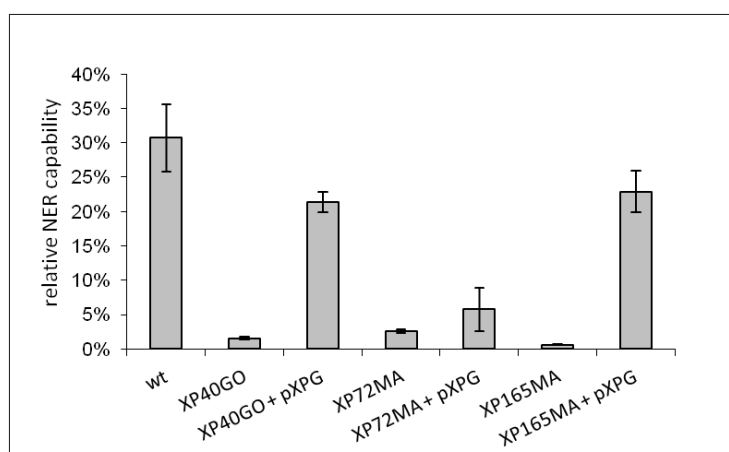


Figure 6A (legend see next page)



B



C

Figure 6: Determination of relative NER capability and assignment of patients' fibroblast cells to their complementation groups with HCR. Cells were transfected in triplicates with either irradiated ($250 \text{ J/m}^2 \text{ UVC}$) or non-irradiated firefly luciferase plasmid together with untreated renilla luciferase plasmid (normalization). Expression of the firefly luciferase correlates with cells' ability to repair UV-induced DNA lesions (relative NER capability). Simultaneous co-transfection of plasmids encoding cDNA of the XP gene mutated within the cells increased relative NER capability, thereby assessing patients' complementation groups. Relative NER capability of wild type fibroblasts is the mean of five HCRs ($n=15$). **A:** Relative NER capability of XP-C fibroblasts before and after co-transfection of pXPC. **B:** Relative NER capability of XP-D fibroblasts before and after co-transfection of pXPD. **C:** Relative NER capability in XP-G fibroblasts before and after co-transfection of pXPG.

3.1.2.3. Determination of mRNA expression levels of the mutated XP genes

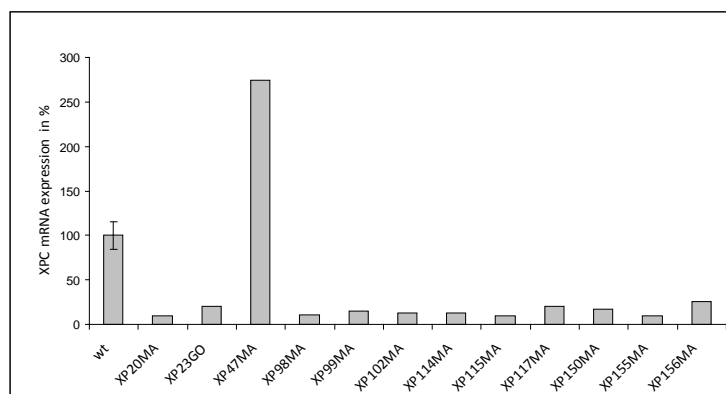
The mRNA expression levels of the XP genes (*XPA* to *XPG*) and the gene coding for polymerase eta (*XPV*) were assessed for a total of 75 XP fibroblast cell cultures. Whole cell RNA was isolated from patient and wild type fibroblast cells (see 2.14.1.6.) and was subjected to reverse transcription PCR to generate cDNA (see 2.14.2.3.). QRT-PCR was performed with QuantiTect[®] SYBR green PCR Kit and QuantiTect[®] Primer Assays (see 2.14.2.4.). The measured Ct values, correlating with the mRNA expression level in a certain sample, were normalized to the two

housekeeping genes β -actin and *GAPDH*. As normal control, mRNA expression of nine wild type fibroblast cell cultures was measured simultaneously. The mean expression level of the wild type cells was set to 100 % to calculate the relative mRNA expression levels of the patients' cells. All mRNA expression levels of the measured genes in % (normalized to both housekeeping genes and relative to the mean wild type expression) are summarized in appendix table A-18.

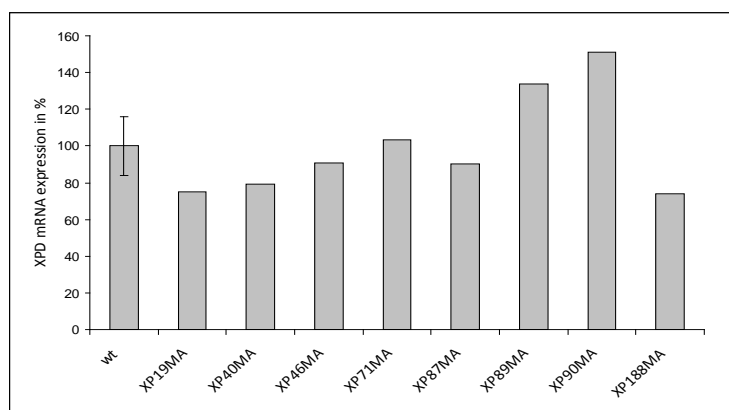
It is already known that XP-C patients generally exhibit reduced *XPC* mRNA levels and, therefore, an abolished protein expression (Cartault *et al.*, 2011; Emmert *et al.*, 2006b; Khan *et al.*, 2006) which might result from nonsense-mediated message decay due to truncating mutations (Lejeune and Maquat, 2005; Maquat, 2005) found in most XP-C patients. Thus, patients XP23GO, XP98MA, XP99MA, and XP115MA, which could not be assigned to complementation group XP-C by HCR (see 2.12.4.2.), were identified as XP-C patients by their reduced *XPC* mRNA levels. The *XPC* mRNA level was decreased in 11 of the 12 XP-C patients. The mean *XPC* mRNA level within these patients was 14.9 % (range from 9.5 % to 25.7 %; $p < 0.001$, Student's T-test) compared to the mean expression level of the nine normal controls set to 100 %. The low range of *XPC* mRNA expression was quite independent of the *XPC* mutation identified although all mutations would lead to truncated *XPC* proteins. Only XP47MA cells, which were later found to harbour an unusual novel *XPC* gene mutation with deletion of exactly one amino acid, exhibited an over expression of mutated *XPC* mRNA of 274.1 % compared to wild type cells (figure 7A).

The *XPD* mRNA expression level in the XP-D cells was normal compared to wild type expression levels of this gene. Two XP-D cells exhibited a slight up regulation in the *XPD* mRNA expression level of 133.6 % (XP89MA) and 151.3 % (XP90MA). However, *XPD* mRNA expression levels of the other five XP-D patients ranged from 74.1 % (XP188MA) to 103.4 % (XP71MA) which is within the normal variation of the wild type *XPD* mRNA expression (Figure 7B).

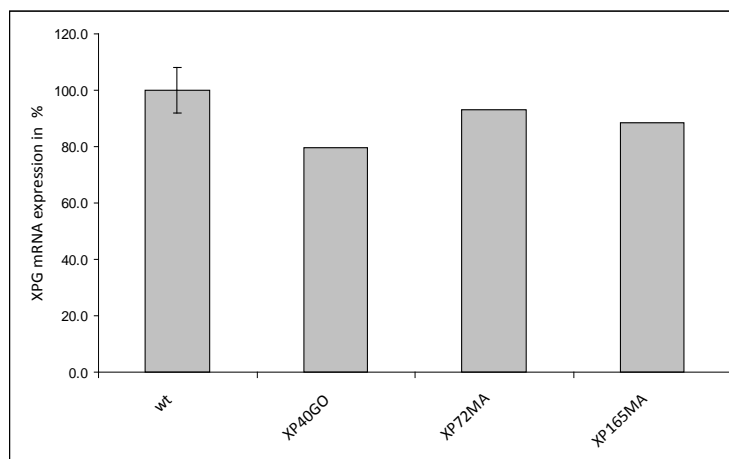
Similar to the XP-D fibroblasts, the XP-G cells revealed normal *XPG* mRNA expression levels. XP72MA exhibited mRNA expression of 93.1 %, XP40GO of 79.4 %, and XP165MA of 88.4 % compared to normal (figure 7C). Thus, the *XPG* mRNA expression in the three XP-G patients' fibroblast cell cultures was within the normal variation of wild type *XPG* mRNA expression.



A



B



C

Figure 7: Determination of mRNA expression levels of the mutated genes via qRT-PCR. Total RNA was isolated from fibroblast cells, reverse transcribed and subjected to qRT-PCR. Expression levels were normalized to expression levels of housekeeping genes β -actin and GAPDH. The mean expression level of nine wild type fibroblast cell cultures was set to 100 % for calculation of the expression levels of the patients' cells. **A:** XPC mRNA expression level in XP-C fibroblasts. **B:** XPD mRNA expression level in XP-D fibroblasts. **C:** XPG mRNA expression level in XP-G fibroblasts.

3.1.2.4. Mutational analysis

The exact genetic defect which is underlying a certain phenotype was determined by genomic DNA sequencing. Genomic DNA was isolated from patients' fibroblast cells (see 2.14.1.1.) and amplified via PCR for sequencing including intron/exon boundaries to allow for detection of splice site mutations which can result in exon skipping. Afterwards, samples were cleaned up (see 2.14.2.1.) and subjected to sequence analysis (see 2.14.2.7.). For sequence alignment *XPC*, *XPD*, and *XPG* reference sequences following the nomenclature of GenBank accession numbers NM_004628, NM_000400, and NM_000123.2, respectively, were used. All mutations identified are summarized in table 3-1.

All 12 XP-C patients carried mutations in a homozygous state indicating possible consanguinity of the parents. Seven different *XPC* mutations were identified. Four of these mutations have not been reported so far. Frameshift mutations, due to deletions or insertions, were most frequent (four of seven mutations) followed by C to T nonsense mutations (two of seven mutations). The most common mutation was a C to T transition at nucleotide position 567 that changed amino acid arginine 155 in exon 4 to a premature stop codon (p.R155X). This mutation was identified in four of the twelve XP-C patients (XP98MA, XP99MA, XP155MA, XP156MA) (Khan *et al.*, 2006). The second most common mutation, found in three of the twelve XP-C patients (XP102MA, XP114MA, XP115MA), was a TG deletion of nucleotides 1747 and 1748 resulting in a frameshift in exon 9 and a truncated *XPC* protein of 572 amino acids with the last 24 amino acids being unrelated to *XPC* (p.Val548AlafsX25) (Chavanne *et al.*, 2000; Khan *et al.*, 2006; Li *et al.*, 1993; Ridley *et al.*, 2005). XP23GO carried a nonsense mutation in the same exon created by a C to T transition at nucleotide position 1839 creating a premature termination codon from amino acid 579 (p.Arg579X) (Chavanne *et al.*, 2000; Gozukara *et al.*, 2001; Khan *et al.*, 2006). Novel frame shift mutations were found in patients XP20MA, XP117MA, and XP150MA. XP20MA carried an AG deletion at nucleotide position 446 and 447 in exon 3 leading to a truncated *XPC* protein of 119 amino acids with the last three being unrelated to *XPC* (p.Ala116TyrfsX4). The A insertion at nucleotide position 1525 in exon 9 in patient XP117MA creates a truncated *XPC* protein of 492 amino acids including the last 17 amino acids being unrelated to *XPC* (p.R475EfsX18). The C deletion at nucleotide position 2271 in XP150MA results in a frame shift starting with amino acid 723 in exon 12 and creating a stop codon after 43 amino acids being unrelated to *XPC* (p.Gln723SerfsX44). Patient XP47MA carried the only mutation not resulting in a truncated *XPC* protein. The deletion of three base pairs, ATC, at nucleotide position 2538 to 2540 in exon 14 creates an inframe single amino acid deletion of amino acid isoleucine 812.

Seven different missense mutations were found in the XP-D patients. Six of them have been described previously. Half of the XP-D patients (XP19MA, XP40MA, XP46MA, XP188MA) carried homozygous mutations while the other half (XP71MA, XP87MA, XP90MA, XP89MA) was compound heterozygous. Most frequent mutation was a G to A transition at nucleotide position 2079 in exon 22 resulting in an amino acid exchange from arginine 683 to glutamine which was found in homozygous state in XP19MA, XP40MA, XP46MA, and in heterozygous state in XP71MA (Kobayashi *et al.*, 2002). The second mutation of XP71MA was a G to C transversion of nucleotide 1878 leading to the amino acid exchange of arginine 616 to proline (Lehmann, 2001). Patient XP188MA carried a homozygous C to T transition at nucleotide 2195 in exon 22 resulting in an amino acid exchange of arginine 722 to tryptophan (Usuda *et al.*, 2011; Taylor *et al.*, 1997). Patients XP87MA and XP89MA carried similar mutations. Both were compound heterozygous for a G to A transition in exon 5 at nucleotide position 366 resulting in amino acid exchange arginine 112 to histidin (Broughton *et al.*, 2001). The second mutation was a G to C transversion of nucleotide 2072 in exon 21 changing aspartic acid 681 to histidin, which has not been described before. However, amino acid exchange of this evolutionary conserved amino acid to asparagine has been described to result in the COFS syndrome (Graham, Jr. *et al.*, 2001). XP90MA carried a G to A transition at nucleotide position 1878 in exon 20 and a G to T transversion at nucleotide position 2078 in exon 22. These missense mutations resulted in the exchange of arginine 616 to glutamine (Falik-Zaccai T.C., 2010) and arginine 683 to tryptophan, respectively (Emmert *et al.*, 2009; Kobayashi *et al.*, 2002).

The three XP-G patients carried five novel *XPG* mutations which have not been reported so far. Patients XP40GO and XP72MA were both compound heterozygous. In XP40GO a C to T transition at nucleotide position 891 changed amino acid 150 into a premature stop codon in exon 4 (p.Q150X). On the other allele a T to C transition at nucleotide position 2776 resulted in an amino acid change from lysine to proline at position 778 in exon 11 (p.L78P). In XP72MA a G to T transversion at nucleotide position 2622 changed amino acid 727 into a stop codon in exon 9 (p.E727X). On the other allele the amino acid tryptophan was changed to serine at position 814 in exon 11 due to a G to C transition at nucleotide position 2884 (p.W814S). Patient XP165MA was homozygous for a missense mutation in exon 11. A G to A transversion at nucleotide position 2856 changed amino acid glycine 805 to arginine in exon 11 (p.G805R).

Table 3-1 Summary of mutations identified in XP-C, XP-D and XP-G patients

Gene	Protein	Nucleotide	Exon	Patient ID
<i>XPC</i>	p.A116YfsX4	c.446_447delAG	3	XP20MA
<i>XPC</i>	p.R155X	c.567C>T	4	XP155MA XP156MA XP99MA XP98MA
<i>XPC</i>	p.R475EfsX18	c.1525insA	9	XP117MA
<i>XPC</i>	p.V548AfsX25	c.1747_1748delTG	9	XP102MA XP114MA XP115MA
<i>XPC</i>	p.R579X	c.1839C>T	9	XP23GO
<i>XPC</i>	p.Q723SfsX44	c.2271delC	12	XP150MA
<i>XPC</i>	p.I812del	c.2538_2540delATC	14	XP47MA
<i>XPD</i>	p.R112H	c.366G>A	5	XP87MA XP89MA
<i>XPD</i>	p.R616P	c.1878G>C	20	XP71MA
<i>XPD</i>	p.R616Q	c.1878G>A	20	XP90MA
<i>XPD</i>	p.D681H	c.2072G>C	21	XP87MA XP89MA
<i>XPD</i>	p.R683Q	c.2079G>A	22	XP19MA XP40MA XP46MA XP71MA
<i>XPD</i>	p.R683W	c.2078G>T	2	XP90MA
<i>XPD</i>	p.R722W	c.2195C>T	2	XP188MA
<i>XPG</i>	p.Q150X	c.891C>T	4	XP40GO
<i>XPG</i>	p.E727X	c.2622G>T	9	XP72MA
<i>XPG</i>	p.L778P	c.2776T>C	11	XP40GO
<i>XPG</i>	p.G805R	c.2856G>A	11	XP165MA
<i>XPG</i>	p.W814S	c.2884G>C	11	XP72MA

3.1.2.5. Conservation status of amino acids in XPG changed by missense mutations in XPC deleted by deletion mutation

The novel *XPC* deletion mutation p.I812del and the three novel *XPG* missense mutations are located in regions which are conserved within these proteins. *XPC* mutation p.I812del is located within the conserved BHD3 domain (amino acids 767 to 831 in human *XPC*) of the *XPC* protein. The region is required for binding of single stranded DNA (Camenisch *et al.*, 2009). The three *XPG* missense mutations p.L778P, p.G805R, and p.W814S are also located within a conserved region of the *XPG* protein: the I-region (amino acids 753 to 881 in human *XPG*) forms together with the N-region (amino acids 1 to 95 in human *XPG*) the active site of the endonuclease (Constantinou *et al.*, 1999). Sequence alignments of a stretch of *XPCs'* BHD3 domain (figure 8A) and *XPGs'* I-region (figure 8B) from human, mouse, and *Drosophila melanogaster* were performed and revealed the affected amino acid residues I812 (*XPC*), L778 (*XPG*), G805 (*XPG*), and W814 (*XPG*) to be conserved throughout these species.



Figure 8: Alignment of a stretch of amino acid sequences of the BHD3 domain from the *XPC* protein (A) and the I-region from the *XPG* protein (B). Amino acids which are affected in the patients are framed.

3.2. Characterization of the five novel *XPG* mutations

3.2.1. Functional relevance of the five novel *XPG* mutations

Complementation ability of the *XPG* alleles carrying mutations p.Q150X, p.E727X, p.G805R, p.L778P, and p.W814S (*XPG*_{mut}) was tested applying HCR (see 2.12.4.2.). Therefore, mutations were introduced into pXPG by site directed mutagenesis (see 2.14.2.2.) generating pXPG_{mut} plasmids (pXPG_{Q150X}, pXPG_{E727X}, pXPG_{G805R}, pXPG_{L778P}, and pXPG_{W814S}) to test the allele specific relevance of the mutations for NER. XP-G fibroblasts were simultaneously co-transfected with UVC irradiated or non-irradiated pcmvLUC, pRL-CMV for normalization, and pXPG_{mut}.

None of the mutated alleles could complement the NER capability compared to wild type pXPG. A slight residual repair activity was retained with XPG_{L778P} and XPG_{W814S}, whereas repair activity was completely abolished with XPG_{G805R} and the two truncated proteins XPG_{Q150X} and XPG_{E727X} (figure 9).

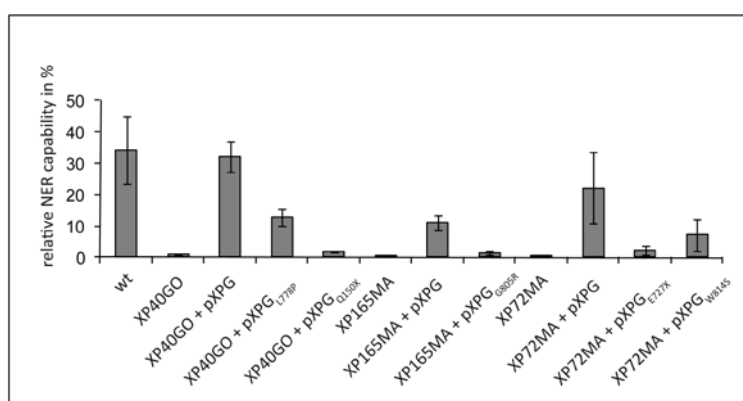


Figure 9: Determination of the allele specific complementation ability of the novel *XPG* mutations by HCR. Allele specific pXPG_{mut} expression vectors were generated from pXPG by site directed mutagenesis for all five mutations. Host cell reactivation was utilized and pXPG as well as pXPG_{mut} expression vectors were co-transfected along with the luciferase reporter gene plasmids pcmvLUC and pRL-CMV. Repair capability is depicted as percent luciferase expression (irradiated vs. unirradiated pcmvLUC). At least n=6 transfections were performed. NER capability of wild type (wt1) cells is the mean value of n=9 transfections.

3.2.2. Interaction of XPG_{mut} with TFIH

Previous studies revealed that XPG-TFIH interaction is impaired in XP-G/CS patients harbouring truncated XPG proteins but not in XP-G patients harbouring at least one missense mutation (Arab *et al.*, 2010; Ito *et al.*, 2007). To test the *XPG* mutations for TFIH interaction, C-terminal mycHis-tagged XPG expression vectors were constructed for the expression of wild type XPGmycHis and XPG_{mut}mycHis fusion proteins (figure 10). *XPG* cDNA was inserted into the

pcDNA3.1/myc-His(-)A (pcDNA) expression vector utilizing NotI (5') and KpnI (3'). Wild-type XPG cDNA was amplified from pXPG plasmid with forward primer XPGmycHis_for and reverse primer XPGmycHis_rev each carrying a NotI (5') or a KpnI (3') restriction site, respectively, and subcloned into pcDNA. For generation of the two truncated proteins XPG₁₋₁₅₀mycHis and XPG₁₋₇₂₇mycHis forward primer XPGmycHis_for was used again together with reverse XPGQ150mycHis_rev or XPGE727mycHis_rev, respectively. For the XPG_{mut}mycHis constructs carrying one of the three missense mutations wild type pXPGmycHis was used as template for site directed mutagenesis using primer G805Rfor/G805Rrev, L778Pfor/L778Pprev, and W814for/W814rev (primer sequences are summarized in table 2-9).

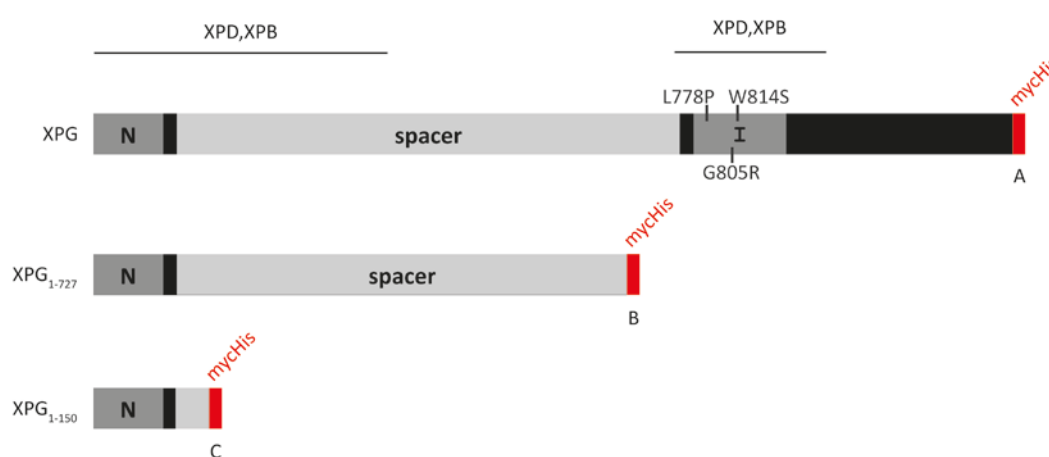


Figure 10: Schematic representation of pXPG(mut)mycHis constructs. The endonuclease motifs, N- and I-region, and interaction sites of XPG with TFIIH subunits XPB and XPD are indicated. **A:** The three missense mutations, which were introduced as single mutations in three pXPG_{mut}mycHis plasmids, are marked in the full length protein scheme. **B:** Scheme of the truncated XPGmycHis protein comprising amino acids 1-727. **C:** Scheme of the truncated XPGmycHis protein comprising amino acids 1-150.

For control purpose, the functionality of wild type XPGmycHis in NER context was analyzed by HCR and complementation of XP40GO fibroblasts (see 2.12.4.2.). As expected, the short mycHis-tag had no influence on the functionality of XPG in NER. The relative NER capacity of XP40GO cells increased from 1.4 % to 20.6 % by co-transfection of pXPGmycHis (figure 11). Therefore, it can be assumed that the mycHis-tag does not influence the function of the XPG protein within the cells.

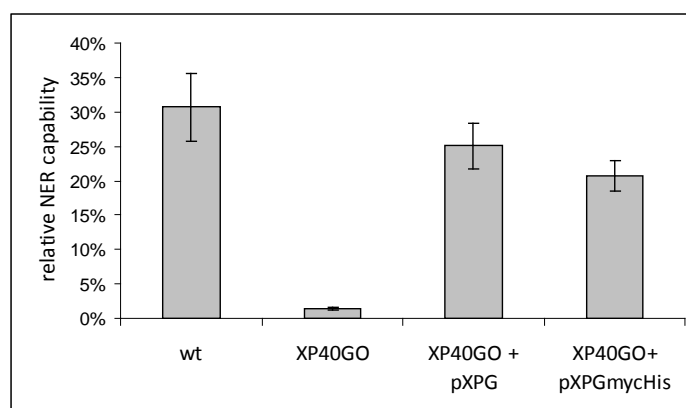


Figure 11: Determination of the complementation ability of XPGmycHis with HCR. Functionality of the C-terminal mycHis tagged XPG protein was determined by HCR. Expression vector pXPGmycHis was co-transfected along with UVC irradiated and non-irradiated luciferase reporter gene plasmid pcmvLUC in XP40GO cells. Repair capability is depicted as percent luciferase expression (irradiated vs. unirradiated pcmvLUC). At least n=3 transfections were performed. NER capability of wild type (wt 1) cells is the mean value of n=9 transfections.

Investigation of the interaction of XPG_(mut)mycHis constructs with TFIIH subunits was performed by over expression of the fusion proteins in HEK293A cells followed by immunoprecipitation using α myc antibody (see 2.15.2.). Analysis of the putative co-immunoprecipitation (co-IP) of TFIIH subunits XPD and cdk7 was done by Western Blot (2.15.3.).

Both proteins XPD and cdk7 were co-immunoprecipitated with XPG_{wt}mycHis under physiological conditions of 150mM NaCl using α myc antibody. Under the same conditions, co-immunoprecipitation of XPD (figure 12A left side) and cdk7 protein (figure 12C) was not observed or greatly diminished with all five XPG_{mut}mycHis constructs including the three missense mutations. Neither XPG_(mut)mycHis nor XPD or cdk7 were detected by immunoblot analysis of the control IP samples (10B left side and 10D). This indicates that IP and co-IP did not occur due to unspecific binding of the proteins to the IP agarose or the α myc antibody. Moreover, XPD (right sites of figure 12A and 12B) as well as cdk7 (figure 12E) were detected in the input controls (a 65 μ g) of each cell lysate. The immunoblot analysis revealed slightly decreased amount of the XPG_{mut}mycHis proteins (except XPG_{E727}mycHis) compared to wild type XPGmycHis. However, figure 12F shows the result of an immunoprecipitation with different amounts of wild type XPGmycHis: XPD protein is co-immunoprecipitated in both samples, independent from the amount of XPGmycHis.

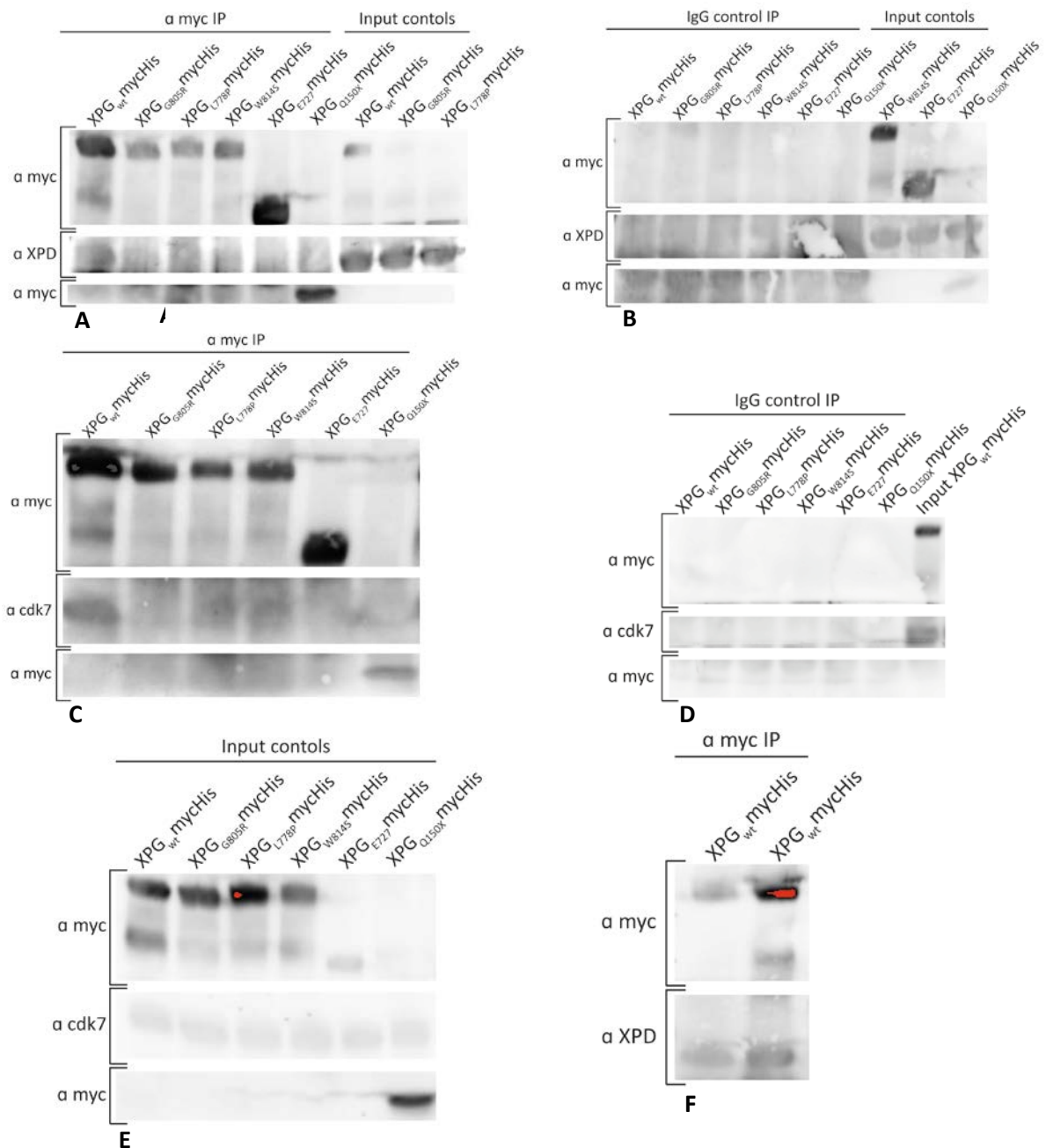


Figure 12: Co-immunoprecipitation of XPD and cdk7 with XPGmycHis. HEK293A cells were transfected with pXPGmycHis and pXPG_{mut}mycHis plasmids. Whole cell extracts were used for immunoprecipitation with α myc antibody as well as α IgG antibody for control purpose. Purified complexes were separated by SDS PAGE in precast 4 % to 12 % gradient gels and immunoblotted with the antibodies indicated. **A:** Analysis of the XPD co-IPs with α myc antibody for XPG_{wt}mycHis and the five XPG_{mut}mycHis proteins (left side). Input controls of transfected cells lysates used for XPD co-IPs (right side). **B:** Analysis of the (XPD co-IP) control IPs with IgG antibody (left side). Input controls of transfected cells used for the XPD co-IPs (right side). **C:** Analysis of the cdk7 co-IPs with α myc antibody for XPG_{wt}mycHis and the five XPG_{mut}mycHis proteins. **D:** Analysis of the (cdk7 co-IP) control IPs with IgG antibody. **E:** Analysis of the input controls of transfected cell lysates used for cdk7 co-IPs. **F:** Analysis of XPD co-IP with different amounts of wild type XPGmycHis protein.

3.2.3. Influence of the XPG mutations on XP protein recruitment to sites of local DNA damage and on subsequent XP protein redistribution

The influence of the novel XPG mutations on recruitment of XP proteins to sites of local DNA photodamage and on subsequent XP protein redistribution was investigated *in vivo* by immunofluorescence. Time-course experiments for XP protein recruitment to DNA photodamage as well as release from photodamage 6 min, 15 min, 30 min, 3 h, and 24 h after UV irradiation in fibroblasts cell cultures from the three XP-G patients were compared to wild type fibroblast cell cultures. Patients and wild type fibroblasts were seeded on glass cover slips and irradiated through 8 μm isopore polycarbonate membrane with 100 J/m² UVC to generate sites of local DNA damage. Antibodies against the XP proteins XPA, XPB, XPC, ERCC1 (complexed with XPF) and XPG were used to examine the recruitment of the corresponding protein to the UV-induced DNA photolesions as well as its redistribution. Removal of DNA photoproducts was studied using antibodies directed against the main UV-induced photolesions CPDs and 6,4PPs. Additionally, double staining against each of the XP proteins together with CPD photolesions was performed for control purpose. For relative quantification at least 100 nuclei were evaluated for the calculation of protein or photodamage spot positive nuclei staining in percent. Results of the quantification of XP protein spot positive nuclei in % in wild type and patients' cells are depicted for each XP protein and two photolesions in figure 13. Pictures of the double staining of each XP protein together with CPD photolesions in the patients' cells are shown in figure 14. Double staining of XPG and CPD is shown in wild type cells. Pictures of the recruitment and redistribution of the XP proteins in XP40GO (exemplary) and wild type cells at different time points are depicted in figure 15.

No recruitment of XPG in the patients' cells

XPG fluorescence staining in wild type cells revealed rapid recruitment of XPG protein to photodamage (21 % and 17 % XPG positive cell nuclei 6 min and 15 min after UV irradiation, respectively). There was also rapid redistribution of wild type XPG protein from the DNA photolesions at 30 min after UV irradiation (only 2 % remaining XPG positive cell nuclei). By 6 h and 24 h after cell irradiation XPG was no longer detectable at sites of DNA photolesions. In contrast, no positive XPG staining in cell nuclei was observed in all three patients' fibroblasts at any time point after UV irradiation indicating no recruitment of mutated XPG to photodamages. The applied XPG antibody 8H7 maps to the C-terminal region of XPG. Thus, truncated proteins XPG_{Q150X} in XP40GO and XPG_{E727X} in XP72MA would not be recognized if

they were expressed, but the XPG proteins containing missense mutation should be recognized (figure 13E).

Early recruitment of other XP proteins is selectively delayed in XP-G patient cells

As expected, all fibroblasts (wild type and XP-G) were stained positive for CPDs (figure 13F, figure 15C) and 6,4PPs (figure 13G, figure 15c) immediately (6 min) after UV irradiation (range from 45 % to 57 % positive cell nuclei). At this time point, wild type and XP-G cells already showed considerable amounts of XP protein localization to the photolesions in the nuclei. The XPA protein was equally rapid recruited in wild type cells as well as in cells from the XP-G patients XP40GO, XP165MA, and XP72MA (50 %, 46 %, 36 %, respectively) (figure 13A). The rapid recruitment of XPB was comparable in wild type, XP40GO, and XP165MA cells (26 %, 15 %, and 22 %, respectively). There was a markedly reduced and delayed XPB recruitment in XP72MA (1 %) (figure 13B). XPC protein was normally recruited in XP165MA cells compared to wild type cells (26 % in XP165MA vs. 21 % in wild type). In XP40GO and XP72MA fibroblasts early XPC recruitment was clearly delayed (7 % and 4 %) (figure 13C). ERCC1 (complexed with XPF) protein recruitment was delayed in all three XP-G patient cells compared to wild type (15 % in XP165MA and 6 % in XP40GO and 1 % in XP72MA vs. 30 % in wild type) (figure 13D).

No redistribution of other XP proteins in all XP-G cells

Thirty minutes after UV irradiation the XP-G cells reached their maximum of XP protein recruitment to photodamage (range from 39 % to 60 %). All XP proteins tested (XPC, XPB, XPA, and ERCC1) were recruited to sites of local photodamage. At this time point, wild type cells already released nearly all XP proteins from DNA lesions (range from 2% to 9 %) (figure 13 A to 13E, figure 15). By 3 h after UV treatment, all XP proteins still persisted at sites of DNA damage in all XP-G cells. In contrast, in wild type fibroblasts the XP proteins were already completely redistributed (figure 13A to 13E, figure 15). After 24 h, redistribution of XP proteins also started in XP-G cells, however, a considerable amount of XP proteins persisted in all patients' cells at sites of local photo- damage (range from 13 % to 49 %). Interestingly, in XP165MA cells, the most severely affected XP-G/CS patient, the XP proteins were found to persist the most (figure 13A to 13E).

Decreased photoproduct removal in XP-G cells

A faster removal of 6,4PPs compared to CPDs has been shown previously (Oh et al., 2007). Thus, the defect in DNA photoproduct removal in XP-G cells was most visible by the removal of 6,4PPs. Immediately (6 min) after UV irradiation, 45 % of the wild type, 56 % of the XP40GO, 40

% of the XP72MA, and 45 % of the XP165MA cells were stained positive for 6,4PPs. Only 1 h later, positive 6,4PP stained wild type cells already decreased to 10 %. In contrast, 48 %, 50 %, and 53 % of the XP40GO, XP72MA, and XP165MA cells, respectively, were still positive for 6,4PP staining. No 6,4PP staining was detectable in the wild type cells 3 h after UV treatment (figure 13G, figure 15C). Indeed, the 6,4PP positive spots decreased also in the XP-G cells, but even after 24 h a complete removal was not observed (15 % in XP40GO, 12 % in XP72MA, 14 % in XP165MA) (figure 13G, figure 15C). This also indicated that all XP-G fibroblasts could nevertheless remove two thirds of their 6,4PPs within 24 h (figure 13G). Accordingly, removal of CPDs was also delayed in fibroblasts from all three XP-G patients' cells compared to wild type fibroblasts. Directly after UVC irradiation, 55 % of the wild type, 57 % of the XP40GO, 57 % of the XP72MA, and 58 % of the XP165MA fibroblasts were stained positive for CDP spots. By 24 h after UV treatment, CPDs were decreased from 55 % to 36 % in wild type cells. In contrast, nearly no removal of CPD was observed in XP40GO, XP72MA, and XP165MA cells (45 %, 45 %, and 48 %, respectively) (figure 13F).

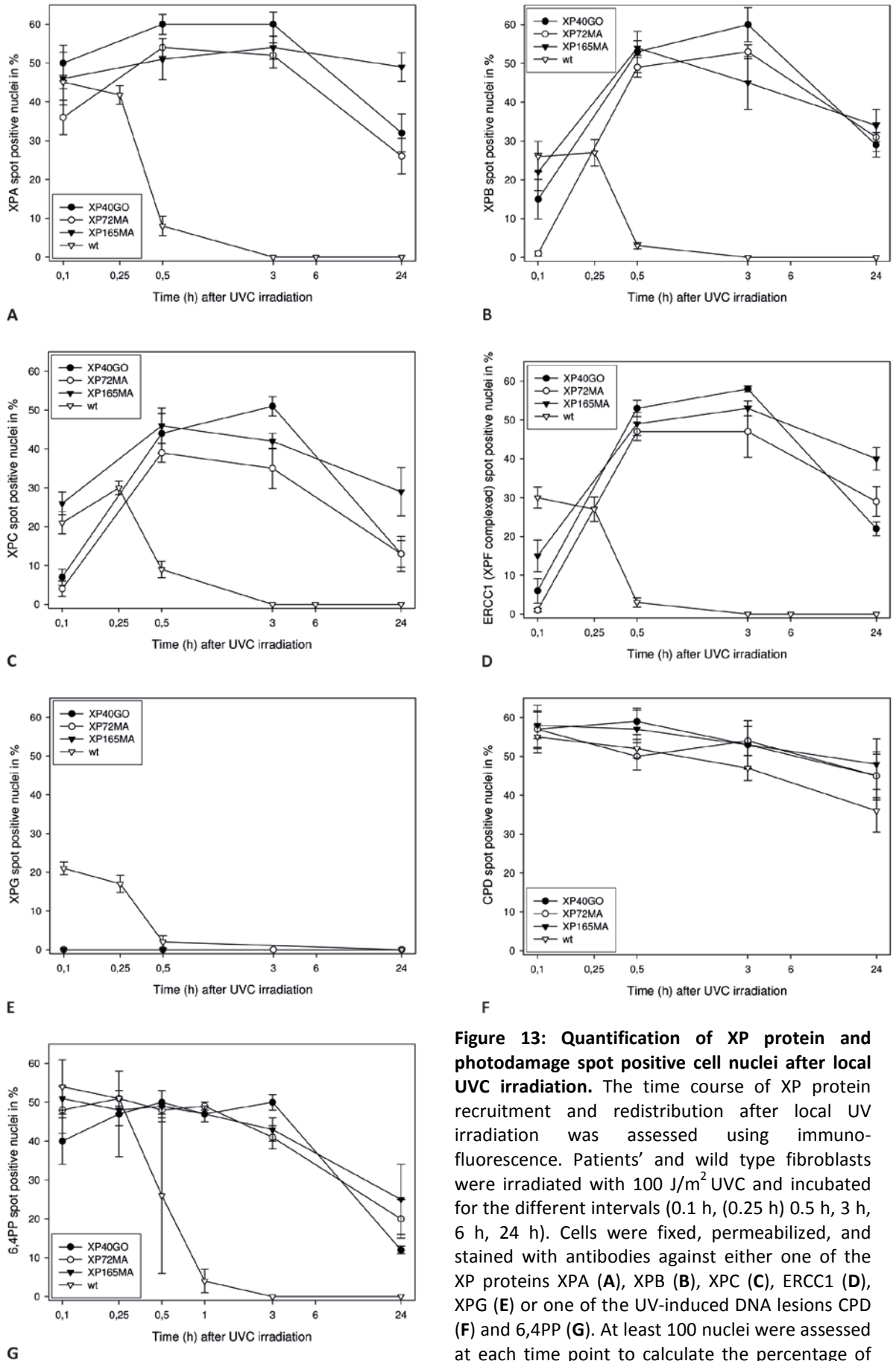


Figure 13: Quantification of XP protein and photodamage spot positive cell nuclei after local UVC irradiation. The time course of XP protein recruitment and redistribution after local UV irradiation was assessed using immunofluorescence. Patients' and wild type fibroblasts were irradiated with 100 J/m² UVC and incubated for the different intervals (0.1 h, 0.25 h, 0.5 h, 3 h, 6 h, 24 h). Cells were fixed, permeabilized, and stained with antibodies against either one of the XP proteins XPA (A), XPB (B), XPC (C), ERCC1 (D), XPG (E) or one of the UV-induced DNA lesions CPD (F) and 6,4PP (G). At least 100 nuclei were assessed at each time point to calculate the percentage of positively stained nuclei.

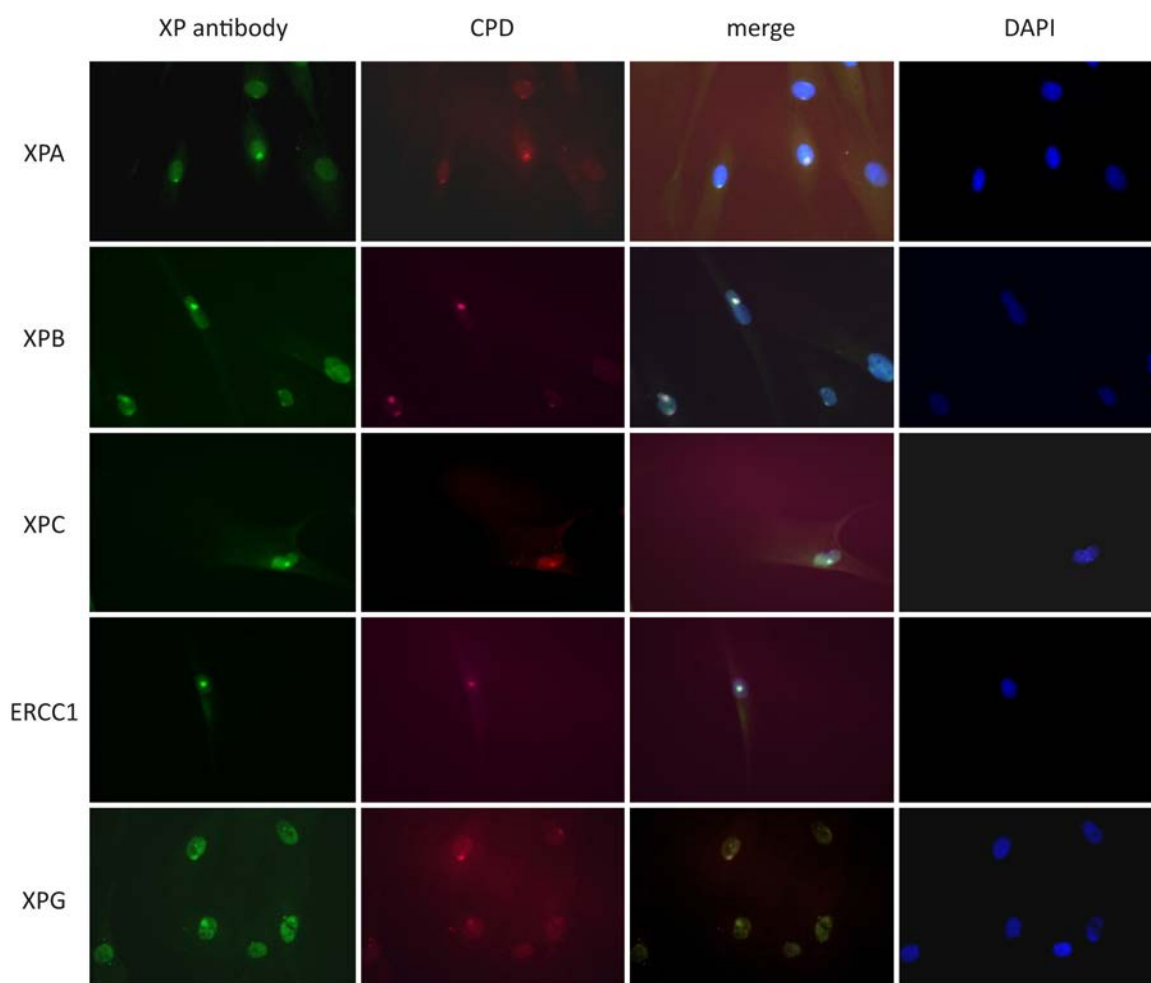


Figure 14: Immunofluorescence double staining of XP proteins and CPD photoproducts. Cells were irradiated with 100 J/m^2 UVC through an $8 \mu\text{m}$ pore filter membrane inducing sites of local DNA photodamage. Afterwards, cells were incubated for 10 min before they were fixed, permeabilized and double stained against the XP proteins indicated and CPD photolesions. Co-localisation of XPA, XPB, XPC and ERCC1 with CPD is shown in XP-G patients' fibroblasts and co-localisation of XPG with CPD is shown wild type cells (bright fluorescent spots within the nuclei).

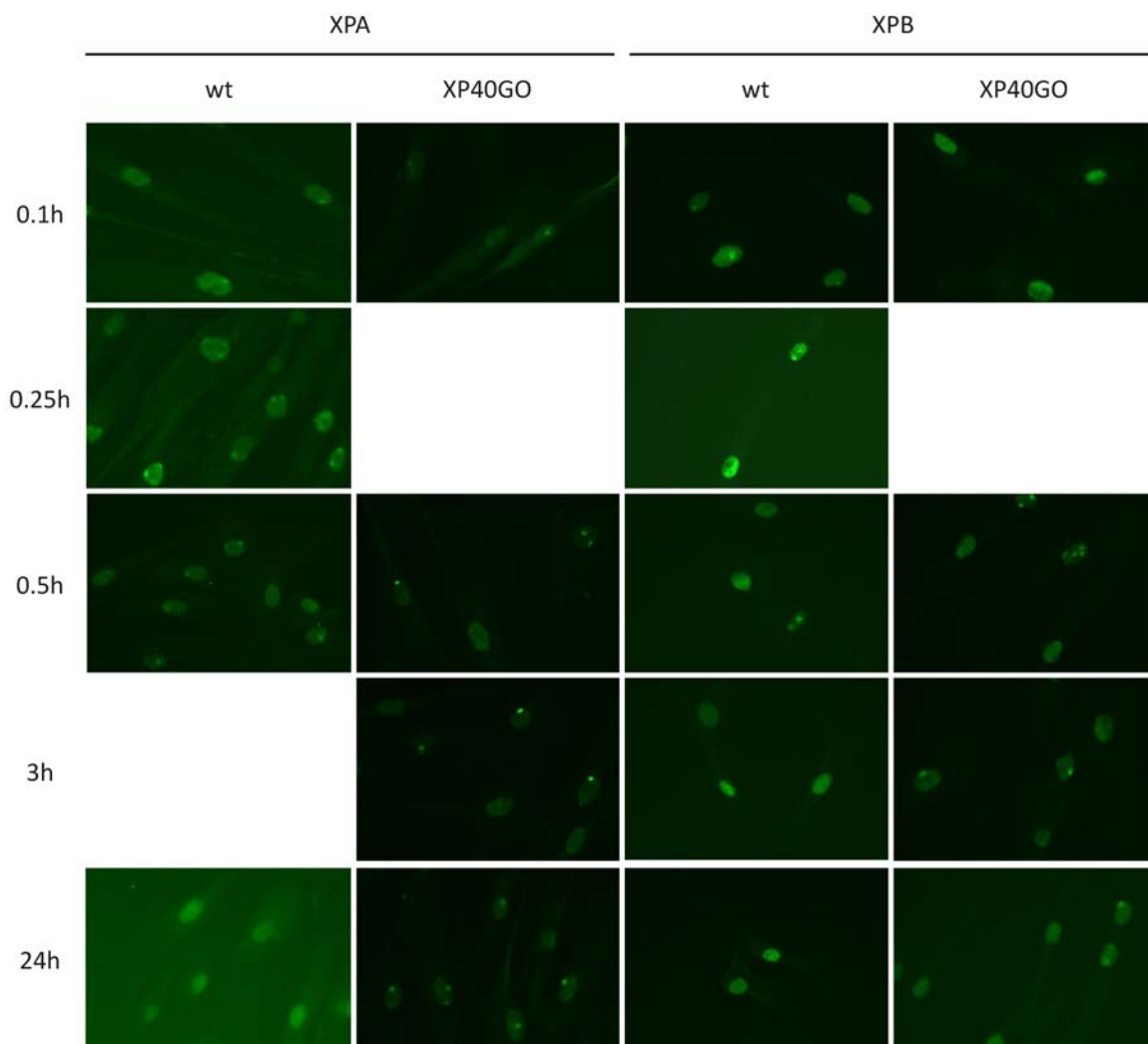


Figure 15A: Immunofluorescence staining of XP proteins in wild type and XP40GO fibroblasts. Cells were irradiated with 100 J/m^2 UVC through an $8 \mu\text{m}$ pore filter membrane inducing sites of local DNA photodamage. Afterwards, cells were further incubated for the time intervals indicated, before they were fixed, permeabilized, and stained with antibodies directed against XP proteins XPA and XPB. Bright fluorescent spots in the nuclei indicate XP proteins localized to UV-induced DNA photolesions.

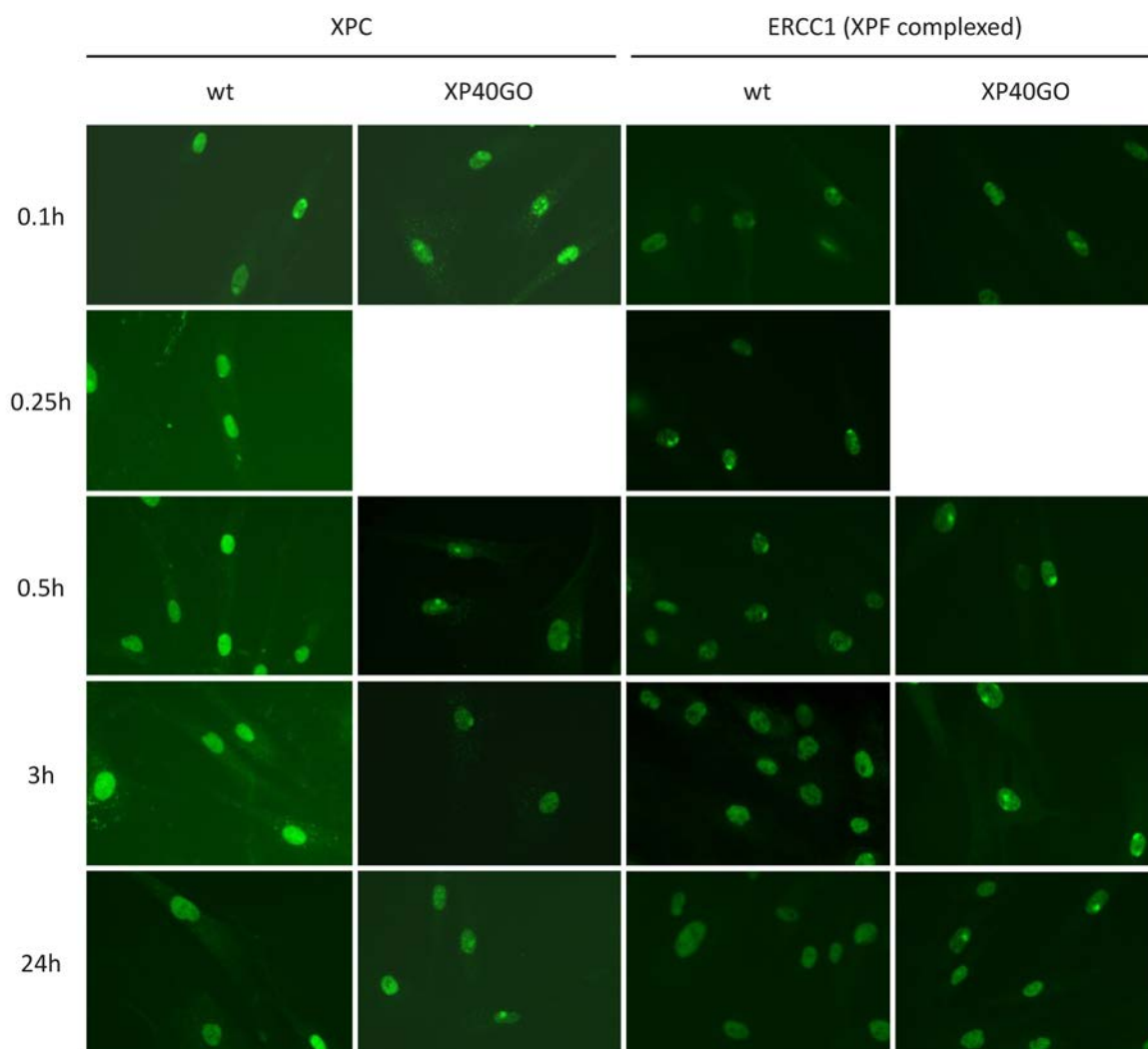


Figure 15B: Immunofluorescence staining of XP proteins in wild type and XP40GO fibroblasts. Cells were irradiated with 100 J/m^2 UVC through an $8 \mu\text{m}$ pore filter membrane inducing sites of local DNA photodamage. Afterwards, cells were further incubated for the time intervals indicated, before they were fixed, permeabilized, and stained with antibodies directed against XP proteins XPC and ERCC1. Bright fluorescent spots in the nuclei indicate XP proteins localized to UV-induced DNA photolesions.

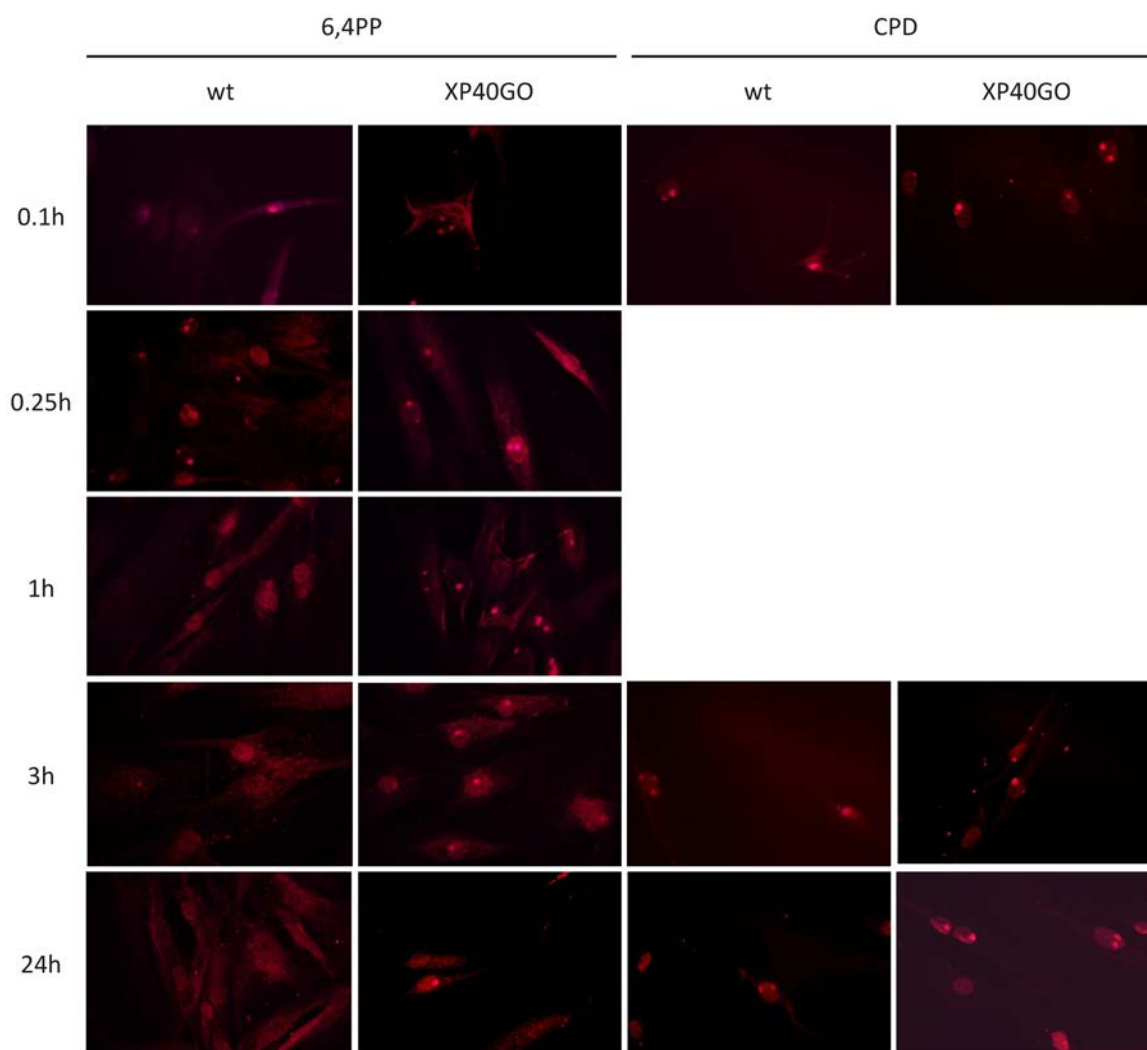


Figure 15C: Immunofluorescence staining of XP proteins in wild type and XP40GO fibroblasts. Cells were irradiated with 100 J/m^2 UVC through an $8 \mu\text{m}$ pore filter membrane inducing sites of local DNA photodamage. Afterwards, cells were further incubated for the time intervals indicated, before they were fixed, permeabilized, and stained with antibodies directed against photolesions 6,4PP and CPD. Bright fluorescent spots in the nuclei indicate XP proteins localized to UV-induced DNA photolesions.

4. Discussion

The three NER defective syndromes Xeroderma pigmentosum, Cockayne Syndrome, and Trichothiodystrophy arise from defects in one of ten genes functioning in the nucleotide excision repair pathways (GGR or TCR) or from defects in the gene encoding the translesional DNA polymerase eta (*XPV*). There is considerable phenotypic heterogeneity between the disorders and different mutations within the same gene may result in different clinical phenotypes (Bootsma, 2002; Kraemer *et al.*, 2007).

Characterization of fibroblasts from NER defect syndrome patients and correlation of the molecular results with patients' course of disease is the first step towards the understanding of the molecular context underlying a certain phenotype. Moreover, these studies improve the prediction of the course of disease for newly diagnosed patients. Therefore, one part of the thesis was the characterization of fibroblast cells from patients suffering from a defect in the nucleotide excision repair.

Seventy-five NER defective primary fibroblast cell cultures, isolated from skin punch biopsies of the patients, were provided from the University Clinics Göttingen and Mannheim. Based on the low frequency of NER associated diseases, this collective represents the largest collection of NER deficient fibroblasts in Germany and is therefore a source of novel information regarding phenotype-genotype correlations.

Cells were intensively analyzed for their phenotypic characteristics regarding their post-UV survival (see 3.1.2.1) and their relative NER capability (see 3.1.2.2.). The assignment of the complementation group was performed (see 3.1.2.2.) and the mRNA expression level of the mutated gene was assessed (see 3.1.2.3.). The genetic defect of 23 primary fibroblast cell cultures was pinpointed during the thesis (see 3.1.2.4.).

Mutational analysis of 12 XP-C, eight XP-D, and three XP-G patients identified ten novel disease-causing mutations: four in the *XPC*, one in the *XPB*, and five in the *XPG* gene. Phenotype-genotype correlation of the *XPG* mutations revealed that missense mutations found in patients XP72MA and XP165MA resulted in the XP/CS complex. This clinical entity normally occurs in XP-G patients harbouring mutations that result in the expression of truncated XPG proteins from both alleles (Emmert *et al.*, 2002; Nouspikel *et al.*, 1997). A destabilized architecture of the transcription factor TFIIH due to impaired XPG-TFIIH interaction has been reported to be responsible for the CS symptoms in these patients (Arab *et al.*, 2010; Ito *et al.*, 2007).

Based on the unusual phenotype-genotype correlation of the XP-G patients the five novel *XPG* gene mutations were comprehensively analyzed on the molecular level in the second part of the theses.

4.1. Clinical symptoms of the patients

4.1.1. Clinical symptoms of XP-C patients

The mean age at XP diagnosis of the 12 XP-C patients analyzed was 8.75 years and the mean age for the development of the first skin cancer was 7.3 years in these patients. All patients who developed skin cancer exhibited at least one non-melanoma skin cancer (NMSC; basal and/or squamous cell carcinoma) in sun-exposed skin areas. The clinical findings are quite comparable to findings of a few studies reporting on larger XP-C patient cohorts. Chavanne et al. reported a mean age of 11.7 years for first skin cancer development in seven XP-C patients from Southern Europe (Chavanne *et al.*, 2000). Khan et al. described development of skin cancers at an early age (Khan *et al.*, 2006), and Soufir et al. found similar clinical symptoms in their group of 56 investigated XP-C patients from Maghreb including photosensitivity and numerous skin cancers (Soufir *et al.*, 2010). It has been found that NMSC and melanoma have a different distribution on XP patients' skin. Similar to the normal population melanomas are more evenly distributed throughout the body, whereas NMSC is mainly located on the head and forearms of the patients (Kraemer *et al.*, 1994). Different mechanisms in the carcinogenesis of NMSC and melanoma may be the reason for this observation. Development of NMSC is predominantly a result of UV-induced DNA damage. The identification of the UV-characteristic C to T and CC to TT signature of mutations in the p53 suppressor gene in NMSC from XP patients supports this assumption on the molecular level (Giglia *et al.*, 1998). The finding that all patients who developed skin malignancies exhibited NMSC clearly demonstrates the importance of DNA repair to especially protect against NMSC.

The XP-C patients showed a rather homogeneous clinical phenotype with pronounced sun sensitivity and skin symptoms prevailing. None of the four newly identified mutations resulted in "XP plus neurological abnormalities". Only one patient (XP20MA) carrying the novel mutation p.A116YfsX4 was described to exhibit an overall reduced intellectual capacity. However, this does not correspond to the common neurological degeneration of "XP plus neurological abnormalities" where neurological symptoms become obvious around the fifth to tenth year of life (Rapin *et al.*, 2000). In line with this study, Khan et al. reported 16 (Khan *et al.*, 2006) and Chavanne et al. 12 XP-C patients with no XP type neurological symptoms (Chavanne *et al.*, 2000). Soufir et al. described 56 XP-C patients of whom 49 carried the same

p.V548AfsX25 mutation that was also found in three patients in this study (Soufir *et al.*, 2010). Only two of those 49 patients showed mental retardation. However, the patients carried the mutation in a homozygous state and there was high consanguinity in the study population. Recently, two XP-C patients from different consanguine XP-C families with the same mutation were described: one with and the other without neurological abnormalities (Khan *et al.*, 2009). The authors concluded that the neurological symptoms probably resulted from another mutated gene due to consanguinity, or from mutation-dependent altered interaction of modifier proteins with XPC. In close mating the proportion of genes shared is 25 % (identical by descent), leading to the chance of homozygosity by descent of 1/8 (Harper, 1988). Thus, close consanguinity confers an increased probability of simultaneous occurrence of other recessive disorders. Nonsyndromic hearing loss has been reported to occur at increased frequency in association with parental consanguinity (Bittles *et al.*, 2004; Sajjad *et al.*, 2008). Patient XP20MA also carried homozygous mutations suggesting the possibility of consanguinity.

4.1.2. Clinical symptoms of the XP-D patients

XP-D was the second most frequent complementation group among the 23 patients analyzed in this study. This is in line with results from Bradford *et al.* assessing a long term follow up of 106 XP patients where 30 XP-D patients also represented the second most common complementation group beside 46 XP-C patients (Bradford *et al.*, 2011). In the present study, the mean age of diagnosis was 9.4 years among the XP-D patients. Four of the five XP-D patients exhibiting the XP phenotype developed skin cancer, but the onset of tumor development was relatively late compared to the 12 XP-C patients (range from 15 years to 52 years in XP-D patients vs. range from 3 years to 14 years in XP-C patients). In addition, XP90MA did not develop skin cancer until the age of 15 years. Taylor *et al.* summarized clinical details of the skin of 17 XP-D patients exhibiting the XP phenotype. Eleven patients also developed no skin cancer until a mean age of 21 years (ranging from 4 to 48 years) (Taylor *et al.*, 1997). This may indicate a later onset of skin cancer in XP-D patients compared to XP-C patients. However, all patients, described by Taylor *et al.*, were reported to be sun sensitive (Taylor *et al.*, 1997). In the present study, XP phenotype patient XP19MA exhibited no increased sun sensitivity. XP plus neurological symptoms often occurs in complementation group XP-D (Bradford *et al.*, 2011), but none of the five XP-D patients exhibiting the XP phenotype showed additional neurological abnormalities.

The XP/CS phenotype in XP89MA was relatively mild compared to other XP/CS patients of complementation group XP-D. Broughton *et al.* described a XP-D patient with severe XP/CS

symptoms who died at the age of 16 months (Broughton *et al.* 1995). Two other XP-D patients suffering from XP/CS symptoms, described by Theron *et al.*, also died at the age of 15 and 24 months. The latter one additionally developed a squamous cell carcinoma (Theron *et al.*, 2005). In contrast to that, XP89MA did not exhibit any skin cancer until the age of 15 years. In addition, beside a slight intellectual impairment, the patient was reported to go to school. Unfortunately, no additional clinical data were available for the two patients suffering from the TTD phenotype, XP87MA and XP188MA.

4.1.3. Clinical symptoms of the XP-G patients

Two of the three XP-G patients, XP72MA and XP165MA, exhibited XP/CS symptoms. The XP/CS phenotype was reflected by sun sensitivity since birth and freckling within the sun-exposed skin areas as well as dwarfism, microcephaly, muscular hypotension, ataxia, and neurological impairment. Patient XP165MA was most severely affected and died at the age of two years from meningitis. Patient XP72MA was more mildly affected and at the age of seven years enrolment in a special school was discussed. Moreover, the patient did not develop any skin cancer until this age. This is in good agreement with previous clinical reports about seven XP/CS complex XP-G patients with early onset of CS symptoms exhibiting similar symptoms of sun sensitivity, short statures, microcephaly, and neurological impairment. These six patients, like XP165MA, had a short lifespan and died at the age of 11 months to 6.5 years. (Arlett *et al.*, 1980; Emmert *et al.*, 2002; Moriwaki *et al.*, 1996; Nospikel *et al.*, 1997; Zafeiriou *et al.*, 2001). Development of skin cancer was only reported for one of these patients, who was severely affected and died at the age of 11 months (Zafeiriou *et al.*, 2001). Compared to the XP-C patients developing their first skin cancer at a mean age of 7.3 years, the absence of skin cancer development in most of the XP/CS patients might be explained by their short lifespan.

4.2. Functional deficits in the NER deficient cells

4.2.1. Increased UV sensitivity in the NER deficient cells

UV sensitivity of fibroblasts from XP patients was first shown by Gartler *et al.* in 1963 (Gartler, 1963). Later on, a defect in the NER pathway was found to be the molecular reason for this observation (Cleaver, 1968; Reed *et al.*, 1969). Additionally, bacterial mutants, defective in excision repair, were also found to exhibit invariably UV sensitivity (Kondo *et al.*, 1970). Therefore, determination of post-UV cell survival became obligatory in the identification of NER deficient fibroblast cells (Broughton *et al.*, 2001; Chavanne *et al.*, 2000; Khan *et al.*, 2006; Khan *et al.*, 2010). Accordingly, fibroblast cells analyzed during this thesis were also examined

for their post-UV survival using the MTT assay. As expected, all cells showed a reduced survival after UV irradiation at both cell densities (5000 cells and 7500 cells).

Mean post-UV survival of the XP-C cells after 30 J/m² UVC was 50 % and 49 % at a density of 5000 and 7500 cells, respectively. XP-D cells tested under the same conditions exhibited a survival of 56 % and 52 %, whereas wild type fibroblasts exhibited a mean post-UV survival of 81 % and 87 %. Other studies reported a more pronounced UV sensitivity for XP-C and XP-D fibroblast cells with survival rates of 10 % and less with similar UVC irradiation doses. Differences in the measured UV sensitivity may result from the experimental procedures used for determination. Chavanne et al. measured unscheduled DNA synthesis of XP-C cells after UV treatment (Chavanne *et al.*, 2000). Khan et al. used the MTS assay for the analysis of XP-C cells' post-UV survival (Khan *et al.*, 2010). This assay is indeed similar to the MTT assay, but the procedure (Imoto *et al.*, 2002) was differing from the protocol performed in this thesis. Broughton et al. assessed survival of XP-D fibroblasts by determination of the apoptosis level of the sub-G1 cell fraction of previously irradiated fibroblasts using flow cytometry (Broughton *et al.*, 2001). Remaining post-UV survival may also result from additional processes of the cells to cope with the DNA damages for example translesional synthesis (Nakajima *et al.*, 2004). Furthermore the XPC protein is dispensable for transcription coupled repair. Thus, XP-C cells are still proficient of TCR and remove photoproducts from actively transcribed DNA strands which is particularly important in non-dividing cells (Kantor *et al.*, 1990).

A clear correlation between clinical sun sensitivity of the XP-C patients and post-UV cell survival is hindered by the absence of appropriate data for eight of the twelve patients. Moreover, it has been reported previously that many XP-C patients do not burn on minimal sun exposure and tan normally despite developing freckles and skin cancers later on in life (Khan *et al.*, 2009). In addition, XPC^{-/-} mice do also not exhibit photosensitivity (Berg *et al.*, 1998).

Among the XP-D patients sun sensitivity was described for XP40MA, XP71MA, XP89MA, and XP90MA whereas XP19MA was described to exhibit no sun sensitivity. In contrast to the clinical results, fibroblasts from XP19MA were more UV sensitive than those of the other four patients. This indicates no correlation between patients' UV sensitivity and post-UV cell survival of their corresponding fibroblasts.

Fibroblasts from two of the three XP-G patients (XP165MA and XP72MA) exhibited a markedly reduced post-UV survival compared to the XP-C and XP-D patients' cells (figure 5 compared to figures 3 and 4). All cells from patient XP165MA died at 12 J/m² UVC and only 2 % (5000 cells)

and 4 % (7500 cells) of fibroblasts from patient XP72MA survived after irradiation with 15 J/m² UVC. In contrast, none of the XP-D or XP-C cells exhibited a survival less than 19 % (XP19MA fibroblasts after 16 J/m² UVC) at any irradiation dose. Such an increased UV sensitivity has been reported previously for XP-G/CS cells from other patients (Emmert *et al.*, 2002; Moriwaki *et al.*, 1996). Additionally, a correlation between cells' post-UV survival and patient's photosensitivity has been described for the XP/CS complex (Emmert *et al.*, 2002; Nospikel *et al.*, 1997; Zafeiriou *et al.*, 2001). In line with these findings, a comparison of the clinical data of XP165MA and XP72MA also paralleled the marked sun sensitivity with the clinical notion of photosensitivity. Furthermore, the most severely affected patient, XP165MA, also revealed the most reduced post-UV cell survival.

4.2.2. Decreased relative NER capability in the NER deficient cells

Relative NER capability of the patients' fibroblasts was determined by HCR. Expression of the firefly reporter gene from the UVC irradiated plasmid vs. expression from the non-irradiated plasmid was markedly reduced in all patients' cells compared to wild type fibroblasts. Low enzyme expression levels reflect the inability of NER deficient fibroblasts to remove UVC induced 6,4PPs and CPDs from the transcribed DNA strand in a proper way. False positive expression levels due to cell division are excluded by the non-replicative character of the reporter gene plasmids. Mean relative NER capacity of five wild type fibroblasts was 30.7 %. This is in line with previous results from Emmert *et al.* (Emmert *et al.*, 2002). All patients' cells exhibited a decreased relative NER capacity as it has been shown previously for XP-C (Khan *et al.*, 2006), XP-D (Emmert *et al.*, 2009; Ueda *et al.*, 2009), and XP-G cells (Emmert *et al.*, 2002; Moriwaki *et al.*, 2012; Yoneda *et al.*, 2007). Mean relative NER capacity of the XP-C cells was somewhat increased (4 %) compared to fibroblasts from XP-D (1.5 %) and XP-G (2 %) patients. Again the intact transcription coupled repair pathway of XP-C cells (Kantor *et al.*, 1990) might be a reason for this slight difference. According to previous studies, the cellular repair deficiency of XP-C, XP-D, and XP-G fibroblasts could be complemented by co-transfection of plasmids expressing wild-type *XPC*, *XPD*, and *XPG* cDNA, respectively (figure 6) (Emmert *et al.*, 2002; Emmert *et al.*, 2009; Khan *et al.*, 2006; Moriwaki *et al.*, 2012; Ueda *et al.*, 2009; Yoneda *et al.*, 2007).

4.3. mRNA levels of the mutated gene are only effected in XP-C patients

The expression of the mRNA level of all XP genes, *XPA* to *XPG*, and the gene coding for DNA polymerase eta, *XPV*, was determined for a total of 75 NER deficient primary fibroblast

cultures and nine wild type primary fibroblast cultures (appendix table A-18). The expression levels were normalized to the expression levels of two housekeeping genes β -actin and *GAPDH* and the mean expression level of the wild type fibroblasts was set to 100 %.

A decreased mRNA expression level in XP-C cells has been reported previously: Khan et al. measured a mean *XPC* mRNA level of 24 % in a total of 16 XP-C patient cells using quantitative real-time PCR. The mean *XPC* mRNA expression in cells from 26 XP-C heterozygotes was 59 % compared to normal cells (Khan *et al.*, 2006). This was also corroborated by and Cartault et al. who reported 10 % *XPC* mRNA expression in XP-C homozygotes and 75 % expression in XP-C heterozygotes compared to wild-type cells (Cartault *et al.*, 2011). In addition, Emmert et al. reported on two XP-C patients with equal insertion/deletion mutations exhibiting *XPC* mRNA expression levels of 36 % and 32 % compared to 100 % expression in wild type cells (Emmert *et al.*, 2006b). The underlying mechanism for this gradually reduced *XPC* mRNA level depending on the number of mutated alleles (59 % and 75 % in heterozygotes vs. 24 % and 10 % in homozygotes) may involve the nonsense-mediated message decay pathway (Lejeune and Maquat, 2005; Maquat, 2005) as all mutations resulted in premature stop codons. However, Northern blot analysis may not be sensitive enough to detect these changes as Chavanne et al. reported no significant differences in XP-C heterozygote parents and only slightly reduced *XPC* mRNA expression in their XP-C homozygote children (60% to 80% of normal) (Chavanne *et al.*, 2000).

In agreement with these previous findings, all XP-C cells which were later found to harbour mutations resulting in truncated XPC proteins exhibited significant decreased *XPC* mRNA expression levels ranging from 9.5 % to 25.7 % ($p < 0.001$) compared to the mean level of nine wild type fibroblast cell cultures set to 100 % (figure 7A). Moreover, fibroblasts from XP23GO, XP98MA, XP99MA, and XP115MA were identified as XP-C cells due to their decreased *XPC* mRNA expression levels (figure 7A). In contrast, the only patient who was later found to harbour a mutation not resulting in a truncated XPC protein but in the deletion of the conserved amino acid isoleucine 812 (figure 8A) revealed an up-regulated *XPC* mRNA level. This is in line with the assumption that the nonsense-mediated message decay pathway is probably involved in the modulation of *XPC* mRNA levels. Nonsense-mediated message decay may not be effective in this case as it depends on the presence of a nonsense codon > 50-55 nucleotides upstream of an exon-exon junction (Lejeune and Maquat, 2005; Maquat, 2005).

Expression levels of mutated *XPD* and *XPG* genes in XP-D and XP-G patients have to be evaluated carefully. In contrast to the *XPC* mRNA expression in XP-C patients, expression levels of *XPD* and *XPG* genes from fibroblasts of corresponding complementation groups have not

extensively been studied previously. Moreover, the mRNA expression levels were determined measuring mRNA of one sample (in duplicates) obtained from non-synchronized patient's fibroblasts. The mRNA level might change with ongoing senescence or during cell cycle (Cho *et al.*, 2001; Zhang *et al.*, 2003). In addition, only two reports on determination of mRNA expression levels were found in the literature: Emmert *et al.* reported a 50 % reduced *XPD* mRNA in a compound heterozygous XP-D patient harbouring a missense mutation (p.R683W) and a deletion mutation resulting in a truncated protein (p.G670AfsX39) (Emmert *et al.*, 2009). XP-D patients analyzed in this thesis were all found to harbour missense mutations, thus, a possible influence on the mRNA level by nonsense mediated message decay should be excluded. Accordingly, *XPD* mRNA expression levels were found to be close to normal with a mean expression level of 102.9 % (ranging from 74.1 % to 151.3 %) (figure 7B). Decreased *XPG* mRNA levels have been reported in two XP-G/CS patients carrying mutations leading to truncated proteins, whereas a patient harbouring at least one missense mutation exhibited a *XPG* mRNA expression of 90 % compared to normal (Emmert *et al.*, 2002). Determination of the *XPG* mRNA expression levels in the three XP-G patients analyzed in this thesis revealed also normal expression of the mutated *XPG* alleles compared to the mean level of nine wild type fibroblast cell cultures (Figure 7C).

Nevertheless, these data have to be verified by additional measurements using mRNA isolated from synchronized cells at best. Attempts to synchronize fibroblast cell cultures by contact inhibition as well as by thymidine treatment (Davis *et al.*, 2001) were not successful until the end of the thesis (data not shown).

4.4. Mutational analysis pinpointed the genetic defect und revealed new disease-causing mutations

4.4.1. Mutational analysis of XP-C fibroblasts

Mutational analysis were performed by genomic DNA sequencing using primer pairs flanking the intron exon boundaries to ensure that disease-causing mutations are detected within the exon and the intron regions. In the *XPC* gene 46 different disease-causing mutations, distributed over the whole gene (16 exons), have been identified so far (McDaniel *et al.*, 2007). XP-C mutations usually result in the XP-phenotype. Two patients exhibiting neurological symptoms have been described previously (Hananian and Cleaver, 1980; Khan *et al.*, 2009). All the seven different *XPC* mutations, found during this thesis, were located within the exon regions and mutational distribution comprises nearly the whole gene from exon 3 to exon 14 (table 3-1). All mutations were present in homozygous state although consanguinity is only

documented for three patients (XP47MA, XP98MA, XP99MA). Interestingly, four of the seven mutations have not been described before. Mutations A116YfsX4 and p.R475EfsX18 were found in two patients with German ancestry (XP20MA and XP117MA, respectively). Mutation p.Q723SfsX44 was found in a patient with Turkish (XP150MA), and the mutation p.I812del in a patient with Iranian (XP47MA) ancestry.

With exception of p.I812del, all mutations would result in truncated proteins either by a missense mutation creating a premature stop codon directly (p.R579X, p.R155X) or by deletions that result in a frame shift leading to an altered amino acid sequence and a premature stop codon (p.A116YfsX4, p.R475EfsX18 p.V548AfsX25, p.Q723SfsX44). This may explain the quite homogeneous clinical phenotype in the XP-C patients as all mutations would result in truncated XPC proteins that are expected to be non-functional. In addition, markedly decreased *XPC* mRNA expression levels indicate that the truncated XPC proteins are probably not expressed (figure 7A) (Cartault *et al.*, 2011; Emmert *et al.*, 2006b; Khan *et al.*, 2006). This differs from other XP genes like *XPD* which is an essential gene. Causative *XPD* mutations comprise missense mutations that still preserve some functional activity (Lehmann, 2001). *XPC* mutation p.A548AfsX25, found in three patients (XP102MA, XP114MA, XP115MA), was recently described as a founder mutation in the Mediterranean region as it was present in 87 % of 86 XP-C patients analyzed by Soufir *et al.* (Soufir *et al.*, 2010). Interestingly, it was shown that the mutation occurred approximately 1,250 years ago applying microsatellite haplotyping (Soufir *et al.*, 2010). This was the time when Muslims from Arabia conquered Southern Europe. In line with these findings, the three patients carrying mutation p.A548VfsX25 are also originated from Arabia.

The newly detected in frame deletion of three nucleotides in XP47MA deserves special notion. It leads to a single amino acid deletion p.I812del. This isoleucine is located within the DNA-binding region of XPC composed of three β -hairpin domains BHD1 (amino acids 633 to 683), BHD2 (amino acids 684 to 741), and BHD3 (amino acids 742 to 831) (figure 16) and is conserved through different species (figure 7A). In co-crystals, the Rad4 protein, which is the yeast orthologue of XPC, has been found to associate with DNA through a large transglutaminase-homology domain (TGD) flanked by domains BHD1, -2 and -3 (Min and Pavletich, 2007). Moreover, Camenisch *et al.* described a two step recognition process of XPC to detect damaged DNA. First the DNA is scanned for non-hydrogen-bonded residues which are prone to flip out resulting in ss DNA. Domains BHD1, and BHD2 are involved in this initial scanning process before the BHD3 domain binds to the resulting ss DNA in the second step (Camenisch *et al.*, 2009). Thus, the BHD3 domain is dispensable for the recruitment of XPC to a

DNA lesion, but it is sufficient for the formation of a stable nucleoprotein complex by its single-stranded DNA binding activity (Camenisch *et al.*, 2009). Deletion of amino acid 812 may impair the stable binding of XPC to damaged DNA thereby impairing NER.



Figure 16: Scheme of the primary structure of XPC with transglutaminase-homology domain (TGD) domain and the three β -hairpin domains. A disordered \sim 180-residue insertion divides the TGD domain of human XPC into two parts (Bunick *et al.*, 2006). Numbers of the first and last amino acid comprising each domain are indicated.

4.4.2. Mutational analysis of XP-D fibroblasts

So far 30 different *XPD* mutations have been listed in the mutational database www.xpmutations.org. Mutations in *XPD* may result in XP, XP/CS, TTD, XP/TDD (Broughton *et al.*, 2001; Lehmann, 2001). It is generally assumed that defects in the *XPD* gene that affect the DNA repair function of the protein result in XP, whereas those impairing the protein function in transcriptional context (TFIIH) result in TTD or CS (Bootsma and Hoeijmakers, 1993; Taylor *et al.*, 1997; Ueda *et al.*, 2009). Missense mutations changing amino acid arginine 683 to glutamine or tryptophan have been reported to be most frequent in XP-D patients (Emmert *et al.*, 2009; Kobayashi *et al.*, 2002; Lehmann, 2001). In agreement with that, five of the eight patients harboured missense mutations at this mutational hot spot: three patients (XP19MA, XP40MA, XP46MA) were homozygous for mutation p.R683Q and two patients were compound heterozygous for mutations p.R683W/p.R616Q (XP90MA) and p.R683Q/p.R616P (XP71MA). Amino acid arginine 683 is located in the helicase domain 2 (HD2) which is one of two Rad51/RecA like domains (HD1 and HD2) in the *XPD* protein (figure 17). Mutations which affect the HD1 ATP-binding edge and the HD2 DNA-binding channel thereby leading to impaired helicase activity, which is important for NER, have been reported to result in XP symptoms (Fan *et al.*, 2008). This gives rise to the XP phenotype of the homozygous affected patients XP19MA, XP40MA, and XP46MA. Additionally, a study from Taylor *et al.* investigated the functionality of missense mutations in the *XPD* gene: mutations were introduced into the *rad15* gene from *Schizosaccharomyces pombe* (*Sch.pombe*) a homologue to the *Saccharomyces cerevisiae* *RAD3* and the human *XPD* gene (Murray *et al.*, 1992). Mutation p.R616P, which is also located within HD2, was unable to rescue the lethal phenotype of *Sch.pombe* lacking *rad15*, whereas p.R683W restored viability. They concluded that missense mutations affecting amino acid arginine 616 result in null mutations not contributing to the patients' phenotype (Taylor *et al.*,

1997). Therefore, the XP phenotype of patients XP90MA and XP71MA probably results from their missense mutation affecting amino acid arginine 683.

Mutations p.R722W and p.R112H were found in homozygous (XP188MA) and heterozygous states (XP87MA and XP89MA), respectively. Amino acid arginine 722 is located within the C-terminal extension (CTE) (figure 17) of the protein (Fan *et al.*, 2008). The CTE is important for interaction with p44 subunit of TFIIH which stimulates the XPD helicase activity (Coin *et al.*, 1998) and supports maintenance of the architecture of the transcription factor (Dubaele *et al.*, 2003). Biochemical characterization of the XPD homolog from *Sulfolobus acidocaldarius* (SaXPD) by Fan *et al.* revealed amino acid arginine 112 located within a domain forming a 4Fe-4S cluster (figure 17) (Fan *et al.*, 2008). The Fe-S cluster is supposed to be needed for efficient damage sensing as proteins containing a 4Fe-4S cluster have been shown to held at sites of damaged DNA where the cluster became oxidized (Yavin *et al.*, 2006). Mutation p.R112H was supposed to reduce framework stability due to the removal of a charged side chain hydrogen bond to Fe ion ligand cysteine 102 (Fan *et al.*, 2008). Both mutations, p.R722W and p.R112H, are described to result in the TTD phenotype (Fan *et al.*, 2008; Lehmann, 2001; Taylor *et al.*, 1997). Modified XPD proteins with these TTD associated mutation types were compared to XP associated mutation p.R683W by functional analysis. *In vitro* helicase and NER assays revealed both, TTD and XP associated mutations, influencing the functionality of modified XPD proteins compared to wild type XPD. Moreover, transactivation activity of certain nuclear receptors was impaired by both types of mutations (Dubaele *et al.*, 2003). These molecular similarities may explain the overlapping symptoms of XP and TTD patients. However, the main difference between TTD and XP associated mutations was the inhibition of basal transcription activity only by TTD associated mutations p.R112H and p.R722W (Dubaele *et al.*, 2003). This supports a transcriptional defect as the main reason for differences in TTD and XP disease-causing mutations (Dubaele *et al.*, 2003; Lehmann, 2001; Taylor *et al.*, 1997). According to this, patient XP188MA exhibited the TDD phenotype. Somehow more difficult is the genotype-phenotype correlation of XP87MA and XP89MA. The second mutation found in these compound heterozygous patients was p.D681H which has not been described previously. However, in the crystal structure of SaXPD from Fan *et al.*, mutation p.D681N, located within HD2, was supposed to disrupt a charged site chain interaction with arginine 531 which is needed to position the arginine at the proposed DNA binding site. Thus, this mutation was proposed to influence helicase activity due to impaired DNA binding (Fan *et al.*, 2008). In a review from Lehmann, mutation p.P681N is described to result in XP symptoms in a compound heterozygous state but the second mutation which may also contributes to the phenotype was

not pointed out (Lehmann, 2001). In addition, Graham et al. reported on a compound heterozygous patient harbouring mutation p.D681N together with the null mutation p.R616W. This patient was reported having the COFS Syndrome. This syndrome shares high similarity with CS although eye defects (i.e. microcornea with optic atrophy) are more severe in COFSS patients compared to CS patients (Graham, Jr. *et al.*, 2001). In the present study, patient XP87MA exhibited the TTD and patient XP89MA the XP/CS phenotype. The possibility of a different clinical outcome despite similar mutations in two individuals has been observed previously by the two XP-C patients one with and one without having neurological abnormalities mentioned above. Additional mutations, in this case due to close consanguinity, were suggested to be responsible for the occurrence of neurological symptoms in only one patient (Khan *et al.*, 2009). Moreover, expression levels of the two affected alleles may differ between patients thereby resulting in different phenotypes: single nucleotide polymorphisms have previously been shown to result in altered *XPB* mRNA expression levels (Wolfe *et al.*, 2007). Differences in the methylation status due to epigenetic variability may also influence gene expression levels (Jaenisch and Bird, 2003) and, in turn, the clinical outcome. Thus, additional factors may also contribute to the development of the different phenotypes in XP87MA and XP89MA.



Figure 17: Scheme of the XPD protein with the helicase domains HD1 and HD2, the 4Fe-S domain and the CTE. Numbers of the first and last amino acid comprising each domain are indicated.

4.4.3. Mutational analysis of XP-G fibroblasts

XP-G is a very rare XP complementation group and to date only 20 XP-G causing mutations have been described in 16 XP-G patients. Six of these patients developed classical XP symptoms (Emmert *et al.*, 2002; Ichihashi *et al.*, 1985; Moriwaki *et al.*, 2012; Norris *et al.*, 1987; Nospikel and Clarkson, 1994; Yoneda *et al.*, 2007); the other ten patients exhibited the XP/CS complex phenotype (Emmert *et al.*, 2002; Lalle *et al.*, 2002; Moriwaki *et al.*, 1996; Nospikel *et al.*, 1997; Zafeiriou *et al.*, 2001). Three patients among the XP/CS group were reported to have a late onset of their CS symptoms (Lalle *et al.*, 2002; Thorel *et al.*, 2004).

A total of five novel disease-causing *XPG* mutations in three patients were identified during this thesis. Two of these patients exhibited XP/CS complex symptoms (XP165MA and XP72MA), whereas no clinical data were available for the third patient (XP40GO). The most

severely affected XP/CS patient, XP165MA, carried the homozygous missense mutation p.G805R, patient XP72MA carried mutations p.E727X and p.W814S mutations, and patient XP40GO carried mutations p.Q150X and p.L778P (table 3-1). All three missense mutations are located within the I-region of XPG. Highly conserved amino acid residues in the I-region (amino acid 1-95) and the N-region (amino acid 753-881) (figure 10) are necessary for XPG's endonuclease proficiency (Constantinou *et al.*, 1999; Hosfield *et al.*, 1998; Lieber, 1997; Shen *et al.*, 1996). An alignment of stretch of the I-region (figure 8B) revealed that the mutated amino acid residues leucine 778, glycine 805, and tryptophan 814 are highly conserved in human, mouse, and *Drosophila melanogaster*. Leucine 778 is also highly conserved through different members of the FEN1 nuclease family (Constantinou *et al.*, 1999). Tryptophan 814 is located near to the highly conserved amino acid residue aspartate 812 which is crucial for XPG cleavage activity (Constantinou *et al.*, 1999). This can readily explain the diminished repair capability of the patients' fibroblasts.

However, previous correlations of mutations in the *XPG* gene and patients' phenotypes have revealed that mutations resulting in truncated XPG proteins generally cause the XP/CS phenotype, whereas at least one missense mutation maintaining a full length protein results in the XP phenotype (Emmert *et al.*, 2002; Nospikel *et al.*, 1997). This is true for the previously reported p.L65P, p.A792V, and p.A874T missense mutations (Emmert *et al.*, 2002; Moriwaki *et al.*, 2012; Nospikel and Clarkson, 1994). Also the p.L858P mutation conferred a milder late-onset phenotype due to its retained ability for limited transcription-coupled repair (Lalle *et al.*, 2002). The only missense mutation associated with a severe early-onset XP/CS complex phenotype is p.P72H which is located in the N-region (Zafeiriou *et al.*, 2001). This particular missense mutation was predicted to greatly destabilize the XPG protein (Thorel *et al.*, 2004).

With regard to these previous phenotype-genotype correlations the identification of missense mutations in two patients with XP/CS prompted to further analyze all five novel *XPG* mutations on a molecular level.

4.5. Influence of the novel XPG mutations

4.5.1. All five XPG mutations influence the functionality of XPG in NER

The influence of the five *XPG* mutations on NER was assessed allele-specifically by HCR assay. All three missense mutations as well as the two truncating mutations resulted in a repair deficit. XPG_{G805R} (XP165MA) retained no, whereas XPG_{W814S} (XP72MA) and XPG_{L778P} (XP40GO) retained limited residual repair activity as assessed allele-specifically by HCR (Figure 9). This fits

well as patient XP165MA, suffering from the most severe phenotype, encodes the non-functional XPG_{G805R} on both alleles. Other missense mutations, p.A792V and p.A874T, which are also located in the I-region, near to mutations p.L778P and p.W814S, were also described to retain some repair capability (Constantinou *et al.*, 1999; Emmert *et al.*, 2002). However, residual activity of proteins XPG_{W814S} and XPG_{L778P} may result from a gene doses effect due to the over expression of the proteins. As expected, the two nonsense mutations, missing at least parts of the I-region, also retained no repair activity. This is consistent with previous findings from Lalle *et al.* who investigated the complementation proficiency of a truncated XPG protein, p.K917NfsX65, which even retained the N- and I-regions. This less truncated XPG protein was also found to be unable to decrease the UV sensitivity in XP-G transfectants (Lalle *et al.*, 2002). Wrong protein folding because of the aberrant primary structure or defective nuclear transport due to the missing C-terminal NLS signal might be reasons for these findings.

4.5.2. Mutations impair interaction with TFIIH

The influence of the five XPG mutations on the interaction with subunits of the transcription factor IIH was investigated by co-immunoprecipitation. One main problem of the co-immunoprecipitation experiments was the amount of $XPG_{mut}mycHis$ protein (except $XPG_{E727}mycHis$) compared to wild type $XPGmycHis$ protein. Often even transfection of twice as many cells with $pXPG_{mut}mycHis$ did not result in similar protein amounts compared to wild type $XPGmycHis$. This may indicate a destabilizing effect of the XPG mutations on the protein level as described for mutation p.P72H (Thorel *et al.*, 2004). Nevertheless, figure 12F shows that wild type $XPG_{mut}mycHis$ was able to co-immunoprecipitate XPD independent from its amount.

XPD was not co-immunoprecipitated with the five $XPG_{mut}mycHis$ proteins (figure 12A). Only traces of $cdk7$ were co-immunoprecipitated with $XPG_{L778P}mycHis$ and $XPG_{W814S}mycHis$. $XPG_{G805R}mycHis$ and the two truncated XPG proteins did not co-immunoprecipitate $cdk7$ at all (figure 12C). If there is a direct interaction between XPG and $cdk7$ in addition to the indirect interactions via XPD and/or MAT1 (Drapkin *et al.*, 1996; Reardon and Sancar, 2002) remains to be investigated. That the truncated XPG proteins $XPG_{1-150}mycHis$ (XP40GO) and $XPG_{1-727}mycHis$ (XP72MA) showed no interaction with XPD or with $cdk7$ is in line with previous studies (Arab *et al.*, 2010; Ito *et al.*, 2007). However, single amino acid residues crucial for XPG-TFIIH interaction have not been described for far. The three novel missense mutations are all located within one XPG region (747-928) which interacts with XPD. Iyer *et al.* (Iyer *et al.*, 1996) identified two XPG-XPD binding regions *in-vitro*: XPG_{1-377} and $XPG_{747-928}$. In addition, single

amino acid residue arginine 992 in XPG has been shown to be crucial for interaction with PCNA (Gary *et al.*, 1997). This supports the findings that missense mutations impair XPG-protein interactions in general and that the single amino acid residues leucine 778, glycine 805, and tryptophan 814 in XPG might be crucial for XPG-TFIIH interaction in particular.

Therefore, the XP/CS complex phenotype of patients XP165MA and XP72MA could be explained by impaired XPG-TFIIH interactions due to the novel truncating as well as the novel missense mutations. Ito *et al.* suggested that XPG and XPD cooperatively mediate the anchoring of CAK to core TFIIH (Ito *et al.*, 2010). The impaired XPG-TFIIH interactions destabilize TFIIH thereby resulting in the dissociation of the cdk7 containing CAK complex from core TFIIH (figure 2) (Arab *et al.*, 2010; Ito *et al.*, 2007). The core TFIIH is involved in nucleotide excision repair whereas CAK is dispensable for NER (Arab *et al.*, 2010). However, CAK activity, as part of holo TFIIH, is involved in general transcription (transcription initiation, promoter escape, and phosphorylation of nuclear receptors) (Arab *et al.*, 2010; Ito *et al.*, 2007; Le *et al.*, 2010; Scharer, 2008). That abnormalities in the transcriptional process, in addition to defective GGR or TCR, cause CS features in XP-G patients was recently reported (Arab *et al.*, 2010; Ito *et al.*, 2007). This is also supported by the notion that XP-A patients, despite their deficiency in GGR and TCR, do not exhibit CS features. Secondly, XPA deficient mice in contrast to XPG deficient mice do not develop CS symptoms (Shiomi *et al.*, 2005). Similarly, certain mutations in the *XPD* gene which lead to a dissociation of CAK from core TFIIH (Ito *et al.*, 2007) and impair the phosphorylation of certain nuclear receptors can give rise to XP/CS complex phenotype (Bastien *et al.*, 2000; Chen *et al.*, 2000; Compe *et al.*, 2005; Drane *et al.*, 2004; Ito *et al.*, 2007; Rochette-Egly *et al.*, 1997). Based on these findings and the proposed functional consequences it can also be fairly assumed that also XP40GO suffered from a severe XP/CS complex phenotype. Although fibroblasts from this patient did not exhibit the XP/CS typical increased UV sensitivity compared to XP-C and XP-D fibroblasts from XP patients.

4.5.3. Mutation-specific effects on repair factor assembly

Effects of the *XPG* mutations on the recruitment of other XP proteins to local DNA photodamage was assessed *in vivo* applying immunofluorescence. *In vitro* and *in vivo* investigations suggest a sequential assembly of the NER factors (Riedl *et al.*, 2003; Volker *et al.*, 2001). As expected, the XPG protein was not recruited to local photodamage in the XP-G fibroblasts (figure 13E). This indicates that all five mutated XPG proteins do not properly interact with other NER proteins. Oh *et al.* also described an impaired recruitment of XPG in XP-G cells (Oh *et al.*, 2007). Overall, a recruitment of XPC, XPB, XPA, and ERCC1 (complexed

with XPF) proteins to local photodamage in all XP-G cells at 30 minutes after UV irradiation was observed. This is in line with previous reports investigating recruitment of XP proteins in XP-G cells with other mutations (Arab *et al.*, 2010; Oh *et al.*, 2007; Thorel *et al.*, 2004). At a very early time point (6 min) XPA was also normally fast recruited indicating that XPG is dispensable for XPA recruitment (Oh *et al.*, 2007). A delayed early recruitment (6 min) of XPC was observed in XP72MA and XP40GO (figure 13C) and early XPB recruitment was delayed in XP72MA (figure 13B). This might reflect that the strong functional interaction between XPC and TFIIH (Araujo *et al.*, 2001) is also affected by the destabilization of TFIIH due to impaired interactions with XPG (Arab *et al.*, 2010; Ito *et al.*, 2007). In any case, ERCC1-XPF recruitment depends on XPG (Riedl *et al.*, 2003). In line with that, early recruitment of ERCC1 was delayed in all three XP-G cell lines (figure 13D).

In wild type cells the XP proteins began already to redistribute from local photodamage 30 min after UV irradiation. By 3 h after UV treatment XP proteins were no longer detectable at sites of DNA damage. Redistribution of XP proteins results from the proceeding repair of DNA photoproducts (Dunand-Sauthier *et al.*, 2005; Oh *et al.*, 2007). In addition, this correlates with the removal of 6,4PPs, which was found to be finished 3 h after irradiation (figure 13G, figure 15C). However, CPD removal was much slower and 36 % of CPDs were still detectable even after 24 h (figure 13F, 15C). A faster removal of 6,4PPs compared to CPDs has been demonstrated previously (Oh *et al.*, 2011). Assuming that NER proficient wild type cells, nevertheless, remove most of the CPDs over time, this may indicate an excessive XP protein recruitment to sites of local DNA damage immediately after UV treatment. This superabundance of XP proteins is sufficient for detection by immunofluorescence. However, after a partial redistribution of the superfluous proteins, the residual proteins, sufficient for proper NER, may not be sufficient for detection by immunofluorescence.

In contrast, defective NER was reflected in XP-G cells by persistence of XPA, XPB, XPC, and ERCC1 proteins at local photodamage even after 24 h (figure 13, figure 15). This is in agreement with observations from Arab *et al.* and Oh *et al.* for cells from other XP-G/CS patients (Arab *et al.*, 2010; Oh *et al.*, 2007) and has also been demonstrated for cells from XP-A, XP-B, and XP-C patients (Oh *et al.*, 2007; Riedl *et al.*, 2003) as well as from XP-D patients with and without neurological symptoms (Boyle *et al.*, 2008). Thus, the impaired redistribution of XP proteins reflects impaired repair being related to the XP symptoms as this is the lowest common denominator of all of these variable phenotypes.

5. Summary and conclusion

A total of 75 NER defective fibroblast cell cultures were provided from the University Clinics of Göttingen and Mannheim for characterization purpose. This represents Germany's largest library of NER defective cells with regard to the low incidences of NER defective syndromes.

The assessment of 23 NER defective fibroblast cell cultures (12 XP-C patients, eight XP-D patients, three XP-G patients) was finished during this thesis. Fibroblasts were characterized for their UV sensitivity and their relative NER capability. Defective genes were determined by complementation assays, and mutational analysis revealed new disease-causing mutations. Five novel *XPG* mutations were further analyzed for their impact on protein function in NER.

Analysis of 12 XP-C fibroblasts identified four new mutations in the *XPC* gene. Correlation of the clinical data revealed the novel *XPC* mutations to result in the XP phenotype. None of the corresponding patients exhibited "XP plus neurological" symptoms. Furthermore, there was no correlation between XP-C fibroblasts' UV sensitivity and the clinical phenotype, as the clinical outcome was quite homogeneous among the XP-C patients.

One new missense mutation in the *XPD* gene (p.D681H) was found in two of the eight XP-D fibroblast cell cultures. Missense mutation p.D681N has been associated previously with the COFS Syndrome in a compound heterozygous patient carrying a null mutation on the other allele. The two patients, analyzed in this thesis, were also compound heterozygous carrying the same TTD-associated mutation on the other allele. Interestingly, one of the patients exhibits the TTD and the other one the XP/CS phenotype. Variable phenotypes may depend on different dominance of the mutated alleles due to SNPs or epigenetic variability. A correlation between fibroblasts' UV sensitivity and the clinical outcome was not obvious within the XP-D patients. Fibroblasts of all eight patients showed increased UV sensitivity. In addition, one patient whose fibroblasts were markedly UV sensitive was described to exhibit no increased UV sensitivity.

Five novel disease-causing *XPG* mutations were identified in three XP-G patients. Assessment of fibroblasts' UV sensitivity with clinical files indicated UV sensitivity of fibroblasts and patients (XP165MA, XP72MA) being paralleled. Missense mutations p.G805R (XP165MA, hom) and p.W814S (XP72MA, het) were correlated with the XP/CS complex. Particularly the CS symptoms associated with at least one missense mutation were surprising at first and lead to a further examination of the five *XPG* mutations on a molecular level:

First, the modified *XPG* proteins impaired repair of UV-induced photolesions. Second, the interaction of *XPG* with TFIIH subunits *XPD* and *cdk7* was impaired due to the mutations. Until

now, only broader regions were known to be involved in the XPG-XPB interaction. Thus, for the first time, single amino acids being crucial for XPG-XPB interaction were identified. Furthermore, the impaired interaction explains the XP/CS phenotype of the patients and gives rise to the assumption that the third patient (XP40GO) may also exhibit XP/CS symptoms. Third, a mutation specific effect on the repair factor assembly was observed by analysis of the recruitment of NER proteins to sites of local DNA damage *in vivo*.

Bibliography

Aboussekhra A, Biggerstaff M, Shivji MK, Vilpo JA, Moncollin V, Podust VN, Protic M, Hubscher U, Egly JM, Wood RD: Mammalian DNA nucleotide excision repair reconstituted with purified protein components. *Cell* 80:859-868 (1995).

Aguilera A, Gomez-Gonzalez B: Genome instability: a mechanistic view of its causes and consequences. *Nat Rev Genet* 9:204-217 (2008).

Arab HH, Wani G, Ray A, Shah ZI, Zhu Q, Wani AA: Dissociation of CAK from core TFIIH reveals a functional link between XP-G/CS and the TFIIH disassembly state. *PLoS One* 5:e11007 (2010).

Araki M, Masutani C, Takemura M, Uchida A, Sugasawa K, Kondoh J, Ohkuma Y, Hanaoka F: Centrosome protein centrin 2/caltractin 1 is part of the Xeroderma pigmentosum group C complex that initiates global genome nucleotide excision repair. *J Biol Chem* 276:18665-18672 (2001).

Araujo SJ, Nigg EA, Wood RD: Strong functional interactions of TFIIH with XPC and XPG in human DNA nucleotide excision repair, without a preassembled repairosome. *Mol Cell Biol* 21:2281-2291 (2001).

Arlett CF, Harcourt SA, Broughton BC: The influence of caffeine on cell survival in excision-proficient and excision-deficient Xeroderma pigmentosum and normal human cell strains following ultraviolet-light irradiation. *Mutat Res* 33:341-346 (1975).

Arlett CF, Harcourt SA, Lehmann AR, Stevens S, Ferguson-Smith MA, Morley WN: Studies on a new case of Xeroderma pigmentosum (XP3BR) from complementation group G with cellular sensitivity to ionizing radiation. *Carcinogenesis* 1:745-751 (1980).

Asahina H, Kuraoka I, Shirakawa M, Morita EH, Miura N, Miyamoto I, Ohtsuka E, Okada Y, Tanaka K: The XPA protein is a zinc metalloprotein with an ability to recognize various kinds of DNA damage. *Mutat Res* 315:229-237 (1994).

Baden HP, Jackson CE, Weiss L, Jimbow K, Lee L, Kubilus J, Gold RJ: The physicochemical properties of hair in the BIDS syndrome. *Am J Hum Genet* 28:514-521 (1976).

Baltimore D: RNA-dependent DNA polymerase in virions of RNA tumour viruses. *Nature* 226:1209-1211 (1970).

Barnes DE, Tomkinson AE, Lehmann AR, Webster AD, Lindahl T: Mutations in the DNA ligase I gene of an individual with immunodeficiencies and cellular hypersensitivity to DNA-damaging agents. *Cell* 69:495-503 (1992).

Bartek J, Bartkova J, Lukas J: DNA damage signalling guards against activated oncogenes and tumour progression. *Oncogene* 26:7773-7779 (2007).

Bastien J, Dam-Stitah S, Riedl T, Egly JM, Chambon P, Rochette-Egly C: TFIIH interacts with the retinoic acid receptor gamma and phosphorylates its AF-1-activating domain through cdk7. *J Biol Chem* 275:21896-21904 (2000).

Berg RJ, Ruven HJ, Sands AT, de Gruijl FR, Mullenders LH: Defective global genome repair in XPC mice is associated with skin cancer susceptibility but not with sensitivity to UVB induced erythema and edema. *J Invest Dermatol* 110:405-409 (1998).

Bittles AH, Sullivan SG, Zhivotovsky LA: Consanguinity, caste and deaf-mutism in Punjab, 1921. *J Biosoc Sci* 36:221-234 (2004).

Bohr VA, Smith CA, Okumoto DS, Hanawalt PC: DNA repair in an active gene: removal of pyrimidine dimers from the DHFR gene of CHO cells is much more efficient than in the genome overall. *Cell* 40:359-369 (1985).

Bootsma D, Hoeijmakers JH: DNA repair. Engagement with transcription. *Nature* 363:114-115 (1993).

Bootsma D, Kraemer KH, Cleaver JE, Hoeijmakers JH: Nucleotide excision repair syndromes: Xeroderma pigmentosum, Cockayne Syndrome, and Trichothiodystrophy. In: Vogelstein B, Kinzler KW, editors. *The Genetic Basis of Human Cancer*. 2. McGraw-Hill, New York pp. 211–237(2002).

Boshart M, Weber F, Jahn G, Dorsch-Hasler K, Fleckenstein B, Schaffner W: A very strong enhancer is located upstream of an immediate early gene of human cytomegalovirus. *Cell* 41:521-530 (1985).

Botta E, Nardo T, Orioli D, Guglielmino R, Ricotti R, Bondanza S, Benedicenti F, Zambruno G, Stefanini M: Genotype-phenotype relationships in trichothiodystrophy patients with novel splicing mutations in the XPD gene. *Hum Mutat* 30:438-445 (2009).

Boyle J, Ueda T, Oh KS, Imoto K, Tamura D, Jagdeo J, Khan SG, Nadem C, DiGiovanna JJ, Kraemer KH: Persistence of repair proteins at unrepaired DNA damage distinguishes diseases with ERCC2 (XPD) mutations: cancer-prone Xeroderma pigmentosum vs. non-cancer-prone trichothiodystrophy. *Hum Mutat* 29:1194-1208 (2008).

Bradford PT, Goldstein AM, Tamura D, Khan SG, Ueda T, Boyle J, Oh KS, Imoto K, Inui H, Moriwaki S, Emmert S, Pike KM, Raziuddin A, Plona TM, DiGiovanna JJ, Tucker MA, Kraemer KH: Cancer and neurologic degeneration in Xeroderma pigmentosum: long term follow-up characterises the role of DNA repair. *J Med Genet* 48:168-176 (2011).

Bradford, MM: A rapid and sensitive method for the quantitation of microgram quantities of protein utilizing the principle of protein-dye binding. *Anal Biochem* 72: 248-254 (1976)

Broughton BC, Berneburg M, Fawcett H, Taylor EM, Arlett CF, Nardo T, Stefanini M, Menefee E, Price VH, Queille S, Sarasin A, Bohnert E, Krutmann J, Davidson R, Kraemer KH, Lehmann AR: Two individuals with features of both Xeroderma pigmentosum and trichothiodystrophy highlight the complexity of the clinical outcomes of mutations in the XPD gene. *Hum Mol Genet* 10:2539-2547 (2001).

Broughton BC, Thompson AF, Harcourt SA, Vermeulen W, Hoeijmakers JH, Botta E, Stefanini M, King MD, Weber CA, Cole J, et al.: Molecular and cellular analysis of the DNA repair defect in a patient in Xeroderma pigmentosum complementation group D who has the clinical features of Xeroderma pigmentosum and Cockayne syndrome. *Am J Hum Genet* 56:167-74 (1995).

- Bunick CG, Miller MR, Fuller BE, Fanning E, Chazin WJ: Biochemical and structural domain analysis of xeroderma pigmentosum complementation group C protein. *Biochemistry* 45: 14965–14979 (2006).
- Buschta-Hedayat N, Buterin T, Hess MT, Missura M, Naegeli H: Recognition of nonhybridizing base pairs during nucleotide excision repair of DNA. *Proc Natl Acad Sci USA* 96:6090-6095 (1999).
- Camenisch U, Trautlein D, Clement FC, Fei J, Leitenstorfer A, Ferrando-May E, Naegeli H: Two-stage dynamic DNA quality check by Xeroderma pigmentosum group C protein. *EMBO J* 28:2387-2399 (2009).
- Canceill D, Ehrlich SD: Copy-choice recombination mediated by DNA polymerase III holoenzyme from *Escherichia coli*. *Proc Natl Acad Sci USA* 93:6647-6652 (1996).
- Canceill D, Viguera E, Ehrlich SD: Replication slippage of different DNA polymerases is inversely related to their strand displacement efficiency. *J Biol Chem* 274:27481-27490 (1999).
- Cartault F, Nava C, Malbrunot AC, Munier P, Hebert JC, N'guyen P, Djeridi N, Pariaud P, Pariaud J, Dupuy A, Austerlitz F, Sarasin A: A new XPC gene splicing mutation has lead to the highest worldwide prevalence of Xeroderma pigmentosum in black Mahori patients. *DNA Repair (Amst)* 10:577-585 (2011).
- Ceska TA, Sayers JR, Stier G, Suck D: A helical arch allowing single-stranded DNA to thread through T5 5'-exonuclease. *Nature* 382:90-93 (1996).
- Chavanne F, Broughton BC, Pietra D, Nardo T, Browitt A, Lehmann AR, Stefanini M: Mutations in the XPC gene in families with Xeroderma pigmentosum and consequences at the cell, protein, and transcript levels. *Cancer Res* 60:1974-1982 (2000).
- Chen D, Riedl T, Washbrook E, Pace PE, Coombes RC, Egly JM, Ali S: Activation of estrogen receptor alpha by S118 phosphorylation involves a ligand-dependent interaction with TFIIH and participation of CDK7. *Mol Cell* 6:127-137 (2000).
- Cho RJ, Huang M, Campbell MJ, Dong H, Steinmetz L, Sapinoso L, Hampton G, Elledge SJ, Davis RW, Lockhart DJ: Transcriptional regulation and function during the human cell cycle. *Nat Genet* 27:48-54 (2001).
- Chodaparambil JV, Edayathumangalam RS, Bao Y, Park YJ, Luger K: Nucleosome structure and function. *Ernst Schering Res Found Workshop* 57:29-46 (2006).
- Chun SG, Shaeffer DS, Bryant-Greenwood PK: The Werner's Syndrome RecQ helicase/exonuclease at the nexus of cancer and aging. *Hawaii Med J* 70:52-55 (2011).
- Cleaver JE: Defective repair replication of DNA in Xeroderma pigmentosum. *Nature* 218:652-656 (1968).
- Cleaver JE, Lam ET, Revet I: Disorders of nucleotide excision repair: the genetic and molecular basis of heterogeneity. *Nat Rev Genet* 10:756-768 (2009).

- Coin F, Marinoni JC, Rodolfo C, Fribourg S, Pedrini AM, Egly JM: Mutations in the XPD helicase gene result in XP and TTD phenotypes, preventing interaction between XPD and the p44 subunit of TFIIH. *Nat Genet* 20:184-188 (1998).
- Coin F, Oksenysh V, Egly JM: Distinct roles for the XPB/p52 and XPD/p44 subcomplexes of TFIIH in damaged DNA opening during nucleotide excision repair. *Mol Cell* 26:245-256 (2007).
- Compe E, Drane P, Laurent C, Diderich K, Braun C, Hoeijmakers JH, Egly JM: Dysregulation of the peroxisome proliferator-activated receptor target genes by XPD mutations. *Mol Cell Biol* 25:6065-6076 (2005).
- Constantinou A, Gunz D, Evans E, Lalle P, Bates PA, Wood RD, Clarkson SG: Conserved residues of human XPG protein important for nuclease activity and function in nucleotide excision repair. *J Biol Chem* 274:5637-5648 (1999).
- Cormack RS, Somssich IE: Rapid amplification of genomic ends (RAGE) as a simple method to clone flanking genomic DNA. *Gene* 194:273-276 (1997).
- Crovato F, Borrone C, Rebora A: Trichothiodystrophy--BIDS, IBIDS and PIBIDS? *Br J Dermatol* 108:247 (1983).
- de Laat WL, Sijbers AM, Odijk H, Jaspers NG, Hoeijmakers JH: Mapping of interaction domains between human repair proteins ERCC1 and XPF. *Nucleic Acids Res* 26:4146-4152 (1998).
- Davis PK, Ho A, Dowdy SF: Biological method for cell-cycle synchronization of mammalian cells. *Biotechniques* 30:1322-1331 (2001).
- De Weerd-Kastelein EA, Keijzer W, Bootsma D: Genetic heterogeneity of Xeroderma pigmentosum demonstrated by somatic cell hybridization. *Nat New Biol* 238:80-83 (1972).
- De Boer J, Hoeijmakers JH: Nucleotide excision repair and human syndromes. *Carcinogenesis* 21:453-460 (2000).
- De Bont R, van Larebeke N: Endogenous DNA damage in humans: a review of quantitative data. *Mutagenesis* 19:169-185 (2004).
- Despras E, Daboussi F, Hyrien O, Marheineke K, Kannouche PL: ATR/Chk1 pathway is essential for resumption of DNA synthesis and cell survival in UV-irradiated XP variant cells. *Hum Mol Genet* 19:1690-1701 (2010).
- Dollfus H, Porto F, Caussade P, Speeg-Schatz C, Sahel J, Grosshans E, Flament J, Sarasin A: Ocular manifestations in the inherited DNA repair disorders. *Surv Ophthalmol* 48:107-122 (2003).
- Drane P, Compe E, Catez P, Chymkowitch P, Egly JM: Selective regulation of vitamin D receptor-responsive genes by TFIIH. *Mol Cell* 16:187-197 (2004).
- Drapkin R, Le RG, Cho H, Akoulitchev S, Reinberg D: Human cyclin-dependent kinase-activating kinase exists in three distinct complexes. *Proc Natl Acad Sci USA* 93:6488-6493 (1996).

Dubaele S, Proietti De SL, Bienstock RJ, Keriell A, Stefanini M, Van HB, Egly JM: Basal transcription defect discriminates between Xeroderma pigmentosum and trichothiodystrophy in XPD patients. *Mol Cell* 11:1635-1646 (2003).

Dunand-Sauthier I, Hohl M, Thorel F, Jaquier-Gubler P, Clarkson SG, Scharer OD: The spacer region of XPG mediates recruitment to nucleotide excision repair complexes and determines substrate specificity. *J Biol Chem* 280:7030-7037 (2005).

Dvir A, Conaway JW, Conaway RC: Mechanism of transcription initiation and promoter escape by RNA polymerase II. *Curr Opin Genet Dev* 11:209-214 (2001).

Emmert S, Leibel D, Runger TM: Syndromes with genetic instability: model diseases for (skin) cancerogenesis. *J Dtsch Dermatol Ges* 4:721-731 (2006a).

Emmert S, Slor H, Busch DB, Batko S, Albert RB, Coleman D, Khan SG, bu-Libdeh B, DiGiovanna JJ, Cunningham BB, Lee MM, Crollick J, Inui H, Ueda T, Hedayati M, Grossman L, Shahlavi T, Cleaver JE, Kraemer KH: Relationship of neurologic degeneration to genotype in three Xeroderma pigmentosum group G patients. *J Invest Dermatol* 118:972-982 (2002).

Emmert S, Ueda T, Zumsteg U, Weber P, Khan SG, Oh KS, Boyle J, Laspe P, Zachmann K, Boeckmann L, Kuschal C, Bircher A, Kraemer KH: Strict sun protection results in minimal skin changes in a patient with Xeroderma pigmentosum and a novel c.2009delG mutation in XPD (ERCC2). *Exp Dermatol* 18:64-68 (2009).

Emmert S, Wetzig T, Imoto K, Khan SG, Oh KS, Laspe P, Zachmann K, Simon JC, Kraemer KH: A novel complex insertion/deletion mutation in the XPC DNA repair gene leads to skin cancer in an Iraqi family. *J Invest Dermatol* 126:2542-2544 (2006b).

Enzlin JH, Scharer OD: The active site of the DNA repair endonuclease XPF-ERCC1 forms a highly conserved nuclease motif. *EMBO J* 21:2045-2053 (2002).

Evans E, Fellows J, COFSfer A, Wood RD: Open complex formation around a lesion during nucleotide excision repair provides a structure for cleavage by human XPG protein. *EMBO J* 16:625-638 (1997).

Faghri S, Tamura D, Kraemer KH, DiGiovanna JJ: Trichothiodystrophy: a systematic review of 112 published cases characterises a wide spectrum of clinical manifestations. *J Med Genet* 45:609-621 (2008).

Falik-Zaccai T.C.: A Novel XPD Mutation in a Compound Heterozygote Patient with Mild Sun Sensitivity. *Environmental Mutagen Society 41st Annual Meeting Abstracts* 51 edition: 714 (2010).

Fan L, Arvai AS, Cooper PK, Iwai S, Hanaoka F, Tainer JA: Conserved XPB core structure and motifs for DNA unwinding: implications for pathway selection of transcription or excision repair. *Mol Cell* 22:27-37 (2006).

Fan L, Fuss JO, Cheng QJ, Arvai AS, Hammel M, Roberts VA, Cooper PK, Tainer JA: XPD helicase structures and activities: insights into the cancer and aging phenotypes from XPD mutations. *Cell* 133:789-800 (2008).

Friedberg EC, Walker GC, Siede W, Wood RD, Schultz RA, Ellenberger T: DNA Repair and Mutagenesis. ASM Press, Washington, DC, (2006).

Fujiwara Y, Masutani C, Mizukoshi T, Kondo J, Hanaoka F, Iwai S: Characterization of DNA recognition by the human UV-damaged DNA-binding protein. *J Biol Chem* 274:20027-20033 (1999).

Gartler S: Inborn errors of metabolism at the cell culture level. Ed. Fishbein, M., International Medical Congress, New York, (1963).

Gary R, Ludwig DL, Cornelius HL, MacInnes MA, Park MS: The DNA repair endonuclease XPG binds to proliferating cell nuclear antigen (PCNA) and shares sequence elements with the PCNA-binding regions of FEN-1 and cyclin-dependent kinase inhibitor p21. *J Biol Chem* 272:24522-24529 (1997).

Gates FL: On nuclear derivatives and the lethal action of ultra-violet light. *Science* 68:479-480 (1928).

Giglia G, Dumaz N, Drougard C, Avril MF, ya-Grosjean L, Sarasin A: p53 mutations in skin and internal tumors of Xeroderma pigmentosum patients belonging to the complementation group C. *Cancer Res* 58:4402-4409 (1998).

Giglia-Mari G, Coin F, Ranish JA, Hoogstraten D, Theil A, Wijgers N, Jaspers NG, Raams A, Argentini M, van der Spek PJ, Botta E, Stefanini M, Egly JM, Aebersold R, Hoeijmakers JH, Vermeulen W: A new, tenth subunit of TFIIH is responsible for the DNA repair syndrome trichothiodystrophy group A. *Nat Genet* 36:714-719 (2004).

Giglia-Mari G, Zotter A, Vermeulen W: DNA damage response. *Cold Spring Harb Perspect Biol* 3:a000745 (2011).

Gozukara EM, Khan SG, Metin A, Emmert S, Busch DB, Shahlavi T, Coleman DM, Miller M, Chinsomboon N, Stefanini M, Kraemer KH: A stop codon in Xeroderma pigmentosum group C families in Turkey and Italy: molecular genetic evidence for a common ancestor. *J Invest Dermatol* 117:197-204 (2001).

Graham JM, Jr., nyane-Yeboa K, Raams A, Appeldoorn E, Kleijer WJ, Garritsen VH, Busch D, Edersheim TG, Jaspers NG: Cerebro-oculo-facio-skeletal syndrome with a nucleotide excision-repair defect and a mutated XPD gene, with prenatal diagnosis in a triplet pregnancy. *Am J Hum Genet* 69:291-300 (2001).

Groisman R, Polanowska J, Kuraoka I, Sawada J, Saijo M, Drapkin R, Kisselev AF, Tanaka K, Nakatani Y: The ubiquitin ligase activity in the DDB2 and CSA complexes is differentially regulated by the COP9 signalosome in response to DNA damage. *Cell* 113:357-367 (2003).

Hananian J, Cleaver JE: Xeroderma pigmentosum exhibiting neurological disorders and systemic lupus erythematosus. *Clin Genet* 17:39-45 (1980).

Harper PS: *Practical Genetic Counselling*. Butterworth-Heinemann, Oxford (1988).

Hebra F, Kaposi M: On diseases of the skin including exanthemata volume III., New Sydenham Soc 61ed:252-258 (1874).

Heffron F, Rubens C, Falkow S: Translocation of a plasmid DNA sequence which mediates ampicillin resistance: molecular nature and specificity of insertion. *Proc Natl Acad Sci USA* 72:3623-3627 (1975).

Henning KA, Li L, Iyer N, McDaniel LD, Reagan MS, Legerski R, Schultz RA, Stefanini M, Lehmann AR, Mayne LV, Friedberg EC: The Cockayne syndrome group A gene encodes a WD repeat protein that interacts with CSB protein and a subunit of RNA polymerase II TFIIF. *Cell* 82:555-564 (1995).

Hey T, Lipps G, Sugawara K, Iwai S, Hanaoka F, Krauss G: The XPC-HR23B complex displays high affinity and specificity for damaged DNA in a true-equilibrium fluorescence assay. *Biochemistry* 41:6583-6587 (2002).

Hoeijmakers JH: Genome maintenance mechanisms for preventing cancer. *Nature* 411:366-374 (2001).

Hosfield DJ, Mol CD, Shen B, Tainer JA: Structure of the DNA repair and replication endonuclease and exonuclease FEN-1: coupling DNA and PCNA binding to FEN-1 activity. *Cell* 95:135-146 (1998).

Houtsmuller AB, Rademakers S, Nigg AL, Hoogstraten D, Hoeijmakers JH, Vermeulen W: Action of DNA repair endonuclease ERCC1/XPF in living cells. *Science* 284:958-961 (1999).

Hwang BJ, Ford JM, Hanawalt PC, Chu G: Expression of the p48 Xeroderma pigmentosum gene is p53-dependent and is involved in global genomic repair. *Proc Natl Acad Sci USA* 96:424-428 (1999).

Hwang KY, Baek K, Kim HY, Cho Y: The crystal structure of flap endonuclease-1 from *Methanococcus jannaschii*. *Nat Struct Biol* 5:707-713 (1998).

Ichihashi M, Fujiwara Y, Uehara Y, Matsumoto A: A mild form of Xeroderma pigmentosum assigned to complementation group G and its repair heterogeneity. *J Invest Dermatol* 85:284-287 (1985).

Imoto K, Kobayashi N, Katsumi S, Nishiwaki Y, Iwamoto TA, Yamamoto A, Yamashina Y, Shirai T, Miyagawa S, Dohi Y, Sugiura S, Mori T: The total amount of DNA damage determines ultraviolet-radiation-induced cytotoxicity after uniform or localized irradiation of human cells. *J Invest Dermatol* 119:1177-1182 (2002).

Itin PH, Pittelkow MR: Trichothiodystrophy: review of sulfur-deficient brittle hair syndromes and association with the ectodermal dysplasias. *J Am Acad Dermatol* 22:705-717 (1990).

Itin PH, Sarasin A, Pittelkow MR: Trichothiodystrophy: update on the sulfur-deficient brittle hair syndromes. *J Am Acad Dermatol* 44:891-920 (2001).

Ito S, Kuraoka I, Chymkowitz P, Compe E, Takedachi A, Ishigami C, Coin F, Egly JM, Tanaka K: XPG stabilizes TFIIF, allowing transactivation of nuclear receptors: implications for Cockayne syndrome in XP-G/CS patients. *Mol Cell* 26:231-243 (2007).

Iyer N, Reagan MS, Wu KJ, Canagarajah B, Friedberg EC: Interactions involving the human RNA polymerase II transcription/nucleotide excision repair complex TFIIF, the nucleotide excision

repair protein XPG, and Cockayne syndrome group B (CSB) protein. *Biochemistry* 35:2157-2167 (1996).

Jaenisch R, Bird A: Epigenetic regulation of gene expression: how the genome integrates intrinsic and environmental signals. *Nat Genet* 33 Suppl: 245-54 (2003).

Jaspers NG, Raams A, Silengo MC, Wijgers N, Niedernhofer LJ, Robinson AR, Giglia-Mari G, Hoogstraten D, Kleijer WJ, Hoeijmakers JH, Vermeulen W: First reported patient with human ERCC1 deficiency has cerebro-oculo-facio-skeletal syndrome with a mild defect in nucleotide excision repair and severe developmental failure. *Am J Hum Genet* 80:457-466 (2007).

Jorizzo JL, Atherton DJ, Crouse RG, Wells RS: Ichthyosis, brittle hair, impaired intelligence, decreased fertility and short stature (IBIDS syndrome). *Br J Dermatol* 106:705-710 (1982).

Jorizzo JL, Crouse RG, Wheeler CE, Jr.: Lamellar ichthyosis, dwarfism, mental retardation, and hair shaft abnormalities. A link between the ichthyosis-associated and BIDS syndromes. *J Am Acad Dermatol* 2:309-317 (1980).

Kantor GJ, Barsalou LS, Hanawalt PC: Selective repair of specific chromatin domains in UV-irradiated cells from Xeroderma pigmentosum complementation group C. *Mutat Res* 235:171-180 (1990).

Kee Y, D'Andrea AD: Expanded roles of the Fanconi anemia pathway in preserving genomic stability. *Genes Dev* 24:1680-1694 (2010).

Keeney S, Chang GJ, Linn S: Characterization of a human DNA damage binding protein implicated in Xeroderma pigmentosum E. *J Biol Chem* 268:21293-21300 (1993).

Khan SG, Oh KS, Emmert S, Imoto K, Tamura D, DiGiovanna JJ, Shahlavi T, Armstrong N, Baker CC, Neuburg M, Zalewski C, Brewer C, Wiggs E, Schiffmann R, Kraemer KH: XPC initiation codon mutation in Xeroderma pigmentosum patients with and without neurological symptoms. *DNA Repair (Amst)* 8:114-125 (2009).

Khan SG, Oh KS, Shahlavi T, Ueda T, Busch DB, Inui H, Emmert S, Imoto K, Muniz-Medina V, Baker CC, DiGiovanna JJ, Schmidt D, Khadavi A, Metin A, Gozukara E, Slor H, Sarasin A, Kraemer KH: Reduced XPC DNA repair gene mRNA levels in clinically normal parents of Xeroderma pigmentosum patients. *Carcinogenesis* 27:84-94 (2006).

Khan SG, Yamanegi K, Zheng ZM, Boyle J, Imoto K, Oh KS, Baker CC, Gozukara E, Metin A, Kraemer KH: XPC branch-point sequence mutations disrupt U2 snRNP binding, resulting in abnormal pre-mRNA splicing in Xeroderma pigmentosum patients. *Hum Mutat* 31:167-175 (2010).

Kleijer WJ, Laugel V, Berneburg M, Nardo T, Fawcett H, Gratchev A, Jaspers NG, Sarasin A, Stefanini M, Lehmann AR: Incidence of DNA repair deficiency disorders in western Europe: Xeroderma pigmentosum, Cockayne syndrome and trichothiodystrophy. *DNA Repair (Amst)* 7:744-750 (2008).

Kobayashi T, Takeuchi S, Saijo M, Nakatsu Y, Morioka H, Otsuka E, Wakasugi M, Nikaido O, Tanaka K: Mutational analysis of a function of Xeroderma pigmentosum group A (XPA) protein in strand-specific DNA repair. *Nucleic Acids Res* 26:4662-4668 (1998).

- Kobayashi T, Uchiyama M, Fukuro S, Tanaka K: Mutations in the XPD gene in Xeroderma pigmentosum group D cell strains: confirmation of genotype-phenotype correlation. *Am J Med Genet* 110:248-252 (2002).
- Kondo S, Ichikawa H, Iwo K, Kato T: Base-change mutagenesis and prophage induction in strains of *Escherichia coli* with different DNA repair capacities. *Genetics* 66:187-217 (1970).
- Kraemer KH, Lee MM, Andrews AD, Lambert WC: The role of sunlight and DNA repair in melanoma and nonmelanoma skin cancer. The Xeroderma pigmentosum paradigm. *Arch Dermatol* 130:1018-1021 (1994).
- Kraemer KH, Lee MM, Scotto J: Xeroderma pigmentosum. Cutaneous, ocular, and neurologic abnormalities in 830 published cases. *Arch Dermatol* 123:241-250 (1987).
- Kraemer KH, Patronas NJ, Schiffmann R, Brooks BP, Tamura D, DiGiovanna JJ: Xeroderma pigmentosum, trichothiodystrophy and Cockayne syndrome: a complex genotype-phenotype relationship. *Neuroscience* 145:1388-1396 (2007).
- Kraemer KH, Ruenger TM. Genome instability DNA repair and cancer In: Wolff K, Goldsmith LA, Katz SI, Gilchrist BA, Paller AS, Leffell DJ, eds. *Fitzpatrick's Dermatology in General Medicine*. New York: McGraw Hill pp 977-986 (2008).
- Kusumoto R, Masutani C, Sugawara K, Iwai S, Araki M, Uchida A, Mizukoshi T, Hanaoka F: Diversity of the damage recognition step in the global genomic nucleotide excision repair in vitro. *Mutat Res* 485:219-227 (2001).
- Lalle P, Nospikel T, Constantinou A, Thorel F, Clarkson SG: The founding members of Xeroderma pigmentosum group G produce XPG protein with severely impaired endonuclease activity. *J Invest Dermatol* 118:344-351 (2002).
- Laemmli UK. Cleavage of structural proteins during the assembly of the head of bacteriophage T4. *Nature* 227:680-5 (1970)
- Lao Y, Gomes XV, Ren Y, Taylor JS, Wold MS: Replication protein A interactions with DNA. III. Molecular basis of recognition of damaged DNA. *Biochemistry* 39:850-859 (2000).
- Larizza L, Roversi G, Volpi L: Rothmund-Thomson syndrome. *Orphanet J Rare Dis* 5:2 (2010).
- Le MN, Egly JM, Coin F: True lies: the double life of the nucleotide excision repair factors in transcription and DNA repair. *J Nucleic Acids* 2010. pii: 616342 (2010).
- Lehmann AR: The Xeroderma pigmentosum group D (XPD) gene: one gene, two functions, three diseases. *Genes Dev* 15:15-23 (2001).
- Lejeune F, Maquat LE: Mechanistic links between nonsense-mediated mRNA decay and pre-mRNA splicing in mammalian cells. *Curr Opin Cell Biol* 17:309-315 (2005).
- Li L, Bales ES, Peterson CA, Legerski RJ: Characterization of molecular defects in Xeroderma pigmentosum group C. *Nat Genet* 5:413-417 (1993).

- Li L, Lu X, Peterson CA, Legerski RJ: An interaction between the DNA repair factor XPA and replication protein A appears essential for nucleotide excision repair. *Mol Cell Biol* 15:5396-5402 (1995a).
- Li L, Peterson CA, Lu X, Legerski RJ: Mutations in XPA that prevent association with ERCC1 are defective in nucleotide excision repair. *Mol Cell Biol* 15:1993-1998 (1995b).
- Liang C, Kraemer KH, Morris A, Schiffmann R, Price VH, Menefee E, DiGiovanna JJ: Characterization of tiger-tail banding and hair shaft abnormalities in trichothiodystrophy. *J Am Acad Dermatol* 52:224-232 (2005).
- Liang F, Han M, Romanienko PJ, Jasin M: Homology-directed repair is a major double-strand break repair pathway in mammalian cells. *Proc Natl Acad Sci USA* 95:5172-5177 (1998).
- Lieber MR: The FEN-1 family of structure-specific nucleases in eukaryotic DNA replication, recombination and repair. *Bioessays* 19:233-240 (1997).
- Lieber MR: The mechanism of human nonhomologous DNA end joining. *J Biol Chem* 283:1-5 (2008).
- Lindahl T: Instability and decay of the primary structure of DNA. *Nature* 362:709-715 (1993).
- Lu H, Zawel L, Fisher L, Egly JM, Reinberg D: Human general transcription factor IIH phosphorylates the C-terminal domain of RNA polymerase II. *Nature* 358:641-645 (1992).
- Maillard O, Solyom S, Naegeli H: An aromatic sensor with aversion to damaged strands confers versatility to DNA repair. *PLoS Biol* 5:e79 (2007).
- Manceau G, Karoui M, Charachon A, Delchier JC, Sobhani I: [HNPCC (hereditary non-polyposis colorectal cancer) or Lynch syndrome: a syndrome related to a failure of DNA repair system]. *Bull Cancer* 98:323-336 (2011).
- Maquat LE: Nonsense-mediated mRNA decay in mammals. *J Cell Sci* 118:1773-1776 (2005).
- Masutani C, Kusumoto R, Yamada A, Dohmae N, Yokoi M, Yuasa M, Araki M, Iwai S, Takio K, Hanaoka F: The XPV (Xeroderma pigmentosum variant) gene encodes human DNA polymerase eta. *Nature* 399:700-704 (1999).
- Matsuda T, Saijo M, Kuraoka I, Kobayashi T, Nakatsu Y, Nagai A, Enjoji T, Masutani C, Sugawara K, Hanaoka F, .: DNA repair protein XPA binds replication protein A (RPA). *J Biol Chem* 270:4152-4157 (1995).
- Matsunaga T, Mu D, Park CH, Reardon JT, Sancar A: Human DNA repair excision nuclease. Analysis of the roles of the subunits involved in dual incisions by using anti-XPG and anti-ERCC1 antibodies. *J Biol Chem* 270:20862-20869 (1995).
- McDaniel LD, Rivera-Begeman A, Doughty AT, Schultz RA, Friedberg EC: Validation of XP-C pathogenic variations in archival material from a live XP patient. *DNA Repair (Amst)* 6:115-120 (2007).

- Meira LB, Graham JM, Jr., Greenberg CR, Busch DB, Doughty AT, Ziffer DW, Coleman DM, Savre-Train I, Friedberg EC: Manitoba aboriginal kindred with original cerebro-oculo- facio-skeletal syndrome has a mutation in the Cockayne syndrome group B (CSB) gene. *Am J Hum Genet* 66:1221-1228 (2000).
- Mellon I, Spivak G, Hanawalt PC: Selective removal of transcription-blocking DNA damage from the transcribed strand of the mammalian DHFR gene. *Cell* 51:241-249 (1987).
- Min JH, Pavletich NP: Recognition of DNA damage by the Rad4 nucleotide excision repair protein. *Nature* 449:570-575 (2007).
- Moggs JG, Yarema KJ, Essigmann JM, Wood RD: Analysis of incision sites produced by human cell extracts and purified proteins during nucleotide excision repair of a 1,3-intrastrand d(GpTpG)-cisplatin adduct. *J Biol Chem* 271:7177-7186 (1996).
- Monnat RJ, Jr.: Human RECQ helicases: roles in DNA metabolism, mutagenesis and cancer biology. *Semin Cancer Biol* 20:329-339 (2010).
- Moriwaki S, Stefanini M, Lehmann AR, Hoeijmakers JH, Robbins JH, Rapin I, Botta E, Tanganelli B, Vermeulen W, Broughton BC, Kraemer KH: DNA repair and ultraviolet mutagenesis in cells from a new patient with Xeroderma pigmentosum group G and cockayne syndrome resemble Xeroderma pigmentosum cells. *J Invest Dermatol* 107:647-653 (1996).
- Moriwaki S, Takigawa M, Igarashi N, Nagai Y, Amano H, Ishikawa O, Khan SG, Kraemer KH: Xeroderma pigmentosum complementation group G patient with a novel homozygous missense mutation and no neurological abnormalities. *Exp Dermatol* 21:304-307 (2012).
- Moser J, Kool H, Giakzidis I, Caldecott K, Mullenders LH, Fousteri MI: Sealing of chromosomal DNA nicks during nucleotide excision repair requires XRCC1 and DNA ligase III alpha in a cell-cycle-specific manner. *Mol Cell* 27:311-323 (2007).
- Mu D, Hsu DS, Sancar A: Reaction mechanism of human DNA repair excision nuclease. *J Biol Chem* 271:8285-8294 (1996).
- Mu D, Sancar A: Model for XPC-independent transcription-coupled repair of pyrimidine dimers in humans. *J Biol Chem* 272:7570-7573 (1997).
- Mullis K, Faloona F, Scharf S, Saiki R, Horn G, Erlich H: Specific enzymatic amplification of DNA in vitro: the polymerase chain reaction. *Cold Spring Harb Symp Quant Biol* 51 Pt 1:263-73 (1986).
- Murray JM, Doe CL, Schenk P, Carr AM, Lehmann AR, Watts FZ: Cloning and characterisation of the *S. pombe* rad15 gene, a homologue to the *S. cerevisiae* RAD3 and human ERCC2 genes. *Nucleic Acids Res* 20:2673-2678 (1992).
- Nakabayashi K, Amann D, Ren Y, Saarialho-Kere U, Avidan N, Gentles S, MacDonald JR, Puffenberger EG, Christiano AM, Martinez-Mir A, Salas-Alanis JC, Rizzo R, Vamos E, Raams A, Les C, Seboun E, Jaspers NG, Beckmann JS, Jackson CE, Scherer SW: Identification of C7orf11 (TTDN1) gene mutations and genetic heterogeneity in nonphotosensitive trichothiodystrophy. *Am J Hum Genet* 76:510-516 (2005).

- Nakajima S, Lan L, Kanno S, Takao M, Yamamoto K, Eker AP, Yasui A: UV light-induced DNA damage and tolerance for the survival of nucleotide excision repair-deficient human cells. *J Biol Chem* 279:46674-46677 (2004).
- Nance MA, Berry SA: Cockayne syndrome: review of 140 cases. *Am J Med Genet* 42:68-84 (1992).
- Nelson JA, Gnann JW, Jr., Ghazal P: Regulation and tissue-specific expression of human cytomegalovirus. *Curr Top Microbiol Immunol* 154:75-100 (1990).
- Ng JM, Vermeulen W, van der Horst GT, Bergink S, Sugawara K, Vrieling H, Hoeijmakers JH: A novel regulation mechanism of DNA repair by damage-induced and RAD23-dependent stabilization of Xeroderma pigmentosum group C protein. *Genes Dev* 17:1630-1645 (2003).
- Nishi R, Okuda Y, Watanabe E, Mori T, Iwai S, Masutani C, Sugawara K, Hanaoka F: Centrin 2 stimulates nucleotide excision repair by interacting with Xeroderma pigmentosum group C protein. *Mol Cell Biol* 25:5664-5674 (2005).
- Nocentini S, Coin F, Saijo M, Tanaka K, Egly JM: DNA damage recognition by XPA protein promotes efficient recruitment of transcription factor II H. *J Biol Chem* 272:22991-22994 (1997).
- Norris PG, Hawk JL, Avery JA, Giannelli F: Xeroderma pigmentosum complementation group G-- report of two cases. *Br J Dermatol* 116:861-866 (1987).
- Nospikel T, Clarkson SG: Mutations that disable the DNA repair gene XPG in a Xeroderma pigmentosum group G patient. *Hum Mol Genet* 3:963-967 (1994).
- Nospikel T, Lalle P, Leadon SA, Cooper PK, Clarkson SG: A common mutational pattern in Cockayne syndrome patients from Xeroderma pigmentosum group G: implications for a second XPG function. *Proc Natl Acad Sci USA* 94:3116-3121 (1997).
- Nospikel T: Nucleotide excision repair: variations on versatility. *Cell. Mol. Life Sci.* 66: 994 – 1009 (2009).
- O'Donovan A, Davies AA, Moggs JG, West SC, Wood RD: XPG endonuclease makes the 3' incision in human DNA nucleotide excision repair. *Nature* 371:432-435 (1994).
- Oh KS, Imoto K, Boyle J, Khan SG, Kraemer KH: Influence of XPB helicase on recruitment and redistribution of nucleotide excision repair proteins at sites of UV-induced DNA damage. *DNA Repair (Amst)* 6:1359-1370 (2007).
- Oh KS, Imoto K, Emmert S, Tamura D, DiGiovanna JJ, Kraemer KH: Nucleotide excision repair proteins rapidly accumulate but fail to persist in human XP-E (DDB2 mutant) cells. *Photochem Photobiol* 87:729-733 (2011).
- Oksenysh V, de Jesus BB, Zhovmer A, Egly JM, Coin F: Molecular insights into the recruitment of TFIIH to sites of DNA damage. *EMBO J* 28:2971-2980 (2009).

- Park CH, Mu D, Reardon JT, Sancar A: The general transcription-repair factor TFIIH is recruited to the excision repair complex by the XPA protein independent of the TFIIIE transcription factor. *J Biol Chem* 270:4896-4902 (1995).
- Park CH, Sancar A: Formation of a ternary complex by human XPA, ERCC1, and ERCC4(XPF) excision repair proteins. *Proc Natl Acad Sci USA* 91:5017-5021 (1994).
- Park MS, Valdez J, Gurley L, Kim CY: Characterization of a putative helix-loop-helix motif in nucleotide excision repair endonuclease, XPG. *J Biol Chem* 272:27823-27829 (1997).
- Petrini JH: The Mre11 complex and ATM: collaborating to navigate S phase. *Curr Opin Cell Biol* 12:293-296 (2000).
- Pfeifer GP: Formation and processing of UV photoproducts: effects of DNA sequence and chromatin environment. *Photochem Photobiol* 65:270-283 (1997).
- Ponti G, Ponz de LM: Muir-Torre syndrome. *Lancet Oncol* 6:980-987 (2005).
- Price VH, Odom RB, Ward WH, Jones FT: Trichothiodystrophy: sulfur-deficient brittle hair as a marker for a neuroectodermal symptom complex. *Arch Dermatol* 116:1375-1384 (1980).
- Rapin I, Lindenbaum Y, Dickson DW, Kraemer KH, Robbins JH: Cockayne syndrome and Xeroderma pigmentosum. *Neurology* 55:1442-1449 (2000).
- Rastogi RP, Richa, Kumar A, Tyagi MB, Sinha RP: Molecular mechanisms of ultraviolet radiation-induced DNA damage and repair. *J Nucleic Acids* 592980 (2010).
- Reardon JT, Ge H, Gibbs E, Sancar A, Hurwitz J, Pan ZQ: Isolation and characterization of two human transcription factor IIH (TFIIH)-related complexes: ERCC2/CAK and TFIIH. *Proc Natl Acad Sci USA* 93:6482-6487 (1996).
- Reardon JT, Sancar A: Molecular anatomy of the human excision nuclease assembled at sites of DNA damage. *Mol Cell Biol* 22:5938-5945 (2002).
- Reed WB, Landing B, Sugarman G, Cleaver JE, Melnyk J: Xeroderma pigmentosum. Clinical and laboratory investigation of its basic defect. *JAMA* 207:2073-2079 (1969).
- Ridley AJ, Colley J, Wynford-Thomas D, Jones CJ: Characterisation of novel mutations in Cockayne syndrome type A and Xeroderma pigmentosum group C subjects. *J Hum Genet* 50:151-154 (2005).
- Riedl T, Hanaoka F, Egly JM: The comings and goings of nucleotide excision repair factors on damaged DNA. *EMBO J* 22:5293-5303 (2003).
- Robins P, Jones CJ, Biggerstaff M, Lindahl T, Wood RD: Complementation of DNA repair in Xeroderma pigmentosum group A cell extracts by a protein with affinity for damaged DNA. *EMBO J* 10:3913-3921 (1991).
- Roche Y, Zhang D, Segers-Nolten GM, Vermeulen W, Wyman C, Sugasawa K, Hoeijmakers J, Otto C: Fluorescence correlation spectroscopy of the binding of nucleotide excision repair protein XPC-hHR23B with DNA substrates. *J Fluoresc* 18:987-995 (2008).

- Rochette-Egly C, Adam S, Rossignol M, Egly JM, Chambon P: Stimulation of RAR alpha activation function AF-1 through binding to the general transcription factor TFIID and phosphorylation by CDK7. *Cell* 90:97-107 (1997).
- Roth DB, Porter TN, Wilson JH: Mechanisms of nonhomologous recombination in mammalian cells. *Mol Cell Biol* 5:2599-2607 (1985).
- Rotman G, Shiloh Y: ATM: from gene to function. *Hum Mol Genet* 7:1555-1563 (1998).
- Saijo M, Kuraoka I, Masutani C, Hanaoka F, Tanaka K: Sequential binding of DNA repair proteins RPA and ERCC1 to XPA in vitro. *Nucleic Acids Res* 24:4719-4724 (1996).
- Sajjad M, Khattak AA, Bunn JE, Mackenzie I: Causes of childhood deafness in Pukhtoonkhwa Province of Pakistan and the role of consanguinity. *J Laryngol Otol* 122:1057-1063 (2008).
- Sander M, Cadet J, Casciano DA, Galloway SM, Marnett LJ, Novak RF, Pettit SD, Preston RJ, Skare JA, Williams GM, Van HB, Gollapudi BB: Proceedings of a workshop on DNA adducts: biological significance and applications to risk assessment Washington, DC, April 13-14, 2004. *Toxicol Appl Pharmacol* 208:1-20 (2005).
- Sanger F, Air GM, Barrell BG, Brown NL, Coulson AR, Fiddes CA, Hutchison CA, Slocombe PM, Smith M: Nucleotide sequence of bacteriophage phi X174 DNA. *Nature* 265:687-95. (1977)
- Sarker AH, Tsutakawa SE, Kostek S, Ng C, Shin DS, Peris M, Campeau E, Tainer JA, Nogales E, Cooper PK: Recognition of RNA polymerase II and transcription bubbles by XPG, CSB, and TFIID: insights for transcription-coupled repair and Cockayne Syndrome. *Mol Cell* 20:187-198 (2005).
- Scharer OD: Hot topics in DNA repair: the molecular basis for different disease states caused by mutations in TFIID and XPG. *DNA Repair (Amst)* 7:339-344 (2008).
- Scherly D, Nospikel T, Corlet J, Ucla C, Bairoch A, Clarkson SG: Complementation of the DNA repair defect in Xeroderma pigmentosum group G cells by a human cDNA related to yeast RAD2. *Nature* 363:182-185 (1993).
- Shen B, Nolan JP, Sklar LA, Park MS: Essential amino acids for substrate binding and catalysis of human flap endonuclease 1. *J Biol Chem* 271:9173-9176 (1996).
- Shiomi N, Mori M, Kito S, Harada YN, Tanaka K, Shiomi T: Severe growth retardation and short life span of double-mutant mice lacking Xpa and exon 15 of Xpg. *DNA Repair (Amst)* 4:351-357 (2005).
- Shivji MK, Podust VN, Hubscher U, Wood RD: Nucleotide excision repair DNA synthesis by DNA polymerase epsilon in the presence of PCNA, RFC, and RPA. *Biochemistry* 34:5011-5017 (1995).
- Soufir N, Ged C, Bourillon A, Austerlitz F, Chemin C, Sary A, Armier J, Pham D, Khadir K, Roume J, Hadj-Rabia S, Bouadjar B, Taieb A, de VH, Benchiki H, Grandchamp B, Sarasin A: A prevalent mutation with founder effect in Xeroderma pigmentosum group C from north Africa. *J Invest Dermatol* 130:1537-1542 (2010).

- Southern PJ, Berg P: Transformation of mammalian cells to antibiotic resistance with a bacterial gene under control of the SV40 early region promoter. *J Mol Appl Genet* 1:327-341 (1982).
- Staresinic L, Fagbemi AF, Enzlin JH, Gourdin AM, Wijgers N, Dunand-Sauthier I, Giglia-Mari G, Clarkson SG, Vermeulen W, Scharer OD: Coordination of dual incision and repair synthesis in human nucleotide excision repair. *EMBO J* 28:1111-1120 (2009).
- Stucki M, Jonsson ZO, Hubscher U: In eukaryotic flap endonuclease 1, the C terminus is essential for substrate binding. *J Biol Chem* 276:7843-7849 (2001).
- Sugasawa K: UV-induced ubiquitylation of XPC complex, the UV-DDB-ubiquitin ligase complex, and DNA repair. *J Mol Histol* 37:189-202 (2006).
- Sugasawa K, Akagi J, Nishi R, Iwai S, Hanaoka F: Two-step recognition of DNA damage for mammalian nucleotide excision repair: Directional binding of the XPC complex and DNA strand scanning. *Mol Cell* 36:642-653 (2009).
- Sugasawa K, Ng JM, Masutani C, Iwai S, van der Spek PJ, Eker AP, Hanaoka F, Bootsma D, Hoeijmakers JH: Xeroderma pigmentosum group C protein complex is the initiator of global genome nucleotide excision repair. *Mol Cell* 2:223-232 (1998).
- Sugasawa K, Okamoto T, Shimizu Y, Masutani C, Iwai S, Hanaoka F: A multistep damage recognition mechanism for global genomic nucleotide excision repair. *Genes Dev* 15:507-521 (2001).
- Sugasawa K, Okuda Y, Saijo M, Nishi R, Matsuda N, Chu G, Mori T, Iwai S, Tanaka K, Tanaka K, Hanaoka F: UV-induced ubiquitylation of XPC protein mediated by UV-DDB-ubiquitin ligase complex. *Cell* 121:387-400 (2005).
- Svejstrup JQ, Vichi P, Egly JM: The multiple roles of transcription/repair factor TFIIH. *Trends Biochem Sci* 21:346-350 (1996).
- Svoboda DL, Taylor JS, Hearst JE, Sancar A: DNA repair by eukaryotic nucleotide excision nuclease. Removal of thymine dimer and psoralen monoadduct by HeLa cell-free extract and of thymine dimer by *Xenopus laevis* oocytes. *J Biol Chem* 268:1931-1936 (1993).
- Takao M, Abramic M, Moos M, Jr., Otrin VR, Wootton JC, McLenigan M, Levine AS, Protic M: A 127 kDa component of a UV-damaged DNA-binding complex, which is defective in some Xeroderma pigmentosum group E patients, is homologous to a slime mold protein. *Nucleic Acids Res* 21:4111-4118 (1993).
- Tanaka K, Kawai K, Kumahara Y, Ikenaga M, Okada Y: Genetic complementation groups in cockayne syndrome. *Somatic Cell Genet* 7:445-455 (1981).
- Tang J, Chu G: Xeroderma pigmentosum complementation group E and UV-damaged DNA-binding protein. *DNA Repair (Amst)* 1:601-616 (2002).
- Tapias A, Auriol J, Forget D, Enzlin JH, Scharer OD, Coin F, Coulombe B, Egly JM: Ordered conformational changes in damaged DNA induced by nucleotide excision repair factors. *J Biol Chem* 279:19074-19083 (2004).

Taylor EM, Broughton BC, Botta E, Stefanini M, Sarasin A, Jaspers NG, Fawcett H, Harcourt SA, Arlett CF, Lehmann AR: Xeroderma pigmentosum and trichothiodystrophy are associated with different mutations in the XPD (ERCC2) repair/transcription gene. *Proc Natl Acad Sci USA* 94:8658-8663 (1997).

Temin HM, Mizutani S: RNA-dependent DNA polymerase in virions of Rous sarcoma virus. *Nature* 226:1211-1213 (1970).

Thacker J, Chalk J, Ganesh A, North P: A mechanism for deletion formation in DNA by human cell extracts: the involvement of short sequence repeats. *Nucleic Acids Res* 20:6183-6188 (1992).

Theron T, Fousteri MI, Volker M, Harries LW, Botta E, Stefanini M, Fujimoto M, Andressoo JO, Mitchell J, Jaspers NG, McDaniel LD, Mullenders LH, Lehmann AR: Transcription-associated breaks in Xeroderma pigmentosum group D cells from patients with combined features of Xeroderma pigmentosum and Cockayne syndrome. *Mol Cell Biol.* 25:8368-78 (2005).

Thompson LH, Schild D: Homologous recombinational repair of DNA ensures mammalian chromosome stability. *Mutat Res* 477:131-153 (2001).

Thompson LH, Schild D: Recombinational DNA repair and human disease. *Mutat Res* 509:49-78 (2002).

Thoms KM, Kuschal C, Emmert S: Lessons learned from DNA repair defective syndromes. *Exp Dermatol* 16:532-544 (2007).

Thorel F, Constantinou A, Dunand-Sauthier I, Nospikel T, Lalle P, Raams A, Jaspers NG, Vermeulen W, Shivji MK, Wood RD, Clarkson SG: Definition of a short region of XPG necessary for TFIIH interaction and stable recruitment to sites of UV damage. *Mol Cell Biol* 24:10670-10680 (2004).

Tikoo S, Sengupta S: Time to bloom. *Genome Integr* 1:14 (2010).

Tirode F, Busso D, Coin F, Egly JM: Reconstitution of the transcription factor TFIIH: assignment of functions for the three enzymatic subunits, XPB, XPD, and cdk7. *Mol Cell* 3:87-95 (1999).

Tomlinson CG, Atack JM, Chapados B, Tainer JA, Grasby JA: Substrate recognition and catalysis by flap endonucleases and related enzymes. *Biochem Soc Trans* 38:433-437 (2010).

Trego KS, Turchi JJ: Pre-steady-state binding of damaged DNA by XPC-hHR23B reveals a kinetic mechanism for damage discrimination. *Biochemistry* 45:1961-1969 (2006).

Troelstra C, Odijk H, de WJ, Westerveld A, Thompson LH, Bootsma D, Hoeijmakers JH: Molecular cloning of the human DNA excision repair gene ERCC-6. *Mol Cell Biol* 10:5806-5813 (1990).

Tsodikov OV, Enzlin JH, Scharer OD, Ellenberger T: Crystal structure and DNA binding functions of ERCC1, a subunit of the DNA structure-specific endonuclease XPF-ERCC1. *Proc Natl Acad Sci USA* 102:11236-11241 (2005).

- Tsutakawa SE, Classen S, Chapados BR, Arvai AS, Finger LD, Guenther G, Tomlinson CG, Thompson P, Sarker AH, Shen B, Cooper PK, Grasby JA, Tainer JA: Human flap endonuclease structures, DNA double-base flipping, and a unified understanding of the FEN1 superfamily. *Cell* 145:198-211 (2011).
- Ueda T, Compe E, Catez P, Kraemer KH, Egly JM: Both XPD alleles contribute to the phenotype of compound heterozygote Xeroderma pigmentosum patients. *J Exp Med* 206:3031-3046 (2009).
- Usuda T, Saijo M, Tanaka K, Sato N, Uchiyama M, Kobayashi T: A Japanese trichothiodystrophy patient with XPD mutations. *J Hum Genet* 56:77-79 (2011).
- Venema J, van HA, Karcagi V, Natarajan AT, van Zeeland AA, Mullenders LH: Xeroderma pigmentosum complementation group C cells remove pyrimidine dimers selectively from the transcribed strand of active genes. *Mol Cell Biol* 11:4128-4134 (1991).
- Venter JC, Adams MD, Myers EW, Li PW, Mural RJ, Sutton GG, Smith HO, Yandell M, Evans CA, Holt RA, Gocayne JD, Amanatides P et al.: The sequence of the human genome. *Science* 291:1304-1351 (2001).
- Volker M, Mone MJ, Karmakar P, van HA, Schul W, Vermeulen W, Hoeijmakers JH, van DR, van Zeeland AA, Mullenders LH: Sequential assembly of the nucleotide excision repair factors in vivo. *Mol Cell* 8:213-224 (2001).
- Wacker A, Dellweg H, Jacherts D: Thymine dimerization and survival of bacteria. *J Mol Biol* 4:410-412 (1962).
- Wakasugi M, Reardon JT, Sancar A: The non-catalytic function of XPG protein during dual incision in human nucleotide excision repair. *J Biol Chem* 272:16030-16034 (1997).
- Wakasugi M, Sancar A: Order of assembly of human DNA repair excision nuclease. *J Biol Chem* 274:18759-18768 (1999).
- Wang XM, Cui YP, Liu YF, Wei L, Liu H, Wang XL, Zheng ZZ: Cockayne syndrome. *Zhongguo Dang Dai Er Ke Za Zhi* 13:141-144 (2011).
- Winkler GS, Araujo SJ, Fiedler U, Vermeulen W, Coin F, Egly JM, Hoeijmakers JH, Wood RD, Timmers HT, Weeda G: TFIIH with inactive XPD helicase functions in transcription initiation but is defective in DNA repair. *J Biol Chem* 275:4258-4266 (2000).
- Wogan GN, Hecht SS, Felton JS, Conney AH, Loeb LA: Environmental and chemical carcinogenesis. *Semin Cancer Biol* 14:473-486 (2004).
- Wolfe KJ, Wickliffe JK, Hill CE, Paolini M, Ammenheuser MM, Abdel-Rahman SZ: Single nucleotide polymorphisms of the DNA repair gene XPD/ERCC2 alter mRNA expression. *Pharmacogenet Genomics* 17:897-905 (2007).
- Wood RD: DNA damage recognition during nucleotide excision repair in mammalian cells. *Biochimie* 81:39-44 (1999).

Xie Z, Liu S, Zhang Y, Wang Z: Roles of Rad23 protein in yeast nucleotide excision repair. *Nucleic Acids Res* 32:5981-5990 (2004).

Yavin E, Stemp ED, O'shea VL, David SS, Barton JK: Electron trap for DNA-bound repair enzymes: a strategy for DNA-mediated signaling. *Proc Natl Acad Sci USA* 103:3610-3614 (2006).

Yoneda K, Moriue J, Matsuoka Y, Moriwaki S, Moriue T, Nakai K, Yokoi I, Nibu N, Demitsu T, Kubota Y: Xeroderma pigmentosum complementation group G in association with malignant melanoma. *Eur J Dermatol* 17:540-541 (2007).

Yudkovsky N, Ranish JA, Hahn S: A transcription reinitiation intermediate that is stabilized by activator. *Nature* 408:225-229 (2000).

Zafeiriou DI, Thorel F, Andreou A, Kleijer WJ, Raams A, Garritsen VH, Gombakis N, Jaspers NG, Clarkson SG: Xeroderma pigmentosum group G with severe neurological involvement and features of Cockayne syndrome in infancy. *Pediatr Res* 49:407-412 (2001).

Zhang H, Pan KH, Cohen SN: Senescence-specific gene expression fingerprints reveal cell-type-dependent physical clustering of up-regulated chromosomal loci. *Proc Natl Acad Sci USA* 100:3251-3256 (2003).

Zipper H, Brunner H, Bernhagen J, Vitzthum F: Investigations on DNA intercalation and surface binding by SYBR Green I, its structure determination and methodological implications. *Nucleic Acids Res.* 32:e103 (2004).

Appendix

Data of the post-UV survival of the primary fibroblast cell cultures. Cells were irradiated with increasing doses UVC irradiation and the post-UV survival was determined with MTT assay (see 2.12.4.1.). Results of all twenty-three NER deficient and three wt primary fibroblast cell cultures are listed in table A-1 to A-13.

Table A-1 Post-UV survival of wt fibroblasts at a density of 5000 cells in percent.

5000 cells		0 J/m ²	6 J/m ²	12 J/m ²	18 J/m ²	24 J/m ²	30 J/m ²
wt1	mean (n=4)	100	109	87	92	91	76
	SEM	5,0	4,5	2,3	5,7	3,3	06
wt5	mean (n=4)	100	98	86	86	94	83
	SEM	6,5	4,9	7,7	3,4	1,4	3,5
wt6	mean (n=4)	100	90	94	97	88	83
	SEM	6,1	4,2	4,9	2,9	1,8	1,2

Table A-2 Post-UV survival of wt fibroblasts at a density of 5000 cells in the presence of 1 mM caffeine in percent.

5000 cells, 1 mM caffeine		0 J/m ²	6 J/m ²	12 J/m ²	18 J/m ²	24 J/m ²	30 J/m ²
wt1	mean (n=4)	100	125	101	101	105	90
	SEM	9,3	5,8	4,1	2,3	2,8	2,5
wt5	mean (n=4)	100	141	105	117	114	117
	SEM	9,7	6,1	15,2	4,2	6,3	2,7
wt6	mean (n=4)	100	95	91	95	80	76
	SEM	1,2	2,3	2,7	31	1,5	5,7

Table A-3 Post-UV survival of wt fibroblasts at a density of 7500 cells in percent.

7500 cells		0 J/m ²	6 J/m ²	12 J/m ²	18 J/m ²	24 J/m ²	30 J/m ²
wt1	mean (n=4)	100	99	88	85	85	81
	SEM	6,3	3,2	3,6	0,9	2,1	2,2
wt5	mean (n=4)	100	97	95	90	99	95
	SEM	5,1	6,7	5,5	7,4	4,4	3,4
wt6	mean (n=4)	100	96	90	86	75	85
	SEM	1,9	1,8	1,6	3,0	0,9	1,2

Table A-4 Post-UV survival of wt fibroblasts at a density of 7500 cells in the presence of 1 mM caffeine in percent.

7500 cells, 1mMcaffeine		0 J/m ²	6 J/m ²	12 J/m ²	18 J/m ²	24 J/m ²	30 J/m ²
wt1	mean (n=4)	100	110	100	101	87	85
	SEM	7,8	3,5	3,7	3,1	3,0	3,4
wt5	mean (n=4)	100	146	129	121	126	133
	SEM	10,4	4,1	2,5	7,9	3,8	3,3
wt6	mean (n=4)	100	96	90	86	75	85
	SEM	1,9	1,8	1,6	3,0	0,9	1,2

Table A-5 Post-UV survival of XP-C fibroblasts at a density of 5000 cells in percent.

5000 cells		0 J/m ²	6 J/m ²	12 J/m ²	18 J/m ²	24 J/m ²	30 J/m ²
XP20MA	mean (n=4)	100	110	89	81	60	52
	SEM	10,3	2,8	3,9	4,6	5,2	4,0
XP23GO	mean (n=4)	100	37	40	33	29	26
	SEM	10,0	7,1	10,3	2,6	6,2	1,8
XP47MA	mean (n=4)	100	68	51	48	38	37
	SEM	4,9	2,6	4,6	4,3	3,5	5,9
XP98MA	mean (n=4)	100	95	81	73	50	40
	SEM	5,1	6,8	1,8	2,0	2,0	9,8

XP99MA	mean (n=4)	100	65	61	47	31	36
	SEM	4,5	4,2	3,7	9,5	2,5	2,3
XP102MA	mean (n=4)	100	78	75	77	66	50
	SEM	2,6	4,9	1,2	3,2	9,6	10,9
XP114MA	mean (n=4)	100	78	67	64	56	62
	SEM	5,5	4,3	2,1	5,8	7,1	10,4
XP115MA	mean (n=4)	100	93	78	76	69	59
	SEM	3,6	6,5	3,4	3,6	6,4	2,8
XP117MA	mean (n=4)	100	74	59	52	38	35
	SEM	6,1	4,1	2,4	5,7	3,7	3,8
XP150MA	mean (n=4)	100	86	79	84	70	77
	SEM	8,2	7,7	12,0	9,8	9,1	2,9
XP155MA	mean (n=4)	100	91	77	72	70	65
	SEM	2,5	0,9	7,6	4,5	2,0	2,2
XP156MA	mean (n=4)	100	84	77	64	57	62
	SEM	5,9	2,0	0,2	1,9	1,7	3,9

Table A-6 Post-UV survival of XP-C fibroblasts at a density of 5000 cells in the presence of 1 mM caffeine in percent.

5000 cells, 1mM caffeine		0 J/m ²	6 J/m ²	12 J/m ²	18 J/m ²	24 J/m ²	30 J/m ²
XP20MA	mean (n=4)	100	87	57	27	28	20
	SEM	2,6	19,2	10,3	9,7	37,2	35,1
XP47MA	mean (n=4)	100	40	31	25	19	21
	SEM	15,3	4,3	4,0	10,7	26,3	24,8
XP98MA	mean (n=4)	84	100	86	73	54	45
	SEM	4,2	7,4	1,3	4,0	5,5	4,5
XP99MA	mean (n=4)	100	35	25	22	20	17
	SEM	2,2	6,4	2,0	9,9	7,7	5,0
XP102MA	mean (n=4)	100	87	81	78	73	53

	SEM	4,6	2,4	8,7	4,2	3,3	11,6
XP114MA	mean (n=4)	100	59	35	28	24	21
	SEM	3,6	5,7	1,8	11,7	4,5	2,4
XP115MA	mean (n=4)	100	70	55	52	48	48
	SEM	2,1	1,6	4,3	2,3	2,2	6,7
XP117MA	mean (n=4)	100	67	55	39	34	36
	SEM	12,7	5,2	5,8	4,5	6,5	3,3
XP150MA	mean (n=4)	100	102	102	102	99	94
	SEM	7,4	5,5	6,3	10,3	1,6	3,2
XP155MA	mean (n=4)	100	100	99	89	99	96
	SEM	5,0	8,7	7,5	0,2	2,5	6,4
XP156MA	mean (n=4)	100	92	77	66	54	55
	SEM	5,2	1,1	2,9	2,6	0,4	3,4

Table A-7 Post-UV survival of XP-C fibroblasts at a density of 7500 cells in percent.

7500 cells		0 J/m²	6 J/m²	12 J/m²	18 J/m²	24 J/m²	30 J/m²
XP20MA	mean (n=4)	100	68	55	54	38	27
	SEM	6,6	4,7	9,5	3,7	6,6	5,3
XP23GO	mean (n=4)	100	47	37	40	30	31
	SEM	5,6	6,3	8,8	7,2	6,4	6,3
XP47MA	mean (n=4)	100	72	58	54	46	43
	SEM	3,4	1,5	5,3	4,9	2,6	2,9
XP98MA	mean (n=4)	100	83	70	64	46	41
	SEM	6,5	8,1	4,5	3,6	3,3	11,2
XP99MA	mean (n=4)	100	81	72	61	50	36
	SEM	4,9	2,4	1,9	3,7	3,7	4,3
XP102MA	mean (n=4)	100	89	86	77	78	44
	SEM	4,3	2,5	2,0	6,1	2,0	8,2
XP114MA	mean (n=4)	100	76	53	57	54	51
	SEM	2,8	4,8	7,8	4,4	5,5	1,3

XP115MA	mean (n=4)	100	88	76	74	68	62
	SEM	6,7	5,9	2,0	1,9	4,3	3,1
XP117MA	mean (n=4)	100	77	64	46	44	40
	SEM	3,4	8,9	3,3	4,6	5,5	2,2
XP150MA	mean (n=4)	100	91	88	82	78	78
	SEM	5,6	7,8	6,1	8,3	7,5	5,9
XP155MA	mean (n=4)	100	83	75	73	67	72
	SEM	8,7	7,0	1,8	4,1	2,1	4,5
XP156MA	mean (n=4)	100	86	76	70	69	62
	SEM	3,2	0,7	2,5	2,2	1,5	6,3

Table A-8 Post-UV survival of XP-C fibroblasts at a density of 7500 cells in the presence of 1 mM caffeine in percent.

7500 cells, 1mM caffeine		0 J/m ²	6 J/m ²	12 J/m ²	18 J/m ²	24 J/m ²	30 J/m ²
XP20MA	mean (n=4)	100	48	26	25	18	24
	SEM	14,1	18,5	23,4	18,0	35,8	22,1
XP47MA	mean (n=4)	100	57	44	37	33	29
	SEM	2,8	2,2	5,6	3,2	0,5	6,1
XP98MA	mean (n=4)	100	85	67	61	42	48
	SEM	9,1	1,3	1,9	5,6	3,5	7,1
XP99MA	mean (n=4)	100	45	37	29	23	22
	SEM	2,3	1,7	2,9	6,8	3,6	8,5
XP102MA	mean (n=4)	100	88	88	87	70	49
	SEM	2,8	4,5	2,7	3,6	2,7	8,0
XP114MA	mean (n=4)	100	63	35	31	28	25
	SEM	0,4	4,6	5,0	9,4	3,8	2,6
XP115MA	mean (n=4)	100	74	64	58	57	53
	SEM	0,6	3,2	3,7	2,5	1,9	3,3
XP117MA	mean (n=4)	100	64	51	40	35	34
	SEM	3,7	4,1	2,7	2,3	0,7	0,0

XP150MA	mean (n=4)	100	89	87	80	90	85
	SEM	8,5	6,5	8,6	9,7	1,2	2,6
XP155MA	mean (n=4)	100	103	102	110	120	115
	SEM	3,9	11,3	9,7	8,5	3,7	3,4
XP156MA	mean (n=4)	100	77	74	64	62	54
	SEM	3,4	2,2	2,9	3,4	4,0	7,3

Table A-9 Post-UV survival of XP-D fibroblasts at a density of 5000 cells as well as 10000 cells in the case of XP188MA in percent.

5000 cells		0 J/m ²	6 J/m ²	12 J/m ²	18 J/m ²	24 J/m ²	30 J/m ²
XP46MA	mean (n=4)	100	112	98	94	61	67
	SEM	7,4	1,9	3,7	3,4	0,5	1,0
XP71MA	mean (n=4)	100	81	69	48	46	44
	SEM	10,6	4,2	6,0	5,7	1,2	8,7
XP87MA	mean (n=4)	100	94	75	79	69	74
	SEM	7,5	6,5	4,6	2,4	5,3	3,1
XP90MA	mean (n=4)	100	87	71	56	50	42
	SEM	2,2	2,5	5,5	4,9	2,6	2,1
		0 J/m ²	3 J/m ²	6 J/m ²	9 J/m ²	12 J/m ²	15 J/m ²
XP89MA	mean (n=4)	100	82	42	37	32	34
	SEM	0,7	1,3	3,7	3,2	5,0	4,1
		0 J/m ²	4 J/m ²	8 J/m ²	12 J/m ²	16 J/m ²	20 J/m ²
XP19MA	mean (n=8)	100	74	74	36	22	n.d.
	SEM	7,0	7,6	3,3	6,6	15,4	n.d.
XP40MA	mean (n=8)	100	78	58	63	29	22
	SEM	2,8	2,7	3,5	3,2	4,8	9,4
10000 cells		0	5 J/m ²	10 J/m ²	15 J/m ²	20 J/m ²	25 J/m ²
XP188MA	mean (n=4)	100	100	93	83	53	48
	SEM	3,3	2,3	2,0	5,0	3,2	6,5

Table A-10 Post-UV survival of XP-D fibroblasts at a density of 5000 cells in the presence of 1 mM caffeine in percent.

5000 cells, 1mM caffeine		0 J/m ²	6 J/m ²	12 J/m ²	18 J/m ²	24 J/m ²	30 J/m ²
XP46MA	mean (n=4)	100	103	97	84	74	77
	SEM	6,1	7,4	9,3	11,4	25,7	26,3
XP71MA	mean (n=4)	100	88	63	40	38	46
	SEM	16,5	13,3	12,5	12,3	25,9	25,3
XP87MA	mean (n=4)	100	91	67	61	74	83
	SEM	9,2	7,8	9,9	11,5	11,6	6,0
XP90MA	mean (n=4)	100	91	67	58	47	47
	SEM	1,7	3,6	7,0	8,1	6,4	1,9
		0 J/m ²	3 J/m ²	6 J/m ²	9 J/m ²	12 J/m ²	15 J/m ²
XP89MA	mean (n=4)	100	79	45	44	42	47
	SEM	7,2	1,4	1,8	2,9	3,3	0,8

Table A-11 Post-UV survival of XP-D fibroblasts at a density of 7500 cells in percent.

7500 cells		0 J/m ²	6 J/m ²	12 J/m ²	18 J/m ²	24 J/m ²	30 J/m ²
XP46MA	mean (n=4)	100	95	79	64	53	52
	SEM	5,6	3,2	1,0	2,5	2,3	3,8
XP71MA	mean (n=4)	100	75	61	47	49	46
	SEM	5,1	4,3	3,1	6,5	1,3	13,1
XP87MA	mean (n=4)	100	80	70	70	68	61
	SEM	4,1	3,1	4,3	1,4	2,2	3,5
XP90MA	mean (n=4)	100	83	68	54	48	48
	SEM	2,8	1,5	1,7	2,0	1,9	4,6
		0 J/m ²	3 J/m ²	6 J/m ²	9 J/m ²	12 J/m ²	15 J/m ²
XP89MA	mean (n=4)	100	88	36	28	20	25
	SEM	0,5	2,4	5,1	2,7	7,5	4,4
		0 J/m ²	4 J/m ²	8 J/m ²	12 J/m ²	16 J/m ²	20 J/m ²
XP19MA	mean (n=8)	100	71	53	30	19	n.d.
	SEM	6,3	6,9	9,9	9,9	20,2	n.d.

XP40MA	mean (n=8)	100	80	72	73	42	23
	SEM	1,6	2,1	3,3	2,7	7,0	6,2

Table A-12 Post-UV survival of XP-D fibroblasts at a density of 7500 cells in the presence of 1 mM caffeine in percent.

7500 cells, 1mM caffeine		0 J/m ²	6 J/m ²	12 J/m ²	18 J/m ²	24 J/m ²	30 J/m ²
XP46MA	mean (n=4)	100	83	75	58	54	55
	SEM	7,6	10,1	6,3	6,2	25,2	24,3
XP71MA	mean (n=4)	100	74	50	38	45	53
	SEM	16,8	13,7	16,1	9,8	25,4	24,3
XP87MA	mean (n=4)	100	82	71	62	89	75
	SEM	6,2	3,7	4,9	4,3	4,2	6,3
XP90MA	mean (n=4)	100	84	69	59	49	47
	SEM	3,3	3,3	3,5	7,2	2,0	1,3
		0 J/m ²	3 J/m ²	6 J/m ²	9 J/m ²	12 J/m ²	15 J/m ²
XP89MA	mean (n=4)	100	78	32	32	34	38
	SEM	6,9	1,8	7,8	5,1	1,4	5,0

Table A-13 Post-UV survival of XP-G fibroblasts in percent.

5000 cells		0J/m ²	6J/m ²	12J/m ²	18J/m ²	24J/m ²	30J/m ²
XP40GO	mean (n=4)	100	74	63	50	46	46
	SEM	4,8	3,0	1,9	2,0	1,8	0,8
5000 cells, 1mM caffeine							
XP40GO	mean (n=4)	100	99	93	87	87	82
	SEM	5,9	11,3	8,5	10,6	8,3	7,6
7500 cells							
XP40GO	mean (n=4)	100	82	68	54	54	52
	SEM	3,4	5,1	5,5	3,7	1,6	5,0

7500 cells, 1mM caffeine							
XP40GO	mean (n=4)	100	75	75	68	71	64
	SEM	8,9	8,5	9,1	9,5	4,4	8,3
5000 cells		0J/m²	3J/m²	6J/m²	9J/m²	12J/m²	15J/m²
XP72MA	mean (n=4)	100	86	47	23	8	2
	SEM	16,9	8,4	4,0	9,7	14,0	12,5
5000 cells, 1mM caffeine							
XP72MA	mean (n=4)	100	90	37	15	1	0
	SEM	8,8	2,8	3,7	10,9	15,5	0,0
7500 cells							
XP72MA	mean (n=4)	100	86	48	26	8	4
	SEM	8,7	5,9	4,4	6,3	14,2	9,3
7500 cells, 1mM caffeine							
XP72MA	mean (n=4)	100	76	29	13	2	1
	SEM	5,6	4,5	11,1	4,0	16,1	38,0
5000 cells		0J/m²	4J/m²	8J/m²	12J/m²	16J/m²	20J/m²
XP165MA	mean (n=4)	100	54	3	0	0	0
	SEM	6,6	13,2	23,1	0,0	0,0	0,0
7500 cells							
XP165MA	mean (n=4)	100	62	4	0	0	0
	SEM	3,6	6,9	18,2	0,0	0,0	0,0

Data of relative NER capability of the primary human fibroblast cell cultures. Relative NER capability was determined with HCR (see 2.12.4.2.). HCR results of all twenty-three NER deficient and five wt primary fibroblast cell cultures analyzed during the thesis are listed in tables A-14 to A-17.

Table A-14 Relative NER capability of wt fibroblasts

wt fibroblasts	mean (n=3) repair norm.	SEM
wt1	22,9%	2,3%
wt2	22,4%	1,5%
wt3	20,2%	5,1%
wt4	41%	10,4%
wt5	47,3%	15,1%

Table A-15 Relative NER capability of XP-C fibroblasts

XP-C fibroblasts	mean (n=3) repair norm.	SEM
XP20MA	11,3%	1,2%
XP20MA + XPC	23,6%	0,5%
XP23GO	3,2%	0,6%
XP47MA	4,6%	0,8%
XP47 + pXPC	31,8%	12,3%
XP98MA	4,6%	1,0%
XP99MA	4,5%	0,9%
XP102MA	0,9%	0,3%
XP102MA + pXPC	2,1%	0,4%
XP114MA	0,7%	0,1%

XP114MA + pXPC	4,2%	0,6%
XP115MA	1,9%	0,4%
X117MA	0,9%	0,5%
XP117MA + pXPC	12,0%	5,5%
XP150MA	1,7%	0,3%
XP150 + pXPC	12,5	4,6%
XP155MA	4,5%	0,2%
XP155 + pXPC	11,9%	1,3%
XP156MA	5,4%	0,5%
XP156 + pXPC	21,3%	6,0%

Table A-16 Relative NER capability of XP-D fibroblasts

XP-D fibroblasts	mean (n=3) repair norm.	SEM
XP19MA	0,4%	0,1%
XP19MA + pXPD	1,6	0,1%
XP40MA	2,0%	0,5%
XP40MA + pXPD	11,7%	1,6%
XP46MA	4,7%	0,9%
XP46MA + pXPD	45,7%	16,3%
XP71MA	1,5%	0,4%
XP71MA + pXPD	4,6%	1,0%
XP87MA	0,6%	0,1%
XP87MA + pXPD	28,4%	12,4%

XP89MA	0,4%	0,0%
XP89MA + pXPD	13,5%	0,9%
XP90MA	0,7%	0,0%
XP90MA + pXPD	14,2%	2,7%
XP188MA	1,8%	0,2%
XP188MA + XPD	5,1%	0,7%

Table A-17 Relative NER capability of XP-G fibroblasts

XP-G fibroblasts	mean (n=3) repair norm.	SEM
XP40GO	1,6%	0,2%
XP40GO + pXPG	21,4%	1,5%
XP72MA	2,6%	0,2%
XP72MA + pXPG	5,8%	3,2%
XP165MA	0,6%	0,1%
XP165MA + XPG	22,9%	3,0%

XP gene mRNA expression analysis of 75 NER deficient and nine wt primary human fibroblasts and list of the NER deficient primary human fibroblast cell cultures provided from University clinics Mannheim (MA) and Göttingen (GO). Expression of all seven XP genes (*XPA* to *XPG*) and the gene coding for DNA polymerase eta (*XPV*) was determined for all 75 NER deficient primary human fibroblasts with qRT-PCR (see 2.14.2.4.). Expression levels, listed in table A-18, were calculated relative to the mean mRNA expression level of nine wt fibroblast cell cultures set to 100 %.

Table A-18 List of NER deficient fibroblast cell cultures and mRNA expression of the XP genes of NER deficient fibroblast cell cultures as well as wild type fibroblast cell cultures in %

Fibroblasts	XPA	XPB	XPC	XPD	XPE (DDB2)	XPF	XPG	XPV
XP1MA	86,0	62,4	64,5	145,9	31,8	58,4	64,5	422,4
XP4MA	125,0	109,2	12,0	101,6	171,3	95,7	128,0	262,4
XP5MA	75,4	61,8	97,6	87,6	96,1	65,3	51,3	1,2
XP6ma	166,2	82,4	219,2	52,4	109,7	74,8	85,2	73,0
XP8MA	79,6	75,4	88,5	92,9	116,9	36,3	54,0	2,7
XP11MA	91,1	82,1	84,5	106,4	68,5	38,6	44,3	29,7
XP12MA	93,2	107,8	74,3	86,0	160,5	74,3	116,5	211,8
XP15MA	40,5	84,1	8,3	113,8	169,2	60,9	111,0	108,6
XP19MA	99,1	83,2	145,3	75,0	140,9	90,1	143,7	133,4
XP20GO	93,1	80,7	114,9	111,7	77,6	57,1	66,0	1,8
XP20MA	114,0	83,8	9,5	129,6	193,5	72,0	122,4	141,2
XP23GO	117,7	50,1	20,0	101,4	83,8	80,0	93,9	83,5
XP27GO	106,8	70,2	23,8	116,5	73,8	112,6	69,9	127,0
XP27MA	107,6	85,1	127,7	85,1	149,8	77,7	98,4	0,0
XP28GO	101,4	56,7	79,7	43,2	133,3	68,6	70,5	55,9
XP28MA	104,5	119,7	85,6	94,8	180,1	128,5	121,1	134,2
XP29MA	352,1	264,4	391,4	149,1	986,4	171,7	209,2	324,0
XP29GO	173,6	121,8	31,7	52,3	240,2	205,4	160,8	187,9
XP40GO	91,1	145,1	150,2	122,6	370,8	95,5	79,4	176,2
XP31MA	62,8	78,9	113,4	78,0	81,6	57,7	61,3	31,3
XP31GO	48,4	91,9	138,3	97,8	142,8	99,0	84,2	146,0
XP32MA	142,8	142,3	283,6	109,0	222,0	84,2	138,4	98,1
XP32GO	154,6	101,7	258,3	70,1	93,1	151,6	138,8	96,1
XP35MA	105,0	120,7	172,2	95,5	164,7	134,7	124,5	178,6
XP36MA	103,9	90,7	11,1	81,2	113,3	67,8	84,1	77,7
XP40MA	106,7	81,1	188,3	79,3	96,2	62,4	85,1	125,3
XP46MA	116,7	124,2	184,6	90,8	124,2	105,1	112,7	192,4
XP47MA	148,7	161,3	274,1	120,0	176,0	130,7	133,3	177,7
XP52MA	88,3	72,1	94,9	75,1	144,9	65,0	89,0	55,1
XP58MA	100,7	85,6	13,3	111,2	154,1	74,5	92,5	193,1
XP65MA	99,4	80,2	12,1	100,5	122,5	70,0	86,3	79,8
XP67MA	0,0	0,0	90,0	0,0	62,3	0,0	35,2	0,0
XP70MA	104,8	98,1	24,4	157,5	163,6	84,3	104,4	62,0

XP71MA	79,6	93,9	104,9	103,4	85,1	52,1	86,2	62,4
XP72MA	155,7	116,1	265,6	119,5	198,7	108,9	93,1	185,2
XP74MA	101,5	80,4	160,6	70,0	108,8	98,9	99,9	118,9
XP76MA	71,1	72,6	63,6	110,1	135,4	65,9	69,5	1,2
XP77MA	114,7	79,4	211,6	45,8	105,9	90,2	99,1	111,8
XP87MA	117,5	74,3	58,7	90,3	83,5	56,9	60,8	83,6
XP89MA	107,4	113,3	160,1	133,6	144,0	114,9	115,2	159,8
XP90MA	85,1	113,8	165,5	151,3	253,2	85,0	101,0	38,9
XP93MA	78,7	78,8	72,2	73,5	75,3	64,8	69,1	49,5
XP98MA	95,1	80,3	10,9	68,9	102,4	61,0	77,3	78,9
XP99MA	152,3	82,5	14,6	104,3	132,2	231,8	120,2	112,3
XP102MA	75,6	102,5	12,7	114,6	120,2	146,6	105,9	43,4
XP107MA	64,8	79,3	9,4	104,4	145,1	53,1	53,8	108,0
XP114MA	88,3	79,3	13,3	91,6	65,5	105,6	96,0	68,9
XP115MA	102,5	76,4	9,6	79,1	131,0	129,0	98,5	184,3
XP117MA	140,9	88,2	20,1	79,6	180,7	116,6	113,7	169,5
XP118MA	31,5	140,0	354,6	79,2	279,6	143,9	194,6	225,4
XP131MA	252,2	103,0	178,8	1178,9	272,8	121,5	397,9	188,0
XP134MA	164,4	136,0	14,4	126,9	106,3	124,8	117,4	158,3
XP141MA	205,9	128,1	230,1	86,7	167,6	71,8	105,3	155,1
XP148MA	71,9	102,1	93,0	69,5	117,3	58,3	70,7	135,0
XP150MA	126,7	109,1	17,1	116,9	115,3	117,0	104,5	46,7
XP151MA	138,7	108,6	48,3	44,0	88,5	112,7	98,4	95,2
XP153MA	110,3	107,0	126,1	89,8	151,0	65,3	89,9	130,8
XP155MA	148,2	77,5	10,0	53,0	99,8	125,4	101,6	56,9
XP156MA	202,1	101,4	25,7	111,0	193,4	132,8	154,5	222,5
XP163MA	92,9	102,1	85,5	58,3	104,3	85,4	73,1	121,8
XP165MA	166,5	67,7	12,3	68,7	139,6	100,4	88,4	78,8
XP168MA	89,2	49,9	8,4	75,4	105,3	45,4	63,3	80,3
XP169MA	84,6	87,4	86,0	101,2	80,6	76,3	74,4	28,8
XP170MA	76,6	93,8	83,0	89,7	62,1	114,9	68,2	54,8
XP172MA	157,2	153,8	267,1	116,0	171,4	135,8	1,1	291,0
XP174MA	86,4	83,8	0,0	88,3	105,8	87,8	72,7	106,9
XP176MA	115,5	93,7	110,7	110,2	95,3	70,8	77,1	46,6
XP183MA	103,4	67,2	144,6	107,6	133,5	89,2	101,5	23,5
XP188MA	77,0	80,6	117,0	74,1	39,9	45,9	76,0	35,1
XP189MA	95,4	110,4	122,7	40,4	142,2	98,3	87,6	155,8
XP197MA	98,0	127,7	113,7	83,0	112,2	75,8	100,2	114,3
XP199MA	65,1	89,4	65,7	78,2	62,0	44,3	57,2	15,7
XP566MA	123,8	191,4	200,8	99,7	219,4	214,2	154,7	122,0
XP606MA	130,6	83,0	105,3	126,0	171,4	111,0	111,6	171,5
XP686MA	106,2	131,7	180,6	108,4	125,2	161,4	92,2	156,0
wt1	96,9	143,8	119,3	200,8	133,7	121,8	122,5	244,2
wt2	118,0	105,6	51,7	81,4	85,2	83,2	95,7	79,3
wt3	74,1	109,9	90,4	94,5	89,1	91,4	101,9	23,6
wt4	79,2	60,9	90,1	45,1	76,7	64,2	71,2	40,5

wt5	91,0	90,5	101,9	43,8	80,9	72,3	75,2	90,3
wt6	97,9	97,3	138,8	139,2	93,9	71,9	82,2	147,2
wt7	89,1	78,4	81,8	81,9	112,8	103,3	89,4	81,1
wt8	127,3	102,9	35,4	112,0	95,8	137,8	116,2	65,2
wt9	126,4	110,7	190,6	101,4	131,8	154,1	145,7	128,6

Data of relative complementation ability of pXPG_{mut} plasmids determined with HCR. Plasmids expressing modified XPG proteins according to the five novel XPG mutations identified during this thesis were generated by site directed mutagenesis and the complementation ability was tested applying HCR assay (see 2.12.4.2.).

Table A-19 Relative NER capability of pXPG_{mut} plasmids determined with HCR

XP-G Fibroblasts	repair norm. mean (n=9)	SEM
XP40GO	1,1%	0,1%
XP40GO + pXPG	32,2%	4,7%
XPXP40GO + pXPG_{L778P}	12,8%	2,8%
XP40GO + pXPG_{Q150X}	2,1%	0,2%
XP165MA	0,6%	0,1%
XP165MA + pXPG	11,1%	2,2%
XP165MA + pXPG_{G805R}	1,4%	0,7%
XP72MA	0,7%	0,1%
XP72Ma + pXPG	22,3%	11,1%
XP72MA + pXPG_{E727X}	2,4%	1,4%
XP72MA + pXPG_{W814S}	7,3%	5,1%

Curriculum vitae**Personal data**

Annika Schäfer

Born: Göttingen, Germany

Profession since June 2009

Ph.D. student in the Department of Dermatology, Allergy, and Venerology, in the research group of Prof. Dr. Steffen Emmert

Tertiary education

2004 - 2009 Georg-August-University Göttingen

Studies: Biology

Field of Studies: Biochemistry, Microbiology, Chemistry

Final degree: Diploma

Topic of diploma thesis: Interaktionsstudien an den ABC-Transportern der peroxysomalen Membran, Department of Pediatrics, Prof. Dr. Detlef Doenecke

Professional education

2001- 2002 off-the-job training

Degree: Biological-Technical-Assistant (BTA)

Professional activity

2003 BTA at the iOnGen AG

2004 BTA at the Selecore AG

Language skills

German: native language

English: first language during thesis

Extended qualifications EDV skills in Microsoft Office (Word, Excel, Power Point)

Publications

Molecular genetic analysis of 16 XP-C patients from Germany: environmental factors predominately contribute to phenotype variations.

Schäfer A, Hofmann L, Gratchev A, Laspe P, Schubert S, Schürer A, Ohlenbusch A, Tzvetkov M, Hallermann C, Reichrath J, Schön MP, Emmert S.
Exp Dermatol. 22: 24-9 (2013), Epub 2012 Nov 22.

No association of vitamin D-related polymorphisms and melanoma risk as well as melanoma prognosis- a case control study.

Schäfer A, Emmert S, Krupper L, Schubert S, Tzvetkov M, Mössner R, Reich K, Berking C, Volkenandt M, Pföhler C, Schön MP, Vogt T, König IR, Reichrath J
Arch Dermatol Res [Epub ahead of print] (May 2012)

Skin cancer in organ transplant recipients: Effects of immunosuppressive medication on DNA repair.

Kuschal C, Thoms KM, Schuber S, Schäfer A, Boekmann L, Schön MP, Emmer S
Exp Dermatol 21:2-6 (2012)

Identification of a new fatty acid synthesis-transport machinery at the peroxysomal membrane.

Hillebrand M, Gersting SW, Lotz-Havla AS, Schäfer A, Rosewich H, Valerius O, Muntau AC, Gärtner J
J Biol Chem 287:210-21 (2012)

Temozolomide chemoresistance heterogeneity in melanoma with different treatment regimens: DNA damage accumulation contribution.

Boekmann L, Nickel AC, Kuschal C, Schäfer A, Thoms KM, Schön MP, Thomale J, Emmert S
Melanoma Res 21:206-16 (2011)

Live cell FRET microscopy: homo- and hetero dimerization of two human peroxisomal ABC transporters, the adreboleukodystrophy protein (ALDP, ABCD1) and PMP70 (ABCD3).

Hillebrand M, Verrier SE, Ohlenbusch A, Schäfer A, Söling HD, Wouters SF, Gärtner J
J Biol Chem 282:26997-7005 (2007)

Accepted for publication in Journal of Investigative Dermatology:

Characterization of five novel XPG mutations in three XP-G patients: Missense mutations impair repair and transcription

Schäfer A, Schubert S, Gratchev A, Apel A, Laspe P, Hofmann L, Ohlenbusch A, Mori T, Kobayashi N, Schürer A, Schön MP, Goerdts S, Emmert S

In revision progress for publication in Experimental Dermatology:

Functional and molecular genetic analyses of 9 newly identified XPD-deficient patients reveal a novel mutation resulting in TTD as well as in XP/CS complex phenotypes

Schäfer A, Hofmann L, Gratchev A, Schubert S, Laspe P, Ohlenbusch A, Tzvetkov M, Weishaupt C, Oji V, Schön MP, Emmert S

Acknowledgement

Zunächst gilt mein Dank Prof. Dr. Steffen Emmert für die Überlassung des Themas aber vor allem für seine engagierte Betreuung und Unterstützung während der letzten 3 Jahre. Vielen Dank, dass du jederzeit erreichbar warst, dir Zeit genommen hast und immer ein offenes Ohr hattest!

Bei PD Dr. Wilfried Kramer und Prof. Dr. Jürgen Brockmöller möchte ich mich ganz herzlich für die Übernahme des Referats und des Koreferats bedanken sowie für die Betreuung der Arbeit als Thesis Komitee. Hier gilt mein Dank ebenfalls Prof. Dr. Michael Schön der als drittes Mitglied und offizieller Betreuer das Komitee komplettiert hat.

Beim DFG Graduiertenkolleg 1034 *Die Bedeutung genetischer Polymorphismen in der Onkologie: Von den Grundlagen zur individualisierten Therapie* möchte ich mich bedanken, dass ich als assoziiertes Mitglied an den tollen Angeboten des Kollegs teilnehmen durfte.

Ganz besonders danken möchte ich Antje Apel und Petra Laspe für ihre super Betreuung im Labor und ihre fortwährende Hilfsbereitschaft. Ihr beide seid der (Ruhe-)Pol des Labors, und habt immer wieder super Ideen, wenns praktisch mal das ein oder andere Problem bei den Versuchen gibt. Vielen Dank dafür! Außerdem möchte ich meinem Leidensgenossen ☺ Steffen danken, der sich immer wieder Zeit genommen hat mit mir über meine Ideen und Probleme zu sprechen, mir Anregungen gegeben hat, und mich auch von dem ein oder anderen PC Problem erlösen konnte! Danke auch für die freundliche Übernahme des Schlüsseldiensts...! Auch bei der restlichen Emmert-Truppe möchte ich mich bedanken. Ihr alle seid immer sehr nett und hilfsbereit gewesen und zusammen haben wir ein prima Labor-Klima geschaffen.

Vielen Dank an Merle die mich auch in meiner neuen Arbeitsgruppe weiter Unterstützt hat und immer mit Rat und Tat zur Stelle war, wenn ich sie gebraucht habe. Danke außerdem an Ole für die vielen, vielen Sequenzierungen.

Danken möchte ich vor allem auch meiner Familie und meinen Freunden die immer für mich da waren, mich aufgebaut und ermutigt haben, wenn es die ein oder andere Krise gegeben hat. Danke an Benjamin, dass er einfach da ist. Ganz besonders möchte ich mich bei Karina bedanken, ohne die die Optik (nicht nur der Dr. Arbeit) sicher ganz anders ausgefallen wäre. Vor allem aber, weil du mit mir moralisch an vorderster Front marschiert bist, meine Labor-Launen, nach guten und nach schlechten Tagen, immer wieder aufgefangen hast und einfach die beste Mitbewohnerin der Welt ist!

This work was supported by German Cancer Aid.